On Connections Between Dark Matter and the Baryon Asymmetry

James Andrew Unwin

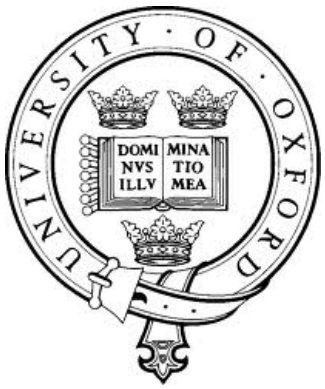

Pembroke College,
University of Oxford.
Trinity Term 2013.

A thesis submitted for the degree of *Doctor of Philosophy*.

Abstract

On Connections Between Dark Matter and the Baryon Asymmetry

A thesis submitted for the degree of *Doctor of Philosophy*, Trinity Term 2013.

James A. Unwin

Pembroke College

This thesis is dedicated to the study of a prominent class of dark matter (DM) models, in which the DM relic density is linked to the baryon asymmetry, often referred to as Asymmetric Dark Matter (ADM) theories. In ADM the relic density is set by a particle-antiparticle asymmetry, in direct analogue to the baryons. This is partly motivated by the observed proximity of the baryon and DM relic densities $\Omega_{\rm DM} \approx 5\Omega_B$, as this can be explained if the DM and baryon asymmetries are linked. A general requisite of models of ADM is that the vast majority of the symmetric component of the DM number density, the DM-antiDM pairs, must be removed for the asymmetry to set the DM relic density and thus to explain the coincidence of $\Omega_{\rm DM}$ and Ω_B. However we shall argue that demanding the efficient annihilation of the symmetric component leads to a tension with experimental constraints in a large class of models.

In order to satisfy the limits coming from direct detection and colliders searches, it is almost certainly required that the DM be part of a richer hidden sector of interacting states. Subsequently, examples of such extended hidden sectors are constructed and studied, in particular we highlight that the presence of light pseudoscalars can greatly aid in alleviating the experimental bounds and are well motivated from a theoretical stance. Finally, we highlight that self-conjugate DM can be generated from hidden sector particle asymmetries, which can lead to distinct phenomenology. Further, this variant on the ADM scenario can circumvent some of the leading constraints.

Acknowledgements

I wish to express my deepest thanks to John March-Russell for support, guidance, and inspiration. I am grateful to my collaborators Uli Haisch, Ed Hardy, Arthur Hebecker, Felix Kahlhoefer, and, especially, Stephen West for an enjoyable and productive time during my DPhil. I am indebted to Alan Barr, Joe Conlon, Rhys Davies, Savas Dimopoulos, Pavel Fileviez Pérez, Mads Frandsen, Peter Graham, Lawrence Hall, Joachim Kopp, Chris McCabe, Matthew McCullough, Apostolos Pilaftsis, Graham Ross, Surjeet Rajendran, Francesco Riva, Raoul Rontsch, Joao Rosa, Subir Sarkar, Fidel Schaposnik, Laura Schaposnik, Kai Schmidt-Hoberg, David Shih, and Timo Weigand for insightful interactions. I would also like to thank Philip Candelas for acting as co-supervisor in the Mathematical Institute and my examiners Joe Conlon and Céline Boehm for their constructive comments.

I am thankful for the hospitality of the CERN theory group, the Institute for Theoretical Physics at Heidelberg University, the Max Planck Institute for Kernphysik (MPIK), Heidelberg, and the Institute for Theoretical Physics at Stanford University during different periods, whilst undertaking work towards this thesis. I gratefully acknowledge that my DPhil research [1–8] has been funded by an EPSRC doctoral scholarship, a Charterhouse European Bursary, a Senior Scholarship at Pembroke College, awards from the Vice-Chancellors Fund and the Esson Bequest, and also through Stipendiary Lectureships at St. John's College and New College.

Finally, I am grateful to my parents and grandparents for their unerring support.

Statement of Originality

This thesis is based on research undertaken between October 2010 and June 2013 and contains no material that has already been accepted, or is concurrently being submitted, for any degree or diploma or certificate or other qualification in this university or elsewhere. To the best of my knowledge and belief this thesis contains no material previously published or written by another person, except where due reference is made in the text.

James A. Unwin June 2013

Contents

1 Introduction and Background

This chapter roughly follows treatments in [9, 10].

The need for additional non-baryonic gravitating matter - *dark matter* - in order to explain astrophysical observations is generally accepted. Moreover, it is also widely held that the dark matter (DM) phenomenon is caused by the existence of new non-relativistic (meta) stable particle species with small or vanishing interactions with photons and hadrons. However, the precise nature of DM is one of the central questions in contemporary theoretical physics and (along with evidence for neutrino masses) is perhaps the most compelling indication of physics beyond the Standard Model (SM).

This thesis is dedicated to the study of a prominent class of DM models, in which the DM relic density is linked to the baryon asymmetry, often referred to as *Asymmetric Dark Matter* (ADM). After outlining the main principles of both traditional DM and ADM in Chap. 1 & 2, respectively, we proceed to carefully examine a crucial requirement on models of ADM in Chap. 3. In Chap. 4, we show that satisfying this theoretical requirement leads to conflict with DM direct detection and collider constraints in a large class of models. We proceed to construct models which satisfy the constraints arising from direct detection and colliders in Chap. 4 & 5, and we examine further experimental limits which can constrain these models. In particular, we demonstrate that viable, motivated models of ADM can be constructed. In Chap. 6 we outline a variant on the ADM scenario which circumvents many of the leading constraints on ADM and which can exhibit distinct phenomenology from traditional models. A summary of the thesis is presented in Chap. 7 with some final remarks.

1.1 The case for dark matter

The earliest indications of deviations in long range gravitational measurements were found by Fritz Zwicky in 1933 [11]. Zwicky estimated the total mass of the galaxy cluster Coma based on the motion of galaxies at the periphery of the cluster, and observed that his result deviated by two orders of magnitude from mass estimates based on the luminosity of the cluster and the number of constituent galaxies. Subsequently, he postulated that this large deviation between measurements was due to the presence of some non-luminous form of matter. Indeed, it was noted that the gravitational force due only to the visible matter would be insufficient for the galaxy cluster to be stable.

Further, evidence for DM comes from observations of galactic rotation curves. If one examines bodies near the galactic edge, the trajectories deviate significantly from naïve expectations of motion under the gravitational effects of just the luminous matter. Rather, the observed velocities of bodies in the periphery of the galaxy are consistent with motion under the gravitational potential generated by an approximately spherical halo of gravitating sources in addition to the observed disk. This lends significant weight to the idea of a DM halo which encompasses the visible galactic disk.

Empirically, the gravitational potential can be inferred by measuring the velocities of bodies at different radial distances from the galactic centre. Take for instance galaxy NGC 6503, the galactic rotation curve for which is shown in Fig. 1 (left) [12]. The plot shows rotational velocities as a function of radial distance for various bodies. Experimental data points are shown with 1σ error bars. The rotational velocity $v_c(r)$ can be calculated for a body at radial distance from the galactic centre r moving under a gravitational potential via Newtonian gravity

$$v_c(r) = \sqrt{\frac{GM(r)}{r}} \ , \qquad M(r) = 4\pi \int_0^r \rho(r') r'^2 \, \mathrm{d}r' \ , \tag{1.1}$$

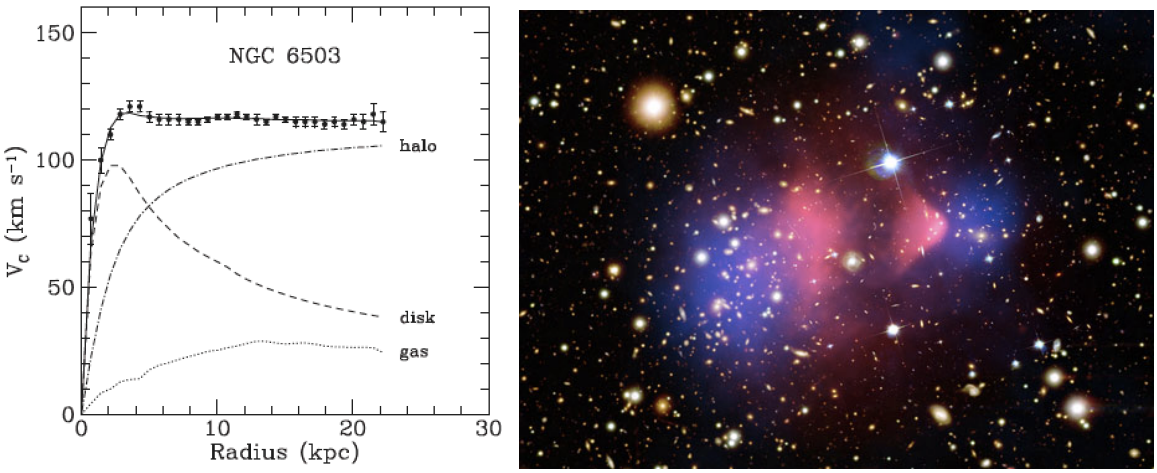

Figure 1. *left.* Galaxy NGC6503 rotation curve [12]. *right.* Bullet cluster [13]. Details in text.

where $G = M_{\rm Pl}^{-2}$ is Newton's constant, with $M_{\rm Pl} = 1.2 \times 10^{19}$ GeV the Planck mass, and ρ is the mass density.

The visible galactic disk, the DM halo, and the intergalactic gas present in the galaxy each contribute differently to the gravitational potential because of their different mass distributions, as dictated by eq. (1.1). A three parameter fit of these components is used to match the data points and is shown in Fig. 1 (left) as the solid line [12]. The contributions of the various components are also indicated, and it is seen that the experimentally observed velocity distribution is consistent with the DM halo hypothesis. Notably, the observed velocity distribution deviates markedly from the naïve expectation based on the visible disk, in particular the radial dependence of the velocity distribution is clearly inconsistent.

One might reasonably suppose that the observed missing mass could be comprised of non-luminous astrophysical bodies composed of normal baryonic matter - such as black holes, neutron stars, brown dwarfs, or rouge planets - collectively referred to as MACHOS (massive compact halo objects). However, whilst these objects certainly

exist, MACHO searches via gravitational microlensing [16] [15] have estimated that their mass contribution is insufficient to account for the total mass density indicated by experimental observations, such as galaxy rotation curves.

Observations of collisions between galaxy clusters have led to further astrophysical anomalies which are attributed to the presence of DM. One famous example is the galaxy cluster 1E0657-558 [13, 14], also known as the *Bullet Cluster*. The Bullet Cluster provides striking evidence for DM, which is encapsulated in Fig. 1 (right). The image combines several pieces of information; the gravitational potential inferred by gravitational lensing is highlighted in blue. The red hue indicates the distribution of hot interstellar gas, as determined by observations of X-ray emissions by the Chandra telescope. It is estimated that such interstellar gas makes up roughly 90% of the visible mass of the galaxy cluster. In the absence of DM one would naturally expect that these regions should coincide, however what is observed is a separation between gravitational and luminous sources. The galaxies and DM of each cluster are essentially collisionless and the motion of these bodies is unimpeded by the collision. In contrast, the hot interstellar gas of each cluster does collide, coalescing in the epicentre, and thus is stripped from the galaxy clusters. Not only does this give compelling empirical evidence for DM, it also puts bounds on the size of the DM self-interaction strength. We shall discuss limits on DM self-interactions further in Chap. 5.

The experimental anomalies discussed above are corroborated by a wealth of further results in astrophysics. In particular, the presence of DM has been inferred in measurements of gravitational lensing (see e.g. [17, 18]), the cosmic microwave background (CMB) [19], and galactic structure formation (see e.g. [20]). Moreover, from these measurements it has been determined that there is roughly five times more DM than baryonic matter in the universe. One might remark that the fact that the present

day DM and baryon densities are comparable is quite curious, and taking this coincidence as a hint of some underlying physical mechanism that sets both of these quantities will be the basis of this thesis, as we shall discuss in the next chapter.

Detailed studies of cosmological structure formation can provide further information on the nature of DM. Density perturbations in the early universe seed structure formation. Notably, if the DM is relativistic then density perturbations at short scales are washed-out, which suppresses small scale structure and, consequently, non-relativistic - *cold* - DM is generally favoured. Relativistic DM is generally in tension with observations; the relevant limits come from the observation of dwarf galaxies which are thought to be formed from density perturbations of ~ 0.1 Mpc [9]. For temperatures above the DM mass (but after the DM is decoupled from the thermal bath, as we shall discuss further below), the DM will escape potential wells and fill under-dense regions, erasing density perturbations smaller than the free streaming length (we use $\hbar = c = k_B = 1$ units)

$$l_F = (1 + z(m_{\rm DM}))l_H \sim \frac{1.66\sqrt{g_*}M_{\rm Pl}}{T_0 m_{\rm DM}} \ , \tag{1.2}$$

where $l_H \sim \frac{M_{\rm Pl}}{m_{\rm DM}^2}$ is the horizon size for $T \sim m_{\rm DM}$, the redshift factor is given by $z(T) = \frac{R_0}{R(T)} - 1$, involving $R(T)$ the cosmic scale factor [9, 10] with $R_0 = R(T_0)$, the present day value, defined at the present temperature $T_0 \simeq 2.73$ K $\simeq 0.23$ meV, and g_* is the number of number of available relativistic degrees of freedom

$$g_* = \sum_{\rm bosons} g_i \left(\frac{T_i}{T}\right)^4 + \frac{7}{8} \sum_{\rm fermions} g_i \left(\frac{T_i}{T}\right)^4 \ , \tag{1.3}$$

where g_i is the number of internal degrees of freedom of the particle. It follows from eq. (1.2) that for thermally produced sub-keV DM density perturbations which lead to dwarf galaxies are erased. Thus the observation of such cosmological structures places

a lower bound on the DM mass (for thermally produced DM)

$$l_F \sim 4 \times 10^{23} \text{ cm} \left(\frac{1 \text{ keV}}{m_{\text{DM}}}\right) \sim 0.1 \text{ Mpc} \left(\frac{1 \text{ keV}}{m_{\text{DM}}}\right) . \tag{1.4}$$

Thus ultra-light ($m_{\text{DM}} \gtrsim$ keV) DM which is highly relativistic - *hot* - is excluded by the observation of dwarf galaxies, also by Lyman alpha forest measurements. However, *warm* DM in the range keV $\lesssim m_{\text{DM}} \lesssim$ MeV, which decouples relativistically but is non-relativistic by radiation-matter equality, is still viable. The conclusion is that either the DM can not be ultra-light, or it must be produced non-thermally, with non-relativistic velocities, such as axion DM [21–24].

1.2 Dark matter production

Having established the empirical case for new non-luminous particle species we next outline the 'freeze-out' picture of how such cosmological DM populations might arise. Consider a population of DM states X which are in thermal equilibrium at temperature T with the visible sector states in the early universe. For simplicity let us assume that the DM has no chemical potential, thus either it is self-conjugate or there is no particle-antiparticle asymmetry between DM and antiDM states. For $T > m_X$ the initial DM number density is set by its thermal distribution $n_X \sim n_\gamma$, where $n_\gamma \propto T^3$ is the number density of photons. We would like to determine the final number density - or *relic density* - which is the quantity that is inferred from observations of the gravitational effects of DM.

If the temperature is much below the DM mass, thermal excitations will not produce DM states and the number density decreases monotonically due to DM pair annihilation to lighter states. As the temperature drops below the DM mass $T < m_X$, and

whilst it remains in equilibrium, its number density is given by a Maxwell-Boltzmann distribution

$$n_X \simeq g_X \left(\frac{m_X T}{2\pi}\right)^{3/2} e^{-m_X/T} \ , \tag{1.5}$$

where g_X is the number of internal degrees of freedom. Once the rate of annihilation Γ drops below the expansion rate of the universe $\Gamma \lesssim H \equiv \frac{1.66\sqrt{g_*}T^2}{M_{\rm Pl}}$ the density of DM states is diluted to the degree that DM pairs rarely meet, and consequently annihilations cease - or *freeze-out*. If particles of a given species are not created or destroyed, then their number density per comoving volume $Y \equiv R^3 n$ is constant. The number density per comoving volume can equivalently be expressed $Y \equiv \frac{n}{s}$ in terms of the entropy density $s = \frac{2\pi^2}{45} g_*^s T^3$, with

$$g_*^s = \sum_{\rm bosons} g_i \left(\frac{T_i}{T}\right)^3 + \frac{7}{8} \sum_{\rm fermions} g_i \left(\frac{T_i}{T}\right)^3 \ . \tag{1.6}$$

For a DM particle created from the thermal bath, the average time before it meets a partner state to annihilate with is

$$\tau = \frac{1}{n_X \langle \sigma v \rangle} \ , \tag{1.7}$$

where σ is the annihilation cross-section and v is the relative velocity of the two states. As discussed above, the DM annihilations freeze-out for $\tau^{-1} \equiv \Gamma \lesssim H$, thus the comoving DM number density becomes constant for

$$H(T_f) \equiv \frac{1.66\sqrt{g_*}T_f^2}{M_{\rm Pl}} = n_X(T_f)\langle \sigma v \rangle \ , \tag{1.8}$$

for T_f the freeze-out temperature, which can be determined for a given model and is characteristically $T_f \sim \frac{m_X}{25}$ (which is only logarithmically sensitive to changes in σ). It

follows that the final DM yield $Y^{(\infty)} \simeq \frac{n_X}{s}\Big|_{T=T_f}$ is given by

$$Y_{\rm FO}^{(\infty)} \sim \frac{1}{M_{\rm Pl}\langle\sigma v\rangle m_X} \ . \tag{1.9}$$

This is illustrated in Fig. 2 and freeze-out is shown in the solid coloured lines, the black line indicates the evolution of the equilibrium (exponentially suppressed) number density, as described by eq. (1.5). Note that increasing the annihilation cross section results in a reduction in the relic density, as indicated by the rightmost arrow in Fig. 2.

An alternative possibility which has recently come to prominence as a general mechanism for DM production is that of DM *freeze-in* [25], based on earlier studies of gravitino production [26]. We outline qualitatively this mechanism for completeness, as it is the only alternative process for thermal production of DM, and also because it shares some features in common with the framework we outline in Chap. 6. In this

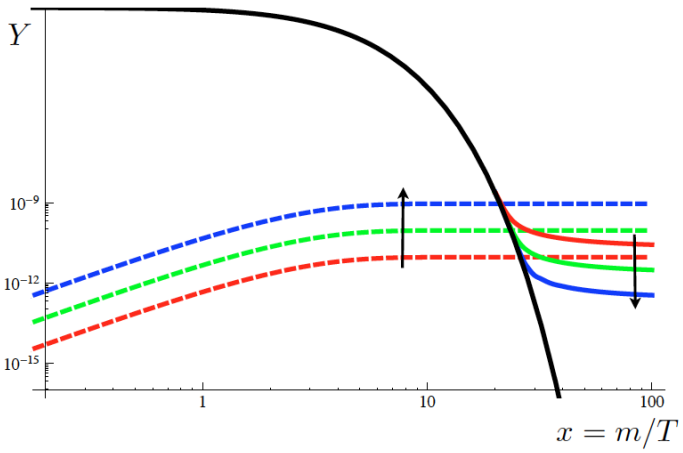

Figure 2. Schematic diagram (from [25]) illustrating the evolution of the DM yield in both freeze-out (solid) and freeze-in (dashed). The black solid line shows the equilibrium yield and the arrows indicate the effect of increasing the coupling strength of the intersector interaction. Note that freeze-out occurs at x ∼20-30, whilst freeze-in is dominated by processes at x ∼2-5.

scenario it is proposed that the DM state X is coupled so feebly to the visible sector that it never reaches thermal equilibrium. It is further assumed that the initial DM abundance is significantly suppressed $n_X \ll n_\gamma$ and in certain constructions the initial DM number density is assumed to be negligible $n_X \approx 0$. Such vanishing initial DM number density may be due to preferential inflaton decay, which does not heat the hidden sector containing the DM.

With the assumption that the hidden sector is significantly colder than the visible sector and, consequently, the DM number density significantly lower than the expected thermal distribution with respect to the visible sector temperature one can study the subsequent thermal evolution due to the feeble connector operator between the two sectors. Processes which connect the thermal bath and the DM can lead to the production of DM states as energy 'leaks' from the visible sector to the hidden sector. For instance let us consider the process $B \to B'X$, involving two states in the visible sector thermal bath B, B'. Parameterising the decay width of B by Γ, which depends on the feeble intersector coupling, it follows that the freeze-in yield at temperature T is parametrically [25]

$$Y_{\rm FI}(T) \sim \frac{M_{\rm Pl} m_B \Gamma}{T^3} \,, \tag{1.10}$$

where m_B is the mass of B. At temperatures significantly above the DM mass the process is suppressed and the operator turns-off once the temperature drops much below the mass of the bath state B, as the number density of B becomes Boltzmann suppressed. This is shown in Fig. 2, where the evolution of the DM comoving number density is given by the coloured dashed lines. Note that the behaviour is opposite to that of freeze-out; with freeze-in there is initially a negligible amount of DM and its yield slowly increases, moreover the evolution of the yield is strongly IR dominated until $T \sim m_B$ is reached and the process switches-off. The parametric expression [25]

for the final DM yield due to freeze-in production is

$$Y_{\rm FI}^{(\infty)} \sim \frac{M_{\rm Pl}\Gamma}{m_B^2} \ . \tag{1.11}$$

Further, whilst in freeze-out increasing the couplings (the annihilation cross section) reduced the DM relic density, with freeze-in larger couplings (i.e. larger Γ) increase the final DM abundance.

Finally, we shall briefly comment on a leading example of non-thermal DM, the QCD axion [21–23]. The axion is well motivated from particle physics, as it is associated to the Peccei-Quinn solution of the strong CP Problem [27]. Specifically, since no symmetries forbid the following term it should be present in the SM Lagrangian

$$\mathcal{L} \supset \frac{\alpha_S}{8\pi}\theta F^{\mu\nu a}\widetilde{F}^a_{\mu\nu} \ , \tag{1.12}$$

where $\widetilde{F}^a_{\mu\nu} = \frac{1}{2}\epsilon^{\mu\nu\sigma\tau}F^a_{\mu\nu}$. However, this term would lead to CP violation in strong interactions and non-observation of such processes constrain $|\theta| < 3 \times 10^{-10}$ [28]. To resolve this apparent conflict with technical naturalness [29], Peccei and Quinn proposed that a spontaneously broken symmetry could be utilised to set $|\theta|$ to zero dynamically. It was subsequently observed by Weinberg and Wilczek [30, 31] that such a mechanism necessarily introduces a new light state, the pseudo-nambo-Goldston boson (PNGB) of the spontaneous broken symmetry. The Weinberg-Wilczek axion, with mass around 10 MeV, was subsequently excluded by experiment, however it has been shown that with further model building PQ-mechanisms with phenomenological acceptable axions can be constructed [32–35].

As the axion has diminutive couplings to photons and baryons, suppressed by the mass scale at which the PQ-symmetry is broken f_a, it can in principle play the role of

DM. Indeed, the interactions between the axion and the SM are so feeble that the axion is never in thermal equilibrium with the visible sector and is not thermally produced. Axion production can proceed via coherent oscillations of the axion field around the minimum of the potential following spontaneous symmetry breaking.

The scale of PQ-breaking and the axion mass are related by $m_a \sim m_\pi f_\pi / f_a$, where f_π and m_π are the mass and decay constant of the pion, respectively. For an axion mass in the range 10^{-6} eV $\lesssim m_a \lesssim 10^{-2}$ eV the observed DM relic density can be reproduced whilst avoiding other astrophysical limits [36, 37]. Although the axion mass is generally expected to be sub-eV, the states are typically produced with small velocities and consequently the free streaming bounds which apply to thermal DM are circumvented. The reader is referred to the review [24] or [9, 10] for further details.

1.3 WIMP dark matter

Next we review the argument for the Weakly Interacting Massive Particles (WIMP) scenario, which is one of the leading frameworks for DM. We begin by observing that the final DM abundance due to thermal freeze-out is parametrically

$$Y_{\rm FO}^{(\infty)} \sim \frac{1}{M_{\rm Pl}\langle\sigma v\rangle m_X} \,. \tag{1.13}$$

Converting the yield (using $\Omega_X h^2 \sim 10^9 \; Y_X \frac{m_X}{\rm GeV}$) and rearranging gives

$$\Omega_X h^2 \sim 0.1 \left(\frac{10^{-26}\ {\rm cm}^3/{\rm s}}{\langle\sigma v\rangle}\right) \,. \tag{1.14}$$

This value of $\langle\sigma v\rangle$, which gives the observed DM relic density $\Omega_{\rm DM} h^2 = 0.1138 \pm 0.0045$ [19], is notable since it is roughly the same order as that expected from particles with

weak gauge interactions

$$\langle \sigma_W v \rangle \simeq G_F^2 T_F^2 \simeq \left(\frac{10^{-5}}{\text{GeV}^2} \right)^2 \left(\frac{m_W}{20} \right)^2 \sim 10^{-26} \text{ cm}^3/\text{s} \, . \tag{1.15}$$

where $G_F \approx 1.2 \times 10^{-5}$ GeV^{-2} is the Fermi constant and we have used the fact that the freeze-out temperature is parametrically $T_F \sim \frac{m}{20}$. Note that the precise cross section will often depend on the DM mass, the masses of other states in the hidden sector, and their couplings, so eq. (1.15) should only be taken as indicative. The coincidence between the weak annihilation cross section with that required to obtain the correct DM relic abundance has been taken as an indication that the DM might be connected with weak scale physics. By comparison to the weak cross section we conclude that for 'weak' couplings and DM masses of 100 GeV - 1 TeV the observed relic abundance can be reproduced.

The WIMP scenario gives intriguing indications that the DM density could be tied to the origin of electroweak symmetry breaking. In particular, it is expected that new physics should enter below the TeV scale in order to resolve the quadratic sensitivity of the Higgs boson mass which enters due the (expected) introduction of high scale physics, generally referred to as the *hierarchy problem*. The leading proposal to solve the hierarchy problem, and for providing a consistent description of physics above the weak scale, is the presence of supersymmetry (SUSY) near the TeV scale (see e.g. [38] for a review). Moreover, SUSY provides a number of additional successes beyond an elegant solution to the hierarchy problem, most prominently, an understanding of electroweak symmetry breaking via radiative corrections [39–41], successful gauge coupling unification [42, 43], and, possibly, a well motivated DM candidate in the form of the lightest SUSY particle (LSP).

In SUSY extensions of the SM the LSP is stable if R-parity $R_p = (-1)^{2s+3(B-L)}$ is conserved, where each particle is assigned an R-parity ± 1 based on its spin s and its global baryon and lepton number charges, B and L. This Z_2 symmetry is partially motivated from the fact that it also forbids several operators which lead to fast proton decay. The SM states are all even under R_p, whereas their superpartners are odd. Thus superpartners must be pair produced and the lightest superpartner is stable. The exact identity of the LSP is rather model dependent, however there are large classes of models in which the LSP is a linear combination of neutral gaugino and Higgsino fields, commonly referred to as the neutralino. Such a neutralino LSP is an appealing candidate for WIMP DM. The mass of the neutralino is expected to be around the weak scale and its couplings are related to the 'weak' couplings by SUSY relations, thus in many instances the neutralino can give the observed DM relic density (see e.g. [44]). Indeed, the fact that SUSY has excellent theoretical motivations, and a natural WIMP candidate, has made it the benchmark for thermal DM in recent years [45].

In the minimal SUSY SM (MSSM) definite predictions can be made about the range of couplings and masses which are permitted for the neutralino. The same couplings which determine the annihilation cross section also enter into the production and scattering cross sections, so in principle the freeze-out hypothesis can be tested by searching for missing energy at colliders or for nuclear scatterings due to WIMPs at DM direct detection experiments. Notably in recent years the sensitivity of direct detection experiments has increased to the level where the WIMP paradigm is starting to be seriously constrained (already scattering by single Z exchange is excluded) and it is expected that within five years much of the WIMP parameter space will have been probed by multiple experiments. Furthermore, one expects the neutralino to be accompanied by superpartners for the other SM fields, however the LHC has now set

stringent bounds on many superparticles [28], in particular new coloured states. As the sparticle masses are pushed higher by LHC searches not only is the SUSY resolution of the hierarchy problem less successful, but also explaining the DM relic density with the neutralino becomes more challenging, as the neutralino mass is forced out of the correct region of parameter space, requiring accidental 'tunings' below the percent level [46–48].

Concurrent with the growing constraints on WIMP DM, and SUSY models in general, there have been several experimental hints for light DM which are hard to accommodate in the WIMP picture. These tentative signals have been observed at DAMA/LIBRA [49, 50], CoGeNT [51], CRESST [52] and CDMS [53], and taken at face value indicate DM with a mass in the region 1-20 GeV. We shall comment on this further in Chap. 7. This has motivated the study of alternative frameworks for DM in which the DM is naturally in this low mass range. Further, one might argue that the WIMP picture fails to resolve perhaps one of the most intriguing puzzles of DM, namely why the DM relic density and the present day baryon density are comparable. The observation that $\Omega_{\rm DM} \simeq 5\Omega_B$ will be one of our leading motivations throughout this thesis. In the next chapter we shall introduce the asymmetric dark matter framework which is motivated by both hints of 1-20 GeV DM, and the desire to explain the proximity of $\Omega_{\rm DM}$ and Ω_B.

2 Asymmetric Dark Matter

This chapter includes excerpts from [1–3].

Asymmetric dark matter [54–124] provides a framework for explaining the existence and comparable magnitudes of the present day baryon density Ω_B and the DM relic density $\Omega_{\rm DM}$. In the standard WIMP picture the origins of Ω_B and $\Omega_{\rm DM}$ are distinct and unrelated. Baryogenesis is conventionally attributed to CP violating processes in baryons or leptons, whilst $\Omega_{\rm DM}$ is assumed to be determined by particle species decoupling from the thermal bath (freeze-out), or out-of-equilibrium species moving towards thermal equilibrium with the visible sector (freeze-in) [25].

A priori, the DM and baryon densities could be different by orders of magnitude and it seems an unreasonable coincidence that they are comparable, particularly given that Ω_B is determined by CP-odd physics, whilst $\Omega_{\rm DM}$ is set by CP-even processes. Consequently, the close proximity $\Omega_{\rm DM} \approx 5\Omega_B$ has motivated a concentrated research effort to construct related genesis mechanisms for baryons and DM, see e.g. [54–65].

2.1 General features

The starting premise for ADM models is relatively simple. Drawing inspiration from the observed matter-antimatter asymmetry which sets the present day baryon density, it has been proposed that the DM relic density could be set by analogous physics. In the SM the proton is perturbatively stable, as it is the lightest particle carrying a conserved (global) baryon number B. In many extensions of the SM, in particular GUT's, we expect that B is violated at some scale, although a linear combination of baryon number and lepton number $B-L$ is preserved (sometimes up to $M_{\rm Pl}$-suppressed effects), indeed

even in the SM B and L are both violated by non-perturbative effects arising from weak gauge interactions. Regardless, as (experimentally) $\tau_p \gtrsim 10^{34}$ s [28], for cosmological purposes the proton can be treated as stable. The fact that the universe contains baryonic matter, and anti-baryons are absent, is indicative of a particle asymmetry in global baryon number. Since baryon annihilations are very efficient, in the absence of an asymmetry the baryon and anti-baryon number densities would both be negligible. The present day baryon density is observed to be $\Omega_b h^2 \approx 0.02$. It follows that the magnitude of the baryon asymmetry must be of order

$$\eta_B \equiv \frac{n_b - n_{\bar{b}}}{n_\gamma} \simeq 10^{-10} \ . \tag{2.1}$$

The asymmetry is sometimes also parameterised in terms of $\Delta_B \equiv \frac{n_\gamma}{s}\eta_B \equiv Y_b - Y_{\bar{b}}$. In the early universe, at some temperature in excess of MeV, an asymmetry must be generated between baryons and antibaryons. This small excess in the number density of baryons over antibaryons is ultimately responsible for the visible matter of the observable universe. As the temperature drops below the proton mass, the number density of (anti)baryons becomes exponentially suppressed, cf. eq. (1.5), and annihilations do not freeze-out until the antibaryon (equilibrium) number density is negligible: $n_{\bar{b}} \sim 10^{-10^5}$. Consequently, n_b is entirely determined by the asymmetry η_B at late times.

One can embark upon a programme to replicate this scenario in the hidden sector and thus set the DM relic density in a similar fashion. Provided the DM mass is not significantly larger than the proton mass (we will discuss the alternative possibility shortly), magnitudes of the baryon and DM asymmetries and masses are related by

$$\frac{\Omega_{\rm DM}}{\Omega_B} \simeq \frac{m_X \eta_{\rm DM}}{m_p \eta_B} \ , \tag{2.2}$$

where $m_p \simeq 0.94$ GeV is the proton mass, and observations indicate that this value should be approximately 5. For the DM to be stable and have a particle-antiparticle asymmetry, in addition to the symmetry which stabilises the state (e.g. Z_2 R-parity), the DM must carry an additional (approximately) conserved quantum number analogous to baryon number, which we denote $\mathscr{X}$. Also, for the DM to have a conserved quantum number it must not be a self-conjugate representation, therefore should be a complex scalar or Dirac fermion. In this framework at low energies $\mathrm{U}(1)_B$ and $\mathrm{U}(1)_{\mathscr{X}}$ are approximate global symmetries of the visible and hidden sector, respectively. However, at higher energies these are no longer good symmetries and only some combination is conserved, for instance $B - L + \mathscr{X}$. This individual violation of B, L and $\mathscr{X}$ allows models to be constructed in which asymmetries in baryon, lepton and DM number are linked, and hence provide the possibility of explaining the relative coincidence of the observed DM and baryon densities.

It is clear from eq. (2.2) that, for judicious choices of DM mass and asymmetry, $\Omega_{\mathrm{DM}} \approx 5\Omega_B$ can be realised. In particular, if the DM asymmetry is a similar magnitude to the baryon asymmetry, then the coincidence of matter densities can be readily explained if the DM mass is similar to the proton mass. Arguably, for the DM-antiDM asymmetry to provide a natural explanation for the close proximity of Ω_{DM} and Ω_B we desire models in which

- The conserved charge of the DM is $\mathcal{O}(1)$ (i.e. comparable to the baryon number of the proton $B = 1$);
- Communication between the hidden and visible sectors should be such that the asymmetries are generated or shared (roughly) equitably;
- The DM mass should be comparable to the proton mass $m_X \sim m_p$.

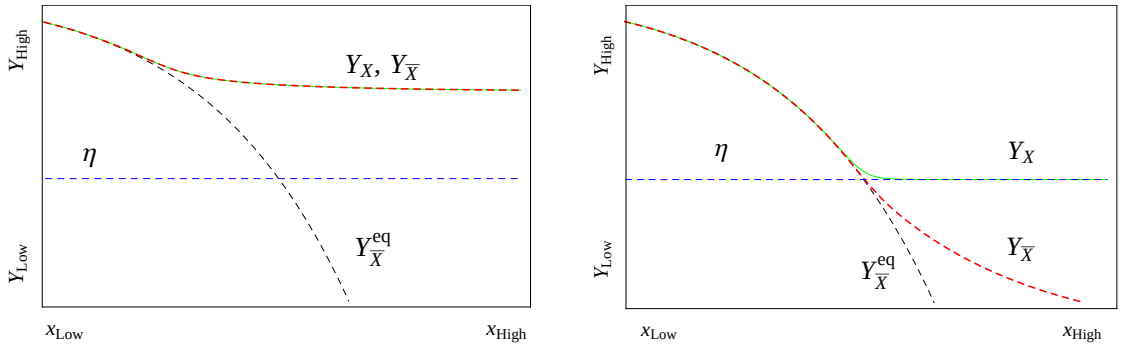

Figure 3. Log plot (from [3]) showing (schematically) Y against $x \propto T^{-1}$. The left panel shows the case where freeze-out happens before the critical temperature, consequently, the asymmetry does not set the final density of X and is comparable to the $\overline{X}$ density. Whereas in the right panel, freeze-out happens after Y_X is set by the asymmetry and $Y_{\overline{X}} \ll Y_X$.

There is some room for variation and changes in one quantity (such as the DM to proton mass ratio) can be absorbed into the other requirements, but the above scenario is the most attractive.

A further requirement on the ADM scenario is that the symmetric component of the DM (the DM-antiDM pairs) must be removed, such that only the residual amount of DM set by the asymmetry determines the relic density. As the asymmetry arises due to CP violating loop-level processes the DM asymmetry is generally suppressed by $\epsilon \sim 10^{-3\pm1}$ relative to the symmetric part. This means that DM annihilations must be efficient, so that the population of $X\overline{X}$ pairs is almost completely annihilated before these interactions freeze-out. This is not an issue for baryon-antibaryon annihilations as the cross section due to the strong force is large; to achieve an analogous removal of the DM symmetric component, the DM annihilation cross section must not be too small. This is illustrated schematically in Fig. 3, which shows the evolution of particle yields. The left panel depicts the case where the DM annihilations are not sufficiently efficient and freeze-out before the asymmetry sets the DM number density, whereas the right panel shows the efficient annihilation scenario in which the $n_{\overline{X}}$ is negligible at late time

and the $n_X \sim \eta_X$. Only the latter case will have the characteristics and phenomenology of ADM. In subsequent chapters we shall discuss this constraint in detail and argue that this provides hints about the likely features of viable ADM models.

2.2 Sharing and cogenesis of particle asymmetries

There is no clear theoretically preferred origin for the observed baryon asymmetry, but a significant number of possible mechanisms have been proposed. As is well known from studies of baryogenesis, in order to generate a particle-antiparticle asymmetry the three Sakharov conditions [125] must be satisfied

- A period of out-of-equilibrium dynamics;
- B-violation;
- C- and CP-violation.

In the ADM framework, there are are several possibilities for the origin of the asymmetries in $\mathscr{X}$ and B. Asymmetries could be generated in any of B, L or $\mathscr{X}$ and subsequently transferred to the other (approximately) conserved quantum numbers. One interesting possibility, which occurs within the SM, is that during the electroweak phase transition (EWPT) non-perturbative sphaleron processes violate $B+L$, although preserve $B-L$, and thus transfer any particle asymmetries between B and L (and vice-versa) [126–128]. Specifically, via a Boltzmann analysis of the evolution of chemical potentials one can derive a relationship between a primordial $B-L$ asymmetry and the asymmetry transferred to B via sphalerons [9, 129] for N_f fermion generations and N_s Higgs doublets

$$B = \frac{8N_f + 4N_s}{22N_f + 13N_s}(B - L) \ . \tag{2.3}$$

For the SM spectrum ($N_f = 3$ and $N_s = 1$), the sharing is around $\sim 35\%$ efficient.

Analogous ADM mechanisms have been proposed in which some primordial asymmetry exists in B, L, or $\mathscr{X}$ and is subsequently shared. This allows for a number of different implementations, for instance, GUT processes can lead to a baryon asymmetry (see e.g. [10]) which can be subsequently transmitted to the DM via some perturbative portal operator [65]. Alternatively, the possibility of generating an L-asymmetry via CP violating decays of heavy right-handed neutrinos with Majorana masses has been studied extensively [130]. It is quite conceivable that an asymmetry in lepton number could then be shared with B and $\mathscr{X}$, possibly via electroweak sphalerons [91], or alternative mechanisms. In particular, this fits well with the expectation of L-violating operators required in the neutrino mass see-saw mechanism involving heavy right-handed neutrinos (see e.g. [131]). Finally, a new scenario for baryogenesis which is possible in models of ADM is that the asymmetry could arise in the hidden sector [76–78] and be subsequently transmitted to the baryons. We shall explore ideas in this direction in Chap. 6.

Alternatively, a more ambitious aim is to construct mechanisms through which the asymmetry in baryons and DM are cogenerated by the same processes. In such *cogenesis* scenarios one assumes that there is no initial asymmetry and that the asymmetries in baryons and DM are simultaneously generated via some out-of-equilibrium CP violating process [120–123]. In certain models of cogenesis the baryon and DM asymmetries are equal and opposite, such that there is no overall asymmetry in the quantity $B - L + \mathscr{X}$. In this case to account for $\Omega_B/\Omega_{\rm DM} \approx 5$, the DM mass m_X must be of similar magnitude to the proton mass. Up to an $\mathcal{O}(1)$ factor, this is also the expected DM mass in ADM models of sharing if the sharing is efficient. Thus 1 GeV $\lesssim m_X \lesssim$ 10 GeV is the preferred ADM mass range and we focus much of our attention on this mass region.

2.3 Aspects of ADM model building

Unlike WIMP DM, in which the neutralino of the MSSM is the benchmark scenario, there is no canonical UV completion for ADM. This is somewhat due to the fact that there is no clear connection between the light (GeV) ADM scale and the (TeV) origin of electroweak symmetry breaking. However, in subsequent chapters we shall argue that the experimental constraints on ADM suggest that the DM could be part of a richer hidden sector and that a simple single state description of ADM is not the correct paradigm. Notably, the visible sector certainly does not exhibit a minimal structure, it features multiple (abelian and non-abelian) gauge interactions and replicated fermion generations, and one might expect that the hidden sector could exhibit an equally complicated spectrum of interacting fields. Arguably, it is questionable to assume that the sector of physics which we have not observed should be significantly simpler than the sector we have. Such a rich hidden sector allows many new possibilities, in particular it is quite plausible that the hidden sector could introduce sufficiently complicated dynamics and large CP violation such that sizeable particle asymmetries can be generated in $\mathscr{X}$.

In the previous section we argued that, for $\eta_{\rm DM}/\eta_B \sim 1$, the natural expectation in ADM models is that the DM mass is comparable to the proton mass, however there is, in fact, another mass range for which $\Omega_{\rm DM} \approx 5\Omega_B$ can be reproduced. For significantly larger DM masses the DM number densities become Boltzmann suppressed and the observed relationship between $\Omega_{\rm DM}$ and Ω_B can be achieved for $m_X \sim$ TeV. However, because this scenario depends on Boltzmann suppression, the DM relic density is exponentially sensitive to changes in parameters. The asymmetries are related to

chemical potentials which enter into the number density, modifying eq. (1.5) as follows

$$n_X \simeq g_X \left(\frac{m_X T}{2\pi}\right)^{3/2} e^{-(m_X-\mu_X)/T}, \qquad n_{\overline{X}} \simeq g_X \left(\frac{m_X T}{2\pi}\right)^{3/2} e^{-(m_X+\mu_X)/T} . \tag{2.4}$$

From which we can express the DM asymmetry in terms of the chemical potential

$$\Delta_X \simeq \frac{n_X - n_{\overline{X}}}{n_X + n_{\overline{X}}} \simeq \tanh\left(\frac{\mu_X}{T}\right) , \tag{2.5}$$

where we have used that in the early universe $n_\gamma \simeq n_X + n_{\overline{X}}$. Further, for temperatures above the proton mass $n_B \simeq n_\gamma \sinh(\mu_B/T)$ and $n_\gamma \sim T^3$, thus for heavy ADM eq. (2.2) is modified

$$\frac{\Omega_{\rm DM}}{\Omega_B} \simeq \frac{m_X(n_X - n_{\overline{X}})}{m_p n_B} \sim \frac{m_X^{5/2}}{T_*^{3/2}} \frac{\eta_X}{\eta_B} e^{-m_X/T_*} , \tag{2.6}$$

where T_* is the temperature at which the operators communicating the asymmetry switch-off, and thus the temperature at which the asymmetry is frozen into both sectors. Supposing, for example, that the asymmetry is transferred by electroweak sphalerons, then $T_* \sim v \simeq 174$ GeV, and hence the observed relationship between the relic densities can be obtained for $m_X \simeq 1.5$ TeV. This result however is exponentially sensitive to both the DM mass m_X and the decoupling temperature T_* and so is less attractive than the standard 1-10 GeV ADM mass range.

The first ADM models were based on this heavy ADM scenario and were proposed in the context of Technicolor extensions of the SM [54–56]. Technicolor is an alternative proposal (to SUSY) for resolving the hierarchy problem (see [132] for a review). It posits that the SM Higgs boson is a fermion bound state under some new gauge symmetry, in which case at some energy near the weak scale the composite nature of the Higgs should be revealed, introducing a UV cutoff to the quadratic sensitivity of the Higgs

mass to high scale physics. The constitute fermion states are light without violating technical naturalness, as they can be protected by a chiral symmetry, similar to the SM fermions. In these models the Higgs boson must be identified with a bosonic bound state (analogous to mesons of hadronic physics) and one also expects fermionic bound states (analogues to the baryons) at comparable energy scales. Further drawing on analogies with hadronic physics, it is quite natural to introduce a global U(1) 'technibaryon' symmetry, hence the technibaryons can carry a conserved quantum number and thus play the role of ADM. As we expect that the fermionic bound states of the model should be at (or above) the scale of the bosonic states, this implies that the stable technibaryons will be heavy (TeV scale) DM, which we have argued is theoretically less appealing, since (multi) TeV ADM requires fine-tuning to provide the correct DM relic density. The first example of light ADM is found in the work of Gelmini, Hall, and Lin [57] (which departs from the Technicolor setting) and such light ADM was then further studied in [58–64]. The recent surge of interest in the ADM scenario can, to some extent, be attributed to a paper of Kaplan, Luty & Zurek [65], which connected this class of models with certain tentative signals in direct detection experiments, and subsequently followed-up by a series of articles by Zurek (and a collection of coauthors) which have studied a myriad of aspects of this subject [67–76].

Without knowledge of the UV completion that describes the connection between the hidden and visible sectors, which should be present to ensure that the baryon and DM asymmetries are comparable, a common approach is to parameterise the physics which connects the visible sector states and the DM via an effective operator description. In particular, the lowest dimension gauge invariant operator in the SM that violates L (but preserves $\mathscr{X} - L$), and thus can provide a portal operator through which an asymmetry can be exchanged between leptons and DM (or vice-versa), is the

(dimension five) Weinberg operator coupled to a scalar DM state ϕ_X: $\phi_X|H^\dagger L|^2$. In the case of fermion DM ψ_X the equivalent operator must be dimension eight in order to preserve Lorentz symmetry. However, for fermion DM there is the dimension six operator $\psi_X u^c d^c d^c$, which allows direct communication between the baryon and DM asymmetries. One might also consider SUSY implementations of ADM. In this case it is expected that SUSY solves the hierarchy problem, however, the LSP can not be the neutralino as it is Majorana, thus self-conjugate, but rather the LSP is a state in the (non-minimal) hidden sector. The number of low dimension portal operators is much greater in the SUSY case since interactions can involve the B and L carrying scalar superpartners of the SM fermions. The lowest dimension B and L violating portal operators are precisely the R_p violating operators of the MSSM coupled to a new DM superfield (which we express below in superfield formalism [38])

$$\boldsymbol{XLH}, \qquad \epsilon_{ij}\boldsymbol{XL}_i\boldsymbol{L}_j\overline{\boldsymbol{E}}, \qquad \boldsymbol{XQL}\overline{\boldsymbol{D}}, \qquad \epsilon_{jk}\boldsymbol{X}\overline{\boldsymbol{U}}_i\overline{\boldsymbol{D}}_j\overline{\boldsymbol{D}}_{\boldsymbol{k}} \ , \tag{2.7}$$

where the indices label generation number. The first three terms of eq. (2.7) connect L and $\mathscr{X}$ numbers, whereas the last operator violates B and $\mathscr{X}$. Being high dimension operators, analogous to the Fermi effective description of weak interactions, in the effective Lagrangian they must be dressed with (an appropriate power of) an inverse mass scale. The mass scale dressing a high dimension operator should be the scale at which the effective description breaks-down, which is parametrically the mass of the heaviest state integrated out in the UV completion from which the operator arises. Notably, the intersector portal operators given above may also be the means by which the symmetric component of the DM annihilates, and this shall be discussed in detail in the next section.

3 The ADM Symmetric Component Problem

This chapter is based on work done in collaboration with John March-Russell and Stephen West, appearing in [1, 2].

In standard theories of baryogenesis an asymmetry η_B is generated between the baryons and anti-baryons which ultimately leads to the visible universe. Due to the strong nuclear force the symmetric component of the baryon density pair-wise annihilates, leaving only a small abundance of baryons set by the asymmetry, and resulting in the matter dominated universe we observe. As discussed in the previous chapter, the ADM framework proposes that the DM undergoes a similar cosmological history to the baryons and that the DM relic density is due to an asymmetry between the DM and its antiparticle. Consequently it is a generic requirement that the vast majority of the symmetric component of the ADM is removed and, thus similar to baryons, the DM must have a relatively large annihilation cross section. We shall denote the DM state X and its anti-particle $\overline{X}$. The forms of the symmetric and asymmetric yields are, respectively

$$\Delta_X \equiv \frac{n_X - n_{\overline{X}}}{s} \ , \qquad\qquad Y_{\rm sym} \equiv \frac{n_X + n_{\overline{X}}}{s} \ . \tag{3.1}$$

As particle asymmetries arise through CP violating loop processes the asymmetric yield is suppressed $\Delta_X \sim \epsilon \, Y_{\rm sym}$, which is typically anticipated to be $\epsilon \lesssim 10^{-2}$.

In principle the DM could annihilate dominantly to either visible sector states or light hidden sector states. As we expect the DM to be 1-10 GeV, if it annihilates to the

visible sector then this likely involves the SM fermions. On the other hand, if the DM X annihilates to light stable hidden sector states Y then the initial energy abundance of the symmetric component will be depleted by the ratio of masses m_Y/m_X. Thus in order for the residual density of X set by the asymmetry to be responsible for $\Omega_{\rm DM}$ it is necessary that there is a sizeable mass splitting between the DM and the light hidden states. This could occur through several mechanism, for instance, the mass of Y could be loop suppressed compared to m_X which provides a sufficient suppression for the relic density of Y to be subdominant provided the CP violating parameter ϵ which relates the symmetric and asymmetric yields is not too small

$$Y_Y \sim \frac{1}{16\pi^2} Y_{\rm sym} \lesssim \Delta_X \sim \epsilon\, Y_{\rm sym}\ . \tag{3.2}$$

Furthermore, light hidden sector vectors and pseudoscalars are very well motivated, the former can arise via a small breaking of a hidden U(1) gauge theory, whilst PNGB occur in many scenarios and are naturally light. On the contrary light hidden sector scalars will suffer from a hierarchy problem analogous to the Higgs and thus are theoretically challenging. Finally, it could be that the light hidden sector states subsequently late decay to the visible sector, this decouples the requirement of efficient annihilation from direct detection limits, however it can potentially lead to signals of energy injection in the early universe.

In this chapter we first we review the standard treatment for calculating the DM relic density in the presence of an asymmetry. Following which we present a comprehensive study of effective operators and compare the requirements for successful ADM models to the experimental limits from direct detection and LHC monojet searches in Sect. 3.2 & 3.3.

3.1 Relic abundance with an asymmetry

The DM asymmetry alters the relic density calculation from the conventional case without an asymmetry. Relic density calculations in the ADM paradigm were recently discussed in [133, 134] and we shall follow these analyses in determining the relic density of the symmetric component. It was found in these previous studies that the annihilation cross section is required to be larger than in the case with no asymmetry. We define the standard variable $x \equiv m/T$, for a particle of mass m at temperature T, and denote by x_f the inverse scaled decoupling temperature of DM and antiDM, assuming that the only $\mathscr{X}$ number changing interactions are pair-annihilations of the DM and its anti-partner. Following [133], the yields for X and $\overline{X}$ in the limit $x \to \infty$ are given by

$$Y_X = \frac{\Delta_X}{1 - \exp\left[-\Delta_X J\omega\right]}, \qquad Y_{\overline{X}} = \frac{\Delta_X}{\exp\left[\Delta_X J\omega\right] - 1}, \tag{3.3}$$

where the quantity ω is defined by

$$\omega = \frac{1}{\sqrt{90}} m_X M_{\rm Pl} \sqrt{g_*} \, . \tag{3.4}$$

and the annihilation integral J is given by

$$J = \int_{x_f}^{\infty} \frac{\langle \sigma v \rangle}{x^2} \, \mathrm{d}x \, . \tag{3.5}$$

Making an expansion of the annihilation cross section (as discussed in Chap. 4, this expansion is not appropriate in the case of light mediators and must be replaced with an alternative analysis and numerical methods)

$$\langle \sigma v \rangle = a + \frac{6b}{x} + \mathcal{O}(x^{-2}), \tag{3.6}$$

allows us to express eq. (3.3) as follows

$$Y_X = \frac{\Delta_X}{1 - \exp\left[-\Delta_X \omega \left(\frac{a}{x_f} + \frac{3b}{x_f^2}\right)\right]}, \qquad Y_{\overline{X}} = \frac{\Delta_X}{\exp\left[\Delta_X \omega \left(\frac{a}{x_f} + \frac{3b}{x_f^2}\right)\right] - 1}. \tag{3.7}$$

Using the tables from DarkSUSY [135] for the temperature dependence of $g_*(T)$, we model the behaviour of x_f via the approximation introduced in [133]

$$x_f = x_{f0}\left(1 + 0.285\frac{a\omega\Delta_X}{x_{f0}^3} + 1.350\frac{b\omega\Delta_X}{x_{f0}^4}\right), \tag{3.8}$$

where x_{f0} is the inverse scaled decoupling temperature in standard freeze-out with no asymmetry. The present relic density is given by

$$\Omega_{\rm DM}h^2 = 2.76 \times 10^8 \left(\Delta_X + Y_{\rm sym}\right)\left(\frac{m_X}{\rm GeV}\right), \tag{3.9}$$

where $h = 69.32 \pm 0.8$ kms^{-1}Mpc^{-1} is the Hubble constant [19]. In the limit $\Delta_X \to 0$, one recovers the standard symmetric DM expressions. In order to realise the requirement that the asymmetric component constitutes the majority of the present relic density, we demand that the symmetric component composes $\leq 1\%$ of the relic density, via the constraint

$$Y_{\rm sym} \leq \frac{1}{100} \times \frac{\Omega_{\rm DM}h^2}{2.76 \times 10^8}\left(\frac{\rm GeV}{m_X}\right). \tag{3.10}$$

Varying the constraint on the symmetric component in a wide range around 1% does not materially affect our conclusions concerning the required annihilation cross section.

3.2 Effective operator connecting dark matter to quarks

Whilst we have commented on possible sources for the DM asymmetry in Chap. 2, for much of this thesis we shall remain agnostic as to its precise origin. Specifically, in this chapter we shall focus on a general feature of ADM from which model independent bounds can be derived. DM annihilation is more efficient for larger values of the inter-sector couplings, however it is precisely these inter-sector couplings which are constrained through direct detection and collider searches. Hence, the need for efficient annihilation results in a tension between cosmological requirements and direct search constraints. Generically, the symmetric part of the DM will be several orders of magnitude larger than the asymmetric component, as the ratio of asymmetric to symmetric DM is of comparable magnitude to the CP violating parameter determining the asymmetry and is typically $\lesssim 10^{-3}$. As a result, these constraints are sufficiently strong to rule out large regions of parameter space.

Since momentum transfer is low in direct detection experiments, mediators with masses ~ 100 MeV or greater are sufficiently heavy to be integrated out. Consequently the variety of portal interactions between the hidden and visible sectors may be parameterised via effective contact operators. We shall demonstrate that the current experimental limits exclude ADM models in which the DM couples to SM quarks with minimal flavour structure via a heavy mediator, for 1 GeV $\lesssim m_X \lesssim$ 100 GeV. However, effective operators do not provide a good description of the collider limits and the relic density calculation for mediators with masses $\lesssim 100$ GeV and, hence, in Chap. 4 we examine the effects of such light mediators.

In Table 1 we list all effective operators up to dimension six connecting SM quarks f to complex scalar ϕ or Dirac fermion ψ DM. Note that $\sigma^{\mu\nu} = \frac{i}{2}(\gamma^\mu\gamma^\nu - \gamma^\nu\gamma^\mu)$ and since $\sigma^{\mu\nu}\gamma^5 = \frac{i}{2}\epsilon^{\mu\nu\rho\sigma}\sigma_{\rho\sigma}$, the operators $\overline{\psi}i\sigma^{\mu\nu}\gamma^5\psi\overline{f}\sigma_{\mu\nu}f$ and $\overline{\psi}\sigma^{\mu\nu}\psi\overline{f}\sigma_{\mu\nu}f$ are equivalent

$\Delta\mathscr{L}$		Int.	Suppression
$\mathcal{O}_s^\phi$:	$\frac{1}{\Lambda}\phi^\dagger\phi\overline{f}f$	SI	1
$\mathcal{O}_v^\phi$:	$\frac{1}{\Lambda^2}\phi^\dagger\partial^\mu\phi\overline{f}\gamma_\mu f$	SI	1
$\mathcal{O}_{va}^\phi$:	$\frac{1}{\Lambda^2}\phi^\dagger\partial^\mu\phi\overline{f}\gamma_\mu\gamma^5 f$	SD	v^2
$\mathcal{O}_p^\phi$:	$\frac{1}{\Lambda}\phi^\dagger\phi\overline{f}i\gamma^5 f$	SD	q^2
$\mathcal{O}_s^\psi$:	$\frac{1}{\Lambda^2}\overline{\psi}\psi\overline{f}f$	SI	1
$\mathcal{O}_v^\psi$:	$\frac{1}{\Lambda^2}\overline{\psi}\gamma^\mu\psi\overline{f}\gamma_\mu f$	SI	1
$\mathcal{O}_a^\psi$:	$\frac{1}{\Lambda^2}\overline{\psi}\gamma^\mu\gamma^5\psi\overline{f}\gamma_\mu\gamma^5 f$	SD	1
$\mathcal{O}_t^\psi$:	$\frac{1}{\Lambda^2}\overline{\psi}\sigma^{\mu\nu}\psi\overline{f}\sigma_{\mu\nu}f$	SD	1
$\mathcal{O}_p^\psi$:	$\frac{1}{\Lambda^2}\overline{\psi}\gamma^5\psi\overline{f}\gamma^5 f$	SD	q^4
$\mathcal{O}_{va}^\psi$:	$\frac{1}{\Lambda^2}\overline{\psi}\gamma^\mu\psi\overline{f}\gamma_\mu\gamma^5 f$	SD	v^2, q^2
$\mathcal{O}_{pt}^\psi$:	$\frac{1}{\Lambda^2}\overline{\psi}i\sigma^{\mu\nu}\gamma^5\psi\overline{f}\sigma_{\mu\nu}f$	SI	q^2
$\mathcal{O}_{ps}^\psi$:	$\frac{1}{\Lambda^2}\overline{\psi}i\gamma^5\psi\overline{f}f$	SI	q^2
$\mathcal{O}_{sp}^\psi$:	$\frac{1}{\Lambda^2}\overline{\psi}\psi\overline{f}i\gamma^5 f$	SD	q^2
$\mathcal{O}_{av}^\psi$:	$\frac{1}{\Lambda^2}\overline{\psi}\gamma^\mu\gamma^5\psi\overline{f}\gamma_\mu f$	SI	v^2
		SD	q^2
$\hat{\mathcal{O}}_s^\phi$:	$\frac{m_q}{\Lambda^2}\phi^\dagger\phi\overline{f}f$	SI	1
$\hat{\mathcal{O}}_s^\psi$:	$\frac{m_q}{\Lambda^3}\overline{\psi}\psi\overline{f}f$	SI	1
$\hat{\mathcal{O}}_p^\psi$:	$\frac{m_q}{\Lambda^3}\overline{\psi}\gamma^5\psi\overline{f}\gamma^5 f$	SD	q^4

Table 1. Set of effective operators $\mathcal{O}$ of dimension six or less connecting SM quarks f to scalar ϕ or fermion ψ DM with universal couplings. We consider three additional natural contact operators $\hat{\mathcal{O}}$ with quark mass dependent couplings, note $\hat{\mathcal{O}} \equiv \frac{m_q}{\Lambda}\mathcal{O}$. It is indicated whether the corresponding direct detection cross section is DM velocity v or momentum transfer q suppressed and if the interaction couples to nuclei in a spin-dependent (SD) or independent (SI) manner [136].

to $\overline{\psi}i\sigma^{\mu\nu}\psi\overline{f}\sigma_{\mu\nu}\gamma^5 f$ and $\overline{\psi}\sigma^{\mu\nu}\gamma^5\psi\overline{f}\sigma_{\mu\nu}\gamma^5 f$, respectively. For definitiveness and to avoid stringent flavour-changing constraints we will typically assume that the contact operators couple universally to all quark flavours. In the case of scalar and pseudoscalar interactions we shall also study the case where the effective coupling to SM quarks is proportional to the relevant quark mass, which is arguably more natural, and we denote these m_q-dependent operators $\hat{\mathcal{O}} \equiv \frac{m_q}{\Lambda}\mathcal{O}$. Operators $\mathcal{O}_p^\phi$, $\mathcal{O}_{pt}^\psi$, $\mathcal{O}_{ps}^\psi$ and $\mathcal{O}_{sp}^\psi$ correspond to CP violating interactions and one might expect their coefficients to be suppressed relative to those of the other, CP conserving, operators, consequently we shall typically omit analysis of these contact interactions for brevity. We have checked that the requirements for efficient annihilation of the symmetric component and experimental limits for these CP violating operators are comparable to examples which will be presented in detail.

The direct detection cross section of certain operators are suppressed by the small DM velocity $v \sim 10^{-3}c$ or momentum transfer $|q| = |p_i - p_f| \lesssim 0.1$ GeV. For operators with suppressed scattering cross sections the current direct detection limits are insufficient to provide any useful constraints on the DM over the whole mass range. However, the high energy production cross sections remain unsuppressed and, consequently, monojet searches provide the leading limits on such operators. Approaches based on effective operators have been employed previously to study the constraints from direct detection and colliders on conventional DM models [68, 136–147], however, the existence of an asymmetry in the hidden sector leads to deviations in the relic density calculations [148].

Whilst there have been previous works on contact operators in the context of ADM [70, 149], in the case of the former the effects of the DM asymmetry are not fully accounted for, while the latter work considers only a limited selection of possible

operators. In the present work we consider the full set of contact operators (correcting some numerical errors contained in previous works) and update the experimental constraints from both direct detection and LHC monojet searches, in particular using the 2012 CMS analysis with 4.67fb^{-1}. Moreover, in subsequent chapters, we go beyond the contact operator analysis and demonstrate that if the DM is connected to SM quarks via exchange of a light mediator state then resonance and threshold effects become very important in determining the exclusion limits.

As remarked previously, if the DM annihilates directly to SM quarks then there is a tension between the efficient removal of the symmetric component and experimental searches. However, if the DM is embedded into a richer hidden sector, with a spectrum of lighter states into which the symmetric component can annihilate (which later decay to the visible sector), then this severs the connection between direct search constraints and cosmological requirements. As we show, effective theories of ADM with $m_X \sim m_p$ and minimal flavour structure which decay directly to SM quarks are excluded for all types of connector operator, this leads to the striking conclusion that in order to realise ADM naturally, the DM must generally be accompanied by additional hidden states of comparable mass or lighter, either to mediate the interactions to the visible sector, or into which the symmetric component of the DM may annihilate. The fact that ADM must be part of a larger hidden sector is an important realisation, since this will generally lead to significant changes to the cosmology and phenomenology, which we shall address in later chapters.

The annihilation cross sections for the operators in Table 1 connecting fermion DM

and SM quarks to $\mathcal{O}(v^2)$ are[1]

$$\sigma^{\mathcal{O}_s^\psi}_{\rm An} v = \frac{3v^2 m_X^2}{8\pi\Lambda^4}\sum_q \left(1-\frac{m_q^2}{m_X^2}\right)^{3/2},$$

$$\sigma^{\mathcal{O}_v^\psi}_{\rm An} v = \frac{3m_X^2}{2\pi\Lambda^4}\sum_q \left(1-\frac{m_q^2}{m_X^2}\right)^{1/2}\left[\left(2+\frac{m_q^2}{m_X^2}\right)+v^2\left(\frac{8m_X^4-4m_q^2m_X^2+5m_q^4}{24m_X^2(m_X^2-m_q^2)}\right)\right],$$

$$\sigma^{\mathcal{O}_a^\psi}_{\rm An} v = \frac{3m_X^2}{2\pi\Lambda^4}\sum_q \left(1-\frac{m_q^2}{m_X^2}\right)^{1/2}\left[\frac{m_q^2}{m_X^2}+v^2\left(\frac{8m_X^4-22m_q^2m_X^2+17m_q^4}{24m_X^2(m_X^2-m_q^2)}\right)\right],$$

$$\sigma^{\mathcal{O}_t^\psi}_{\rm An} v = \frac{6m_X^2}{\pi\Lambda^4}\sum_q \left(1-\frac{m_q^2}{m_X^2}\right)^{1/2}\left[\left(1+2\frac{m_q^2}{m_X^2}\right)+v^2\left(\frac{4m_X^4-11m_X^2m_q^2+16m_q^2)}{24m_X^2(m_X^2-m_q^2)}\right)\right],$$

$$\sigma^{\mathcal{O}_p^\psi}_{\rm An} v = \frac{3m_X^2}{2\pi\Lambda^4}\sum_q \left(1-\frac{m_q^2}{m_X^2}\right)^{1/2}\left[1+\frac{v^2}{8}\left(\frac{2m_X^2-m_q^2}{m_X^2-m_q^2}\right)\right],$$

$$\sigma^{\mathcal{O}_{av}^\psi}_{\rm An} v = \frac{v^2 m_X^2}{4\pi\Lambda^4}\sum_q \left(1-\frac{m_q^2}{m_X^2}\right)^{1/2}\left(2+\frac{m_q^2}{m_X^2}\right),$$

$$\sigma^{\mathcal{O}_{pt}^\psi}_{\rm An} v = \frac{6m_X^2}{\pi\Lambda^4}\sum_q \left(1-\frac{m_q^2}{m_X^2}\right)^{1/2}\left[\left(1-\frac{m_q^2}{m_X^2}\right)+\frac{v^2}{24}\left(4+11\frac{m_q^2}{m_X^2}\right)\right],$$

$$\sigma^{\mathcal{O}_{va}^\psi}_{\rm An} v = \frac{3m_X^2}{\pi\Lambda^4}\sum_q \left(1-\frac{m_q^2}{m_X^2}\right)^{1/2}\left[\left(1-\frac{m_q^2}{m_X^2}\right)+\frac{v^2}{24}\left(4+5\frac{m_q^2}{m_X^2}\right)\right],$$

[1] These expressions correct previous errors in the literature and have been checked both by hand and with `Feyncalc` [150].

while the annihilation cross sections for operators with scalar DM are

$$\sigma^{\mathcal{O}_s^\phi}_{\rm An} v = \frac{3}{4\pi\Lambda^2}\sum_q \left(1-\frac{m_q^2}{m_X^2}\right)^{1/2}\left[\left(1-\frac{m_q^2}{m_X^2}\right)+\frac{3v^2}{8}\frac{m_q^2}{m_X^2}\right],$$

$$\sigma^{\mathcal{O}_v^\phi}_{\rm An} v = \frac{v^2 m_X^2}{4\pi\Lambda^4}\sum_q \left(1-\frac{m_q^2}{m_X^2}\right)^{1/2}\left(2+\frac{m_q^2}{m_X^2}\right),$$

$$\sigma^{\mathcal{O}_{va}^\phi}_{\rm An} v = \frac{3m_X^2}{\pi\Lambda^4}\sum_q \left(1-\frac{m_q^2}{m_X^2}\right)^{1/2}\left[\frac{m_q^2}{m_X^2}+\frac{v^2(7m_q^4-8m_q^2m_X^2+4m_X)}{24m_X^2(m_X^2-m_q^2)}\right].$$

In the above, the cross sections corresponding to scalar or pseudoscalar interactions ($\mathcal{O}_s^\psi$, $\mathcal{O}_p^\psi$ and $\mathcal{O}_s^\phi$) have been provided for the case of universal coupling, the cross sections for the m_q-dependent couplings may be obtained by multiplying the cross section (under the summation) by a factor of m_q^2/Λ^2. To illustrate that the omitted CP violating operators are comparable to the CP conserving interactions we have included the operator $\mathcal{O}_{pt}^\psi$.

These expressions are used to derive the maximum value of the scale Λ permitted to ensure a suitable depletion of the symmetric component for each operator as a function of m_X, where we assume that only one operator is turned on at a time. Imposing the constraint on the symmetric abundance, eq. (3.10), the results obtained are presented graphically in Fig. 5-7. The black curves present upper bounds for Λ for each operator as a function of m_X. The resulting relic density curves may then be constrained through direct detection and collider limits, which we derive in the next section.

3.3 Direct search constraints on contact operators

The constraints on each contact operator in Table 1 depend strongly on whether the corresponding scattering cross section is spin-independent or spin-dependent. If the

scattering cross section is suppressed by powers of v or q then direct detection limits are severely weakened and, in fact, in all cases do not present any significant constraint on the allowed DM mass range. Rather, for the suppressed operators the leading bounds come from collider monojet searches, which we shall discuss shortly.

The cross section for spin-independent elastic scattering of Dirac fermion DM on a target nuclei, with atomic mass A and atomic number Z, at zero momentum transfer is given by [44, 140]

$$\sigma_{SI}^{N_f} = \frac{1}{\pi}\mu_N^2 \left[Z f_p + (A-Z) f_n\right]^2 \ , \tag{3.11}$$

where $\mu_N = \frac{M_X m_N}{(M_X + m_N)}$ is the nucleus-DM reduced mass and $f_{p,n}$ are effective couplings to protons and neutrons. If the DM is instead a complex scalar then this relation is modified

$$\sigma_{SI}^{N_s} = \frac{1}{4\pi}\frac{\mu_N^2}{m_X^2} \left[Z f_p + (A-Z) f_n\right]^2 \ . \tag{3.12}$$

In eq. (3.11) & (3.12) we have expressed the effective couplings to the nucleus in terms of the effective coupling $f_{n,p}$ to nucleons. In turn the couplings $f_{n,p}$ may be expressed in terms of the underlying DM-quark couplings, but this relation is dependent on the nature of the mediator.

If the DM-quark interaction is mediated via a scalar field then [140]

$$f_{p,n} = \sum_{q=u,d,s} G_q f_{Tq}^{(p,n)} \frac{m_{p,n}}{m_q} + \frac{2}{27} f_{TG}^{(p,n)} \sum_{q=c,b,t} G_q \frac{m_{p,n}}{m_q} \ , \tag{3.13}$$

where G_q denotes the effective coupling of the DM to a given quark species. The terms containing $f_{T_q}^{(p,n)}$ describe contributions to the cross section from scattering off light quarks and are proportional to the matrix element of quarks in a nucleon, $f_{T_q}^{(p,n)} \propto \langle \overline{q} q \rangle$.

These $f_{T_q}^{(p,n)}$ have been experimentally determined to have the following values [151]

$$\begin{aligned} f_{Tu}^{p} &= 0.020 \pm 0.004, \quad & f_{Tu}^{n} &= 0.014 \pm 0.003, \\ f_{Td}^{p} &= 0.026 \pm 0.005, \quad & f_{Td}^{n} &= 0.036 \pm 0.008, \\ f_{Ts}^{p} &= 0.118 \pm 0.062, \quad & f_{Ts}^{n} &= 0.118 \pm 0.062. \end{aligned} \tag{3.14}$$

The term containing $f_{TG}^{(p,n)} \equiv 1 - \sum_{u,d,s} f_{Tq}^{(p,n)}$ describes gluon interactions through a heavy quark loops and is approximately 0.84 for protons and 0.83 for neutrons.

On the other hand, if the mediator is a vector field then the contribution from the heavy quarks may be neglected, and the effective nucleon coupling simplifies to

$$f_p = 2G_u + G_d, \quad f_n = G_u + 2G_d. \tag{3.15}$$

The spin-independent scattering cross section per nucleon $\sigma_{SI}^{s,f}$ is given by

$$\sigma_{SI}^{s,f} \approx \frac{1}{A^2} \frac{\mu_p^2}{\mu_N^2} \sigma_{SI}^{N_{s,f}} \ , \tag{3.16}$$

where μ_p is the proton-DM reduced mass. The scattering cross section per nucleon for each of the non-suppressed spin-independent interactions under consideration which couple universally to SM quarks[2] are given by [44, 68]

$$\begin{aligned} \sigma_{\rm SI}^{\mathcal{O}_s^\phi} &\approx \frac{1}{4\pi\Lambda^2} \frac{\mu_p^2}{m_X^2} f_p^2 \ , & \sigma_{\rm SI}^{\mathcal{O}_v^\phi} &\approx \frac{9}{4\pi\Lambda^4} \mu_p^2 \ , \\ \sigma_{\rm SI}^{\mathcal{O}_s^\psi} &\approx \frac{1}{\pi\Lambda^4} \mu_p^2 f_p^2 \ , & \sigma_{\rm SI}^{\mathcal{O}_v^\psi} &\approx \frac{9}{\pi\Lambda^4} \mu_p^2 \ . \end{aligned} \tag{3.17}$$

where $\mu_p = \frac{m_X m_p}{(m_X + m_p)}$ is the nucleon-DM reduced mass and f_p is the DM effective

[2] SI cross section of operators which couple proportional to m_q may be obtained by suitable rescalings; where we have assumed that $f_n \approx f_p$.

couplings to protons. For consistency with later calculations, we use the default values for the factor f_p from `micrOMEGAs` [152] which are consistent with eq. (3.14).

Additionally, the non-suppressed scattering cross sections for the spin-dependent operators of interest are given by [137, 140]

$$\sigma_{\rm SD}^{\mathcal{O}_t^\psi} \simeq 4 \times \sigma_{\rm SD}^{\mathcal{O}_a^\psi} \simeq \frac{16}{\pi \Lambda^4} \mu_p^2 \left(\sum_q \Delta_q^p \right)^2 . \tag{3.18}$$

where the coefficients $\Delta_q^{p,n}$ parameterise the matrix element of the axial (tensorial) current in the nucleon and we use the values derived in [153] from the COMPASS results [154]:

$$\left(\sum_q \Delta_q^p \right)^2 \approx 0.32 . \tag{3.19}$$

Note that in the non-relativistic limit the form of the tensor operators $\overline{q}\sigma^{\mu\nu}q$ coincides with the axial-vector operator $\overline{q}\gamma^\mu\gamma^5 q$ up to a numerical factor [139]. From the scattering cross sections given above we can use the current direct detection limits to place a lower bound on the scale Λ.

The lower bounds placed on Λ by direct detection are displayed in Fig. 5-7 as solid coloured curves. The leading limits (as of March 2012) on spin-independent interactions from direct detection experiments for $m_X \lesssim 1$ GeV come from CRESST [155] (orange), while in the intermediate mass range 1 GeV$\leq m_X \leq$10 GeV the dominant constraints come from a combination of Xenon10 [156] (green) CDMS [157] (cyan) and DAMIC [158] (magenta). For $m_X > 10$ GeV the leading spin-independent limits are provided by the Xenon100 experiment [45] (blue). The strongest direct detection constraints on spin-dependent interactions are from Simple [159] (Stage 2: light purple; Combined: dark purple) for $m_X > 5$ GeV and from CRESST [155] for lighter DM.

A complementary set of constraints on interactions between SM quarks and DM

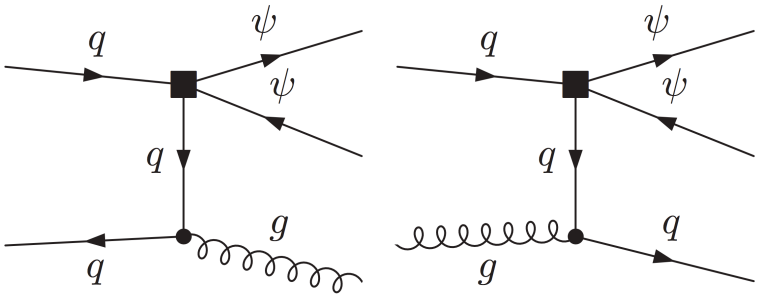

Figure 4. Examples of tree-level monojet events, the square box indicates the presence of a dimension six operator connecting DM ψ to SM quarks q (generated with `FeynArts` [162]).

comes from collider experiments, in particular the recent LHC searches for jets and missing energy [160, 161]. Signals which pass the experimental cuts (detailed shortly) correspond to events with a (relatively-hard) jet as initial state radiation and a subsequent annihilation to DM, as depicted in Fig. 4. Note that LHC monophoton searches provide slightly weaker bounds to those from monojets [161]. Operating at $\sqrt{s} = 7$ TeV, the ATLAS and CMS collaborations reported no apparent excess in the production of jets and missing energy with an integrated luminosity of 1fb^{-1} and 4.67fb^{-1}, respectively. The high p_T ATLAS analysis [160] selected events with a primary jet with $p_T > 250$ GeV and pseudorapidity $|\eta| < 2$, and $\not{E}_T > 220$ GeV, events with a secondary jet with $p_T < 60$ GeV and $|\eta| < 4.5$ were also permitted. The collaboration reported $N_{\text{obs}} = 965$ events. The SM prediction for this process is $N_{\text{SM}} \pm \sigma^2_{\text{SM}} = 1010 \pm 75$ events. Using a χ^2 analysis, following [144], limits (90%CL) may be placed on the total number of signal events N_{DM} consistent with null collider searches by requiring that

$$\chi^2 \equiv \frac{\left(N_{\text{obs}} - N_{\text{SM}} - N_{\text{DM}}(m_X, \Lambda)\right)^2}{N_{\text{DM}}(m_X, \Lambda) + N_{\text{SM}} + \sigma^2_{\text{SM}}} = 2.71 \ . \tag{3.20}$$

Subsequently, the maximum number of signal events N_{DM} can be converted into a

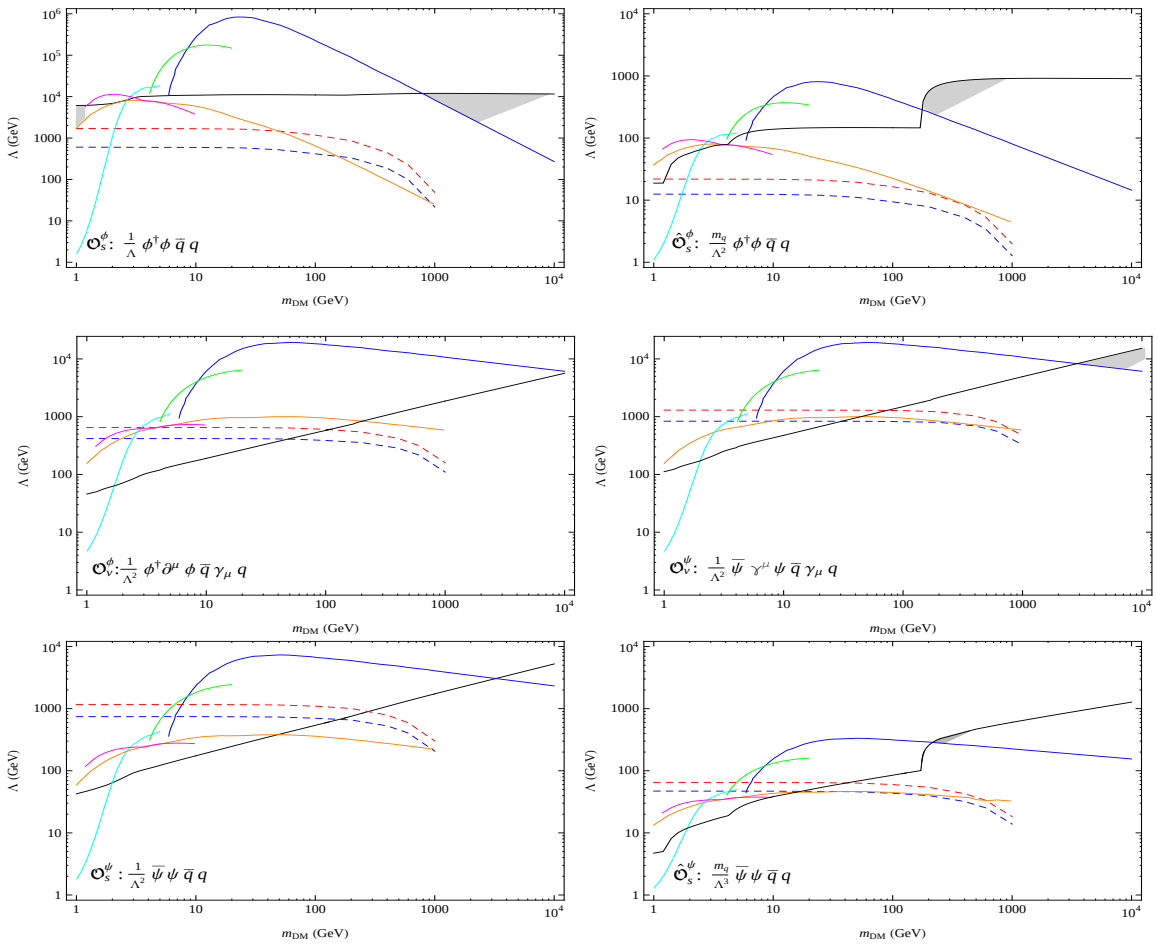

Figure 5. Limits on the scale Λ for the effective operators from direct detection and monojets for scalar DM ϕ and fermion DM ψ, as a function of DM mass $m_{\rm DM}$. The black curve corresponds to the minimum annihilation cross section necessary to reduce the symmetric component to 1%. Constraints are from Xenon100 (blue), Xenon10 (green), CDMS (cyan), CRESST (orange), DAMIC (magenta) and ATLAS $1\,\text{fb}^{-1}$ (red, dashed) and CMS $4.67\,\text{fb}^{-1}$ (blue, dashed) monojet searches. For $m_{\rm DM} \gtrsim \Lambda$ effective operators no longer provide a good description and can not be reliably used to calculate the relic density requirements. Moreover, the monojet limits are no longer reliable much below $\Lambda \lesssim 100$ GeV due to the experimental cuts employed by ATLAS and CMS. Viable models of ADM employing the listed effective operators must lie in the shaded parameter regions. Note that contact operators due to scalar mediators are studied for both universal couplings to quarks and m_q-dependent couplings. We see that, except for the operator $\frac{1}{\Lambda}\phi^\dagger\phi\bar{q}q$ around $m_{\rm DM} \approx 1$ GeV, successful models of ADM involving contact operators are excluded for 1 GeV $\lesssim m_{\rm DM} \lesssim 100$ GeV, which includes the range in which ADM is most well motivated.

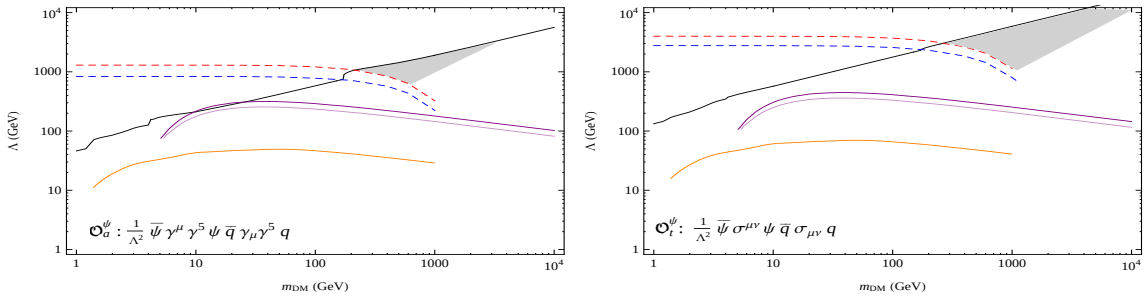

Figure 6. Limits on Λ for operators with spin-dependent direct detection cross sections, viable regions are shaded. Constraints from Simple (Stage 2: light purple; Combined: dark purple), CRESST (orange), ATLAS $1\,\text{fb}^{-1}$ (red, dashed) and CMS $4.67\,\text{fb}^{-1}$ (blue, dashed).

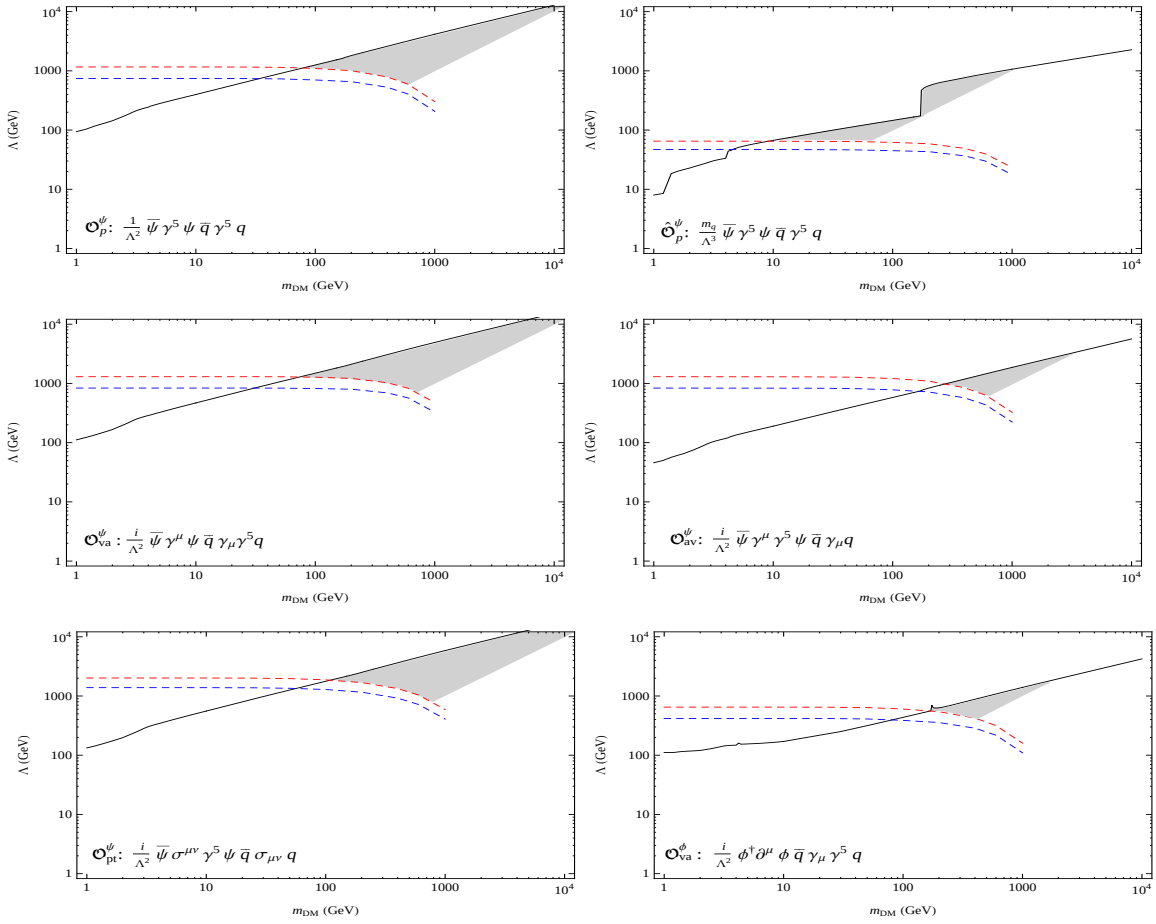

Figure 7. Limits on Λ for operators with v or q suppressed direct detection cross sections, viable parameter regions are shaded. Limits are from ATLAS $1\,\text{fb}^{-1}$ (red, dashed) and CMS $4.67\,\text{fb}^{-1}$ (blue, dashed). The interesting ADM range $m_{\rm DM} \lesssim 10$ GeV is excluded in all cases and, with the exception of the $\frac{m_q}{\Lambda^3}\overline{\psi}\gamma^5\psi\overline{q}\gamma^5 q$ operator, the exclusion is up to $m_{\rm DM} \lesssim 100$ GeV.

limit on the cross section via $N_{\rm DM} = \Delta\sigma \int \mathcal{L}$, where $\int \mathcal{L}$ is the integrated luminosity. From this it follows that the ATLAS null result excludes any new contributions to the production cross section greater than 0.01 pb.

The ATLAS monojet searches have been previously used to place limits on certain models of standard symmetric DM [143–147]. Here we use the LHC monojet bounds to derive constraints on contact interactions between SM and DM states for the ADM scenario and employ the most recent results. The recent CMS search [161] excludes new contributions to the production cross section greater than 0.02 pb and presents a comparable set of constraints to the ATLAS 1 fb^{-1} limits. The CMS analysis considered events with a primary jet with $p_T > 110$ GeV and pseudorapidity $|\eta| < 2.4$, and $\not{E}_T > 350$ GeV, they also allowed events with a secondary jet with $p_T > 30$ GeV, provided the azimuth angle difference of the jets satisfied $\Delta\varphi < 2.5$. CMS observed 1142 events in good agreement with the SM prediction of 1224 ± 101 events.

To calculate the limits on contact operators coupling DM to quarks, we use the program `CalcHEP` [163]. The SM Lagrangian is supplemented with each operator in separate instances and we study the total cross section $pp \to j\overline{X}X$ where X is the DM state and j is a jet. To model the ATLAS search we apply the following cuts on the events $\not{E}_T > 220$ GeV, $p_T > 250$ GeV, and pseudorapidity $|\eta| < 2$ and for CMS we take $\not{E}_T > 350$ GeV, $p_T > 110$ GeV, and pseudorapidity $|\eta| < 2.4$. We do not consider events with additional jets, hadronisation, or parton showering, it has been argued [164, 165] that the latter two simplifications are justified as the primary jet p_T is unaffected by these processes. With these cuts we may reliably assume that the efficiency of the searches is close to 100%. For each operator we determine the minimum value of Λ for which the new contribution to the production cross section is permitted by monojet searches. Since the contact operators are generally suppressed by multiple

powers of Λ, $\mathcal{O}(1)$ changes to the cross section result in only small deviations in the limit on the scale Λ. The resulting limits are plotted in Fig. 5-7 as dashed blue (CMS) and red (ATLAS) curves and supplement the constraints from direct detection.

For $m_X \gtrsim \Lambda$ the contact operators no longer give a good description and one is required to consider the UV completion of the effective theory. Similarly, collider searches do not provide reliable limits on the effective operators if the monojet bound on Λ is comparable to LHC energies, in particular if Λ falls below the p_T cut ~ 100 GeV. This is the case with the operator $\frac{m_q}{\Lambda^2}\phi\phi^\dagger\bar{q}q$, and the fermion DM, scalar and pseudoscalar m_q-dependent operator monojet bounds are close to the limit at which the effective theory breaks down. Consequently, these portal interactions should really be studied in the light mediator regime, which we discuss in detail in Chap. 4. Note, however, that the Tevatron monojet searches utilise much lower momentum cuts, requiring a primary jet with $p_T > 10$ GeV, $|\eta| < 1.1$, and $\not{E}_T > 60$ GeV (90% efficiency), and thus the contact operator description for monojet searches are reliable for $\Lambda \gtrsim 10$ GeV. Moreover, results from CDF [166] lead to constraints which are roughly comparable to the CMS limits for 1 GeV $\lesssim m_X \lesssim 10$ GeV.

To correctly interpret Fig. 5-7, recall that the black curves provide an upper bound on Λ to ensure suitably efficient annihilation of the symmetric component, whilst the coloured curves present lower bounds from searches. A given operator may present a viable ADM model only if there exists some mass region for which a sufficiently low Λ has not been excluded by direct search constraints. It is immediately apparent that there exists a tension between the experimental constraints and the upper bound on Λ required for the efficient annihilation of the symmetric component in all models with heavy mediators.

As argued earlier, the most natural mass range for ADM is 1 GeV $\lesssim m_X \lesssim 10$ GeV

and from the plots in Fig. 5-7 we see that essentially no operators are viable in this preferred mass range. For scalar DM a small region of parameter space remains at $m_X \approx$ 1 GeV for the operator $\frac{1}{\Lambda}\phi\phi^\dagger\bar{q}q$. All of the other spin-independent non-suppressed operators are excluded by direct detection experiments up to at least $m_X \simeq 100$ GeV. The strongest bounds on the remaining fermion DM operators in the ADM mass region are from collider searches, which are sufficient to exclude these operators over the mass range 1 GeV $\lesssim m_X \lesssim$ 10 GeV. With a small number of exceptions the common bound on the scale Λ due to monojet searches is roughly $\Lambda \gtrsim 1$ TeV for $m_X \lesssim 100$ GeV and present stronger bounds than direct detection constraints in several cases. For the non-suppressed spin-independent operators, as the ADM mass range is already excluded by direct detection limits, these collider bounds do not impose significant new constraints. In contrast LHC searches give virtually the sole limits on spin-dependent interactions and the velocity suppressed operators over the mass region of interest.

Inspecting Fig. 5-7 we note that TeV scale ADM (in distinction to ADM in the natural mass range 1 GeV $\lesssim m_X \lesssim$ 10 GeV) allows most effective operators to remove the symmetric component efficiently without conflict with current detection limits. As discussed previously, TeV scale ADM scenario is rather less appealing from a theoretical perspective, since the DM relic density is exponentially sensitive to changes in m_X and the decoupling temperature. Alternatively, in sharing models the operator which transfers the asymmetry may be inefficient, and this can be used to generate discrepancies between the baryon and DM asymmetries. Whilst such constructions permit a wider range of m_X, it as the mass of the DM rises it becomes increasingly difficult to explain the coincidence $\Omega_{\rm DM}/\Omega_B \approx 5$ via the DM asymmetry. Thus, although a wider range of ADM masses are certainly worth contemplating, since a natural expectation in many models of ADM is that the asymmetries in $\mathscr{X}$ and B should be comparable,

we have focused much of our discussion in this chapter on the case that the DM is comparable to the proton mass.

A further source of limits on contact operators come from invisible quarkonium decays [168, 170, 171]. Clearly, only bound states heavier than $2m_X$ can decay invisibly to the DM states. The principle constraints on the ADM region come from decays of the $\Upsilon(1S)$ mesons, as measured at the B-factories BaBar and CLEO [172]. However, we find that the limits on the contact operators of Table 1 coming from these invisible decay searches are not competitive with previous bounds from monojet searches or direct detection. There are also additional constraints on ADM from astrophysics [109, 173–177]. In particular for ADM models with scalar DM there are additional constraints from old compact stars [71, 178, 179]. Specifically, as ADM generally can not annihilates it will accumulate inside astrophysical bodies, which can cause gravitational collapse to a black hole. It has been argued (and is currently under active discussion [180–182]) that the observation of long lived neutron stars places sufficiently strong limits to exclude scalar ADM over a large mass range (including the 1-10 GeV mass range). However, this conclusion can be circumvented with further model building. For instance, these limits no longer apply if the scalar DM is not fundamental, but a composite state of fermions due to some new hidden sector strong dynamics, such that Fermi repulsion of the constituent states arises before the Chandrasekhar limit is reached [179, 183].

3.4 Discussion

If one begins from the well motivated assumptions that ADM with mass $m_X \sim m_p$ annihilates dominantly to SM quarks, and the flavour structure of such DM-quark couplings is minimal, then we have shown (Fig. 5-7) that the current experimental limits allow one to make decisive statements regarding the nature of the hidden sector.

In Fig. 5 it can be seen that contact operators with spin-independent non-suppressed direct detection cross sections are excluded for $\Lambda \lesssim 1$ TeV with universal couplings and up to 200 GeV in the case of m_q dependent couplings. The one exception is the operator $\frac{1}{\Lambda}\phi^\dagger\phi\bar{q}q$ for $m_X \lesssim 1$ GeV. Contact operators with spin-dependent non-suppressed direct detection cross sections are displayed in Fig. 6 and it is seen that these are excluded by monojet searches up to $\Lambda \sim 300$ GeV. Finally, the suppressed direct detection cross sections displayed in Fig. 7 are excluded for $\Lambda \lesssim 100$ GeV with the exception of the pseudoscalar operator $\frac{m_q}{\Lambda^3}\overline{\psi}\gamma^5\psi\bar{q}\gamma^5 q$ which is ruled out in the range $\Lambda \lesssim 10$ GeV. Collating these results we conclude that most contact operators are very strongly constrained and, moreover, that all of the operators are essentially excluded in the interesting, motivated ADM mass region 1 GeV $\lesssim m_X \lesssim$ 10 GeV.

Some caveats to the conclusion presented above are in order. Most prominently, the DM may couple dominantly to leptons. Although such a coupling would go against our expectations from models of flavour and from grand unified theories, if the DM interacts more strongly with leptons compared to quarks, this would greatly relax the monojet bounds and the constraints from DM direct detection [184]. The dominant bounds would now come from monophoton experiments and DM experiments which do not veto on electron recoil, such as DAMA/LIBRA [50]. Alternatively one may attribute a non-minimal flavour structure to the interaction with quarks, for instance, the DM could couple in an isospin violating fashion [185]. There exist studies of the collider limits in both the leptophilic [141] and isospin violating [143] scenarios with reference to conventional models of DM. Whilst possible in the context of ADM models these variant theories require further model building and a dedicated study.

In summary, with these caveats, the combination of direct detection and LHC limits excludes DM-quark contact interaction in the ADM mass region for all contact opera-

tors. With the exception of the pseudoscalar operator $\frac{m_q}{\Lambda^3}\overline{\psi}\gamma^5\psi\overline{q}\gamma^5 q$, all of these contact operators are disallowed by experimental searches for 1 GeV $\lesssim m_X \lesssim$ 100 GeV. The conclusion is striking: models of ADM in which the DM at the natural mass scale (1-10 GeV) and annihilates directly to SM quarks via heavy mediators are essentially excluded. There have been some experimental updates since this analysis was completed. The latest results from Xenon100 [186] and ATLAS [187] slightly improve the bounds on the scale Λ by factors around 1.5 - 3, however the curves in Fig.5-7 are not substantially effected. It has also been subsequently argued [4, 188] that the collider limits on effective operators can be improved if one also includes next-to-leading-order processes, this is especially true for m_q dependent operators for which interactions via heavy quark loops are dominant. Regardless, the analysis above - using the 2011 data - is sufficient to argue our point that ADM models in which the symmetric component annihilates to the quarks via an effective operator are generally excluded in natural constructions. The case of light mediators is not a trivial extension of the effective operator analysis since the results for the monojet and relic density calculations change drastically and we discuss the limits and model building opportunities of light mediators in the next chapter.

4 Towards Successful Annihilation of the Symmetric Component:

Light mediators

This chapter is based on work done in collaboration with John March-Russell and Stephen West, appearing in [1].

In the previous chapter we showed that direct detection [45, 155–159] and collider searches [160, 161, 166] place strong constraints on certain formulations of ADM. Next we shall discuss potential resolutions to the symmetric component problem of ADM, in particular we argue that this strongly motivates the idea that ADM should belong to a rich hidden sector of interacting states. Here we shall examine the limits on models in which the ADM annihilates to quarks via a light mediator, see e.g. [169]. Whilst collider limits are ameliorated in this scenario, direct detection limits (when relevant) remain a stringent constraint. Using the package `micrOMEGAs` [152], we study numerically two specific examples with light mediators, involving scalar and pseudoscalar states in Sect. 4.1 & 4.2. Subsequently in Sect. 4.3 we consider a semi-analytic approach to relate the features of the `micrOMEGAs` results to the underlying physics.

As discussed previously, in order to reproduce the relationship $\Omega_{\rm DM} \simeq 5\ \Omega_B$ in models of ADM it is essential that the DM asymmetry determines $\Omega_{\rm DM}$ and thus we require that the vast majority of the symmetric component must annihilate away. Notably, if the $X\overline{X}$ pairs annihilate to visible sector states then the couplings which ensure efficient annihilation are the same parameters which can be probed by direct detection and collider experiments. The severity of this problem was highlighted in

the previous chapter; we argued that with the reasonable assumptions that the DM annihilates dominantly to SM quarks via a contact operator (i.e. via a heavy mediator) with minimal flavour structure, then limits from direct searches [45, 155–161, 166] exclude the interesting, motivated ADM mass region 1 GeV $\lesssim m_X \lesssim$ 10 GeV for all operators of dimension six or less.

A proper treatment of light mediators requires a careful analysis which includes effects of resonances and mass thresholds. Mediators with mass comparable to, or less than, the momentum cuts employed in the collider searches can lead to a substantial weakening of the monojet bounds. Also, as noted previously, contact operators will not provide a faithful description of the monojet bounds if the limit on Λ is much below the p_T cut. In the presence of a light mediator η the relic density depends upon both the mass m_X of the DM state X and the mass of the mediator m_η. The annihilation of the symmetric component is enhanced in the mass range $m_X \gtrsim m_\eta$, as the annihilation can proceed by the t-channel processes $\overline{X}X \to \eta\eta$. Moreover, when $m_\eta \approx 2m_X$ the annihilation via the s-channel process $\overline{X}X \to \eta \to$ SM is resonantly enhanced. Consequently, the case of GeV scale mediators must be carefully analysed and it is not sufficient to simply adjust the monojet limits as is often the approach taken in the previous literature.

4.1 The light scalar-Higgs portal

To illustrate this general formalism we shall consider a particular example of a scalar state η which mediates interactions between a fermion DM state ψ and the SM quarks via mixing with the SM (or a SM-like) Higgs doublet H. In minimal models of DM it is expected that the mediator connecting the hidden and visible sectors should be a singlet under the SM gauge groups. In this case, mixing with the Higgs after electroweak

symmetry breaking provides the dominant manner by which the mediator state couples to the SM quarks. After electroweak symmetry breaking the scalar mediator and the Higgs will mix inducing interactions between η and the SM quarks [189–191].

To see this consider the Lagrangian contribution which describes the couplings of the two scalar states

$$\mathcal{L} = \lambda_X \eta \overline{\psi}\psi + \mu\eta \left|H\right|^2 + \frac{1}{2}m_\eta^2\eta^2 + V(H)\cdots \tag{4.1}$$

where λ_X is a dimensionless coupling, μ is a parameter with mass dimension one, $V(H)$ is the Higgs potential and the ellipsis contain the SM Yukawa couplings. Rewriting the Higgs as an excitation around its expectation value $H = (v+h)/\sqrt{2}$ gives

$$\mathcal{L} = \lambda_X \eta \overline{\psi}\psi + \sum_q y_q \overline{q} q h + \frac{1}{2}\mu\eta\left|h\right|^2 + \frac{1}{2}\begin{pmatrix}\eta & h\end{pmatrix}\begin{pmatrix} m_\eta^2 & \mu v \\ \mu v & m_h^2\end{pmatrix}\begin{pmatrix}\eta \\ h\end{pmatrix} + \cdots \tag{4.2}$$

where m_h is the Higgs mass and y_q are the SM Yukawas for quarks states q. The resulting mass eigenstates (η_1, h_1) are related to (η, h) via

$$\begin{aligned} \eta &= \cos\theta\ \eta_1 + \sin\theta\ h_1\ , \\ h &= -\sin\theta\ \eta_1 + \cos\theta\ h_1\ , \end{aligned} \tag{4.3}$$

where $\theta \simeq \frac{\mu v}{m_h^2}$ is the mixing parameter. The mass eigenstates can be expressed as follows

$$\begin{aligned} m_{y_1}^2 &\simeq m_\eta^2 - \frac{\mu^2 v^2}{m_h^4}\ , \\ m_{h_1}^2 &\simeq m_h^2 + \frac{\mu^2 v^2}{m_h^4} \simeq m_h^2\ , \end{aligned} \tag{4.4}$$

and the Lagrangian in the mass eigenbasis, to first order in θ, gives

$$\mathcal{L} = \lambda_X \eta_1 \overline{\psi}\psi + \lambda_X \frac{\mu v}{m_h^2} h_1 \overline{\psi}\psi + \frac{1}{2}\mu \eta_1 h_1^2 + \sum_q y_q \bar{q} q h_1 - \sum_q y_q \frac{\mu v}{m_h^2}\, \eta_1 \bar{q} q + V(H) \ . \quad (4.5)$$

Thus the η_1 state has induced couplings to the SM quarks suppressed by the $h - \eta$ mixing parameter. The mixing parameter is parametrically the quotient of the masses of the two states, thus we shall parameterise this interaction in our analysis by $\theta = \lambda' \hat{\theta}$ in terms of the parametric mixing $\hat{\theta} = \frac{m_\eta}{m_h}$ and a dimensionless coupling λ' which absorbs any deviation from this form. Thus the terms in the effective Lagrangian which describe the light mediator interaction between DM and quarks can be written as follows (dropping the subscript on η_1)

$$\mathcal{L} \supset \lambda_X \eta \overline{\psi}\psi + \sum_q (\theta \lambda' y_q) \eta \bar{q} q \ . \quad (4.6)$$

We use `micrOMEGAs` to calculate the required λ_X necessary to obtain the asymmetry dominated relic density, as a function of DM mass m_X. The results are shown in Fig. 8 for a scalar mediator with parameters $\{m_\eta,\ \lambda'\} = \{10\ \text{GeV},\ 1\}, \{50\ \text{GeV},\ 0.1\}$ and are accompanied by the combined direct detection constraints, as used in Chap. 3. Note, LEP searches [192] for mixed Singlet-Higgs states constrain $\lambda' \hat{\theta}$ to be small and influence our choice of values for λ', however varying this parameter will only lead to rescaling of the results. For mediators heavier than a few GeV only the resonance region survives the tension between theoretical and experimental requirements. Moreover, because of the strength of the spin-independent direct searches even lighter mediators are constrained to the point where only a small part of the parameter space survives. For scalar mediators with mass $\lesssim$ few GeV, for $m_X \sim m_\eta$, DM annihilation into η pairs (which later decay to SM states) is allowed by direct detection constraints and

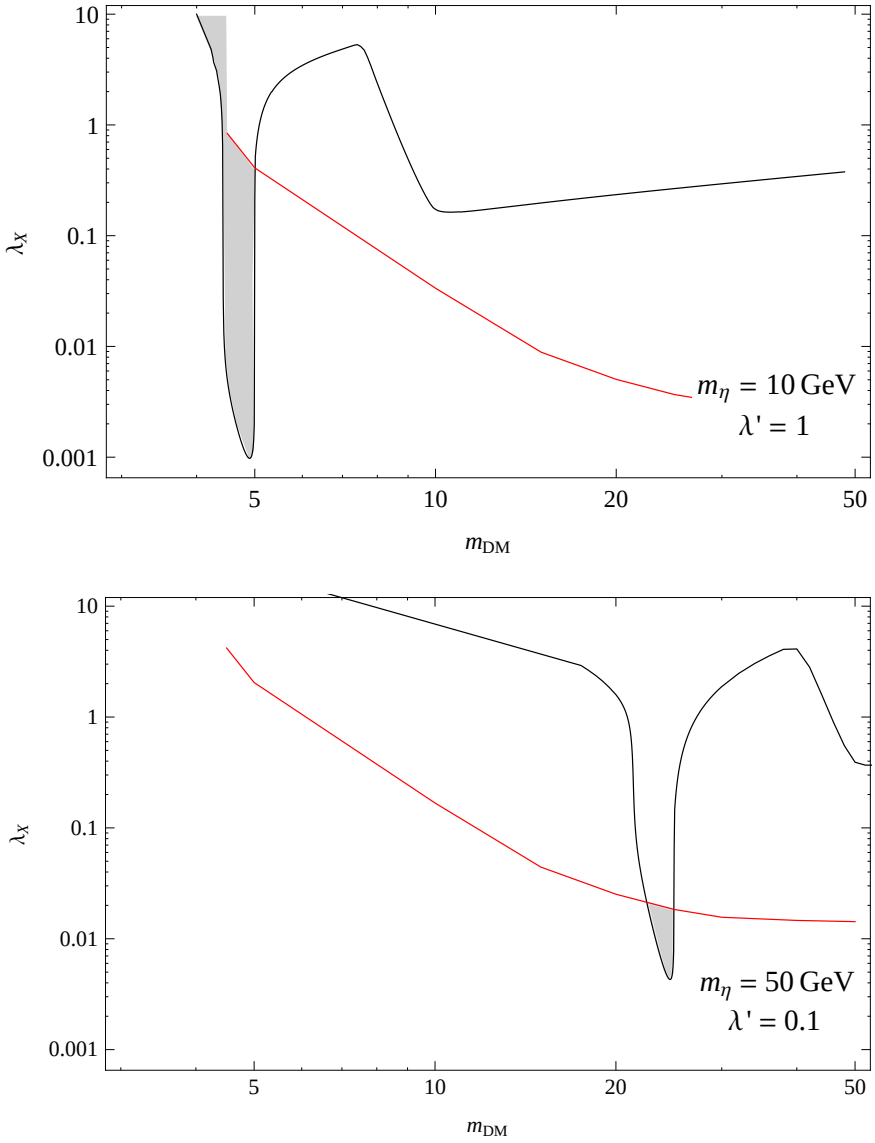

Figure 8. Constraints on a light scalar mediator coupling fermion DM to the visible sector via mixing with a SM-like Higgs with mass $m_h = 125$ GeV. The black curve shows the minimum DM-mediator coupling λ_X required to efficiently annihilate the symmetric component of the DM. The red curve indicates the current combined spin independent direct detection bounds. Constraints from monojet searches are negligible. The allowed parameter space is indicated by the shaded region. For mediators heavier than a few GeV only the resonance region survives the tension between direct detection limits and the requirement for efficient annihilation of the symmetric component.

presents a viable model. However, mediators with $m_\eta \lesssim 10$ GeV or DM with $m_X \lesssim 5$ GeV will lead to additional limits, most prominently searches for quarkonium decays to invisible states [172]. Moreover, this portal interaction will be constrained by future precision measurements of Higgs boson couplings [193–197]. In Sect. 4.3 we give an semi-analytic treatment of ADM relic density in the presence of s-channel resonances $\overline{\psi}\psi \to \eta \to$ SM and t-channel threshold effects $\overline{\psi}\psi \to \eta\eta$.

4.2 The light pseudoscalar portal

Next we shall consider the case of a light pseudoscalar which mediates interactions between DM and the SM quarks. Pseudoscalars are an ideal candidate for light mediator states and present a particularly interesting case as the constraints from direct detection (suppressed by q^4) are negligible. We parametrise the portal interaction connecting a fermion DM state ψ with SM quarks via a pseudoscalar mediator as follows, in analogy with eq. (4.6)

$$\mathcal{L} \supset i\lambda_X a\overline{\psi}\gamma^5\psi + \sum_q i(\hat{\theta}\lambda' y_q)a\overline{q}\gamma^5 f q, \tag{4.7}$$

where, as previously, y_q are the SM Yukawa couplings and $\hat{\theta}$ is the mixing parameter. Such a scenario could occur via mixing with a CP-odd state of an extended Higgs sector (e.g. the A^0 of the MSSM [38]).

In Fig. 9 we display the minimum λ_X required for efficient annihilation of the symmetric component, as a function of m_X, for a portal interaction due to a 10 GeV pseudoscalar mediator a for $\hat{\theta}\lambda' = 0.1, 0.01$ as the black solid curve. By fixing the coupling of the mediator to SM quarks, the size of the DM coupling λ_X to the mediator required for efficient annihilation of the symmetric component is simply a function of

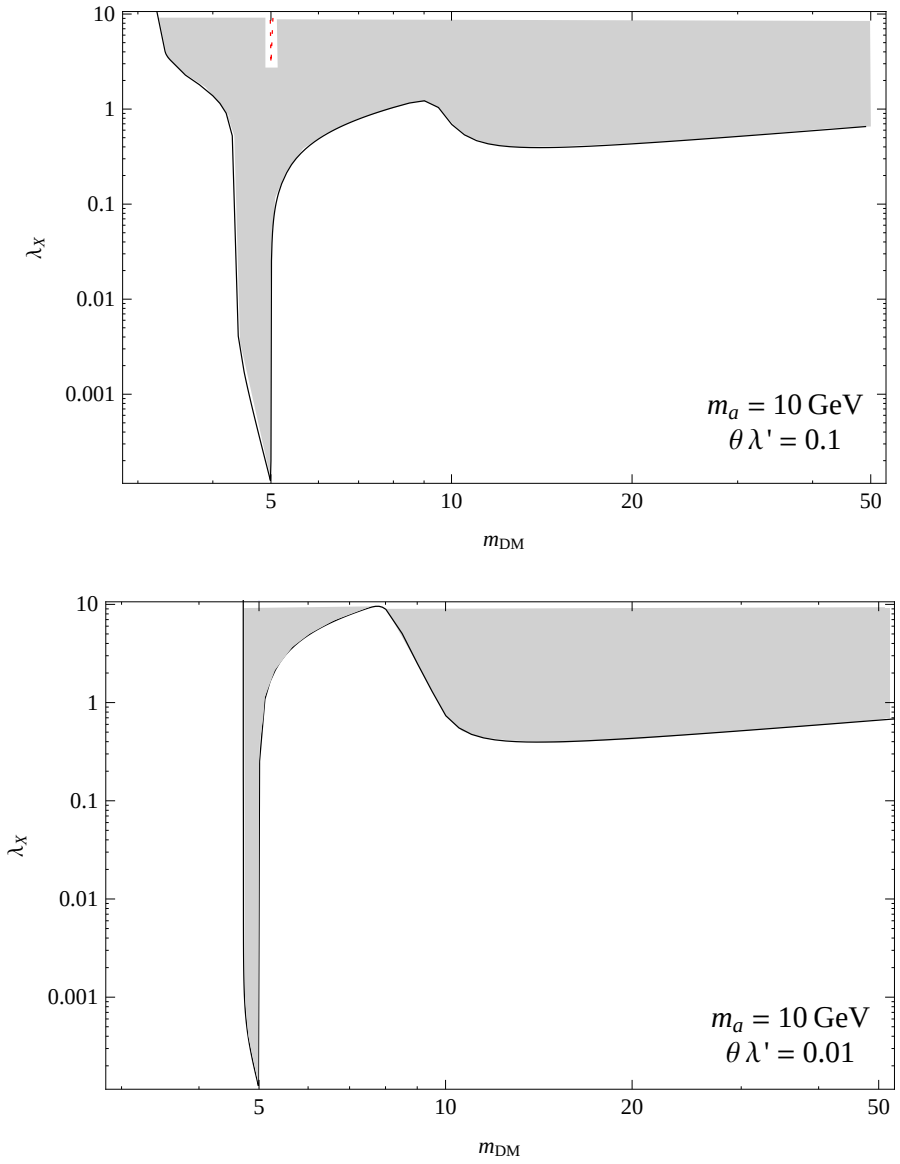

Figure 9. Constraints on a pseudoscalar mediator coupling fermion DM to the visible sector. The solid curve shows the required hidden sector coupling in order to efficiently annihilate the symmetric component. The dashed curve visible near 5 GeV (the resonance region) indicates the LHC monojet limits, as can be seen these do not present significant constraints on the model, this is in contrast to the corresponding contact operator $\mathcal{O}_p^\psi$ studied in Sect. 3.3. Moreover, as the scattering cross section is suppressed by q^4 there are essentially no limits from direct detection. The allowed parameter space is indicated by the shaded region.

the DM mass and the mediator mass. This allows us to present the effects of varying the parameters in a clear manner, which can be readily compared with the previous example of the light scalar-Higgs portal. The leading constraints on the light pseudoscalar portal come from the LHC monojet searches. We use `CalcHEP` to determine the LHC monojet bounds following the same procedure as in Sect. 3.3 and these limits are presented as the red dashed curve in Fig. 9.

4.3 Semi-analytic analysis of light mediators

In this section we shall make some remarks regarding the source of the features exhibited in the relic density calculations with light mediators using a semi-analytic analysis. The introduction of light mediators leads to resonance and mass threshold effects and the dominant process which determines the relic density becomes strongly dependent upon the DM mass. Note also that many models, in particular supersymmetric models, may lead to co-annihilation effects which must be accounted for but this is beyond the scope of these simple models. In correctly specifying the annihilation integral J for light mediators, we shall follow the work of Griest and Seckel [198].

With a light mediator η the standard expansion of $\langle\sigma v\rangle$ used for contact operators, eq. (3.6), is not valid over the whole mass range of the DM, X. There are a number of notable ranges of the DM mass in which the annihilation of the symmetric component is enhanced. In the DM mass range $m_X \gtrsim m_\eta$ the annihilation can proceed by the t-channel process $\overline{X}X \to \eta\eta$. The second region of interest is when $m_\eta \approx 2m_X$, in which case annihilation via s-channel $\overline{X}X \to \eta \to \overline{q}q$ is resonantly enhanced.

To model the effects of resonant production we factor out the pole factor $P(v^2)$

from the cross section

$$P(v^2) = \left[\left(1 - \frac{(2m_X/m_\eta)^2}{1 - \frac{v^2}{4}} \right)^2 + \left(\frac{\Gamma_\eta}{m_\eta} \right)^2 \right]^{-1}. \tag{4.8}$$

Whilst more sophisticated approximations are discussed in [198], this will suffice for our purposes. Following this we can write the thermally averaged cross section in the mass region $m_X \lesssim m_\eta$ as follows

$$\langle \sigma v \rangle_{m_X \lesssim m_\eta} \simeq \left(a_s + \frac{6 b_s}{x} \right) \times P(0), \tag{4.9}$$

where a_s and b_s are the coefficients from the velocity expansion of the cross section corresponding to s-channel $\overline{X}X \to \eta \to \bar{q}q$, assuming a scalar mediator as in Sect. 4.1. From inspection of eq. (4.8) the cross section will be peaked at $m_X \approx m_\eta/2$, in which case the annihilation integral, appearing in eq. (3.3) may be expressed as follows

$$J_{m_X \lesssim m_\eta} \simeq \frac{\left(a_s + \frac{3 b_s}{x_f} \right) \times P(0)}{x_f}. \tag{4.10}$$

In the mass region $m_\eta \gtrsim m_X$ the states η can be pair produced and present the dominant annihilation channel. For DM states with mass $m_X \approx m_\eta$ the final state velocity v_f becomes important and can not be approximated as unity in the velocity expansion of the cross section

$$\sigma v \simeq (a_t + b_t v^2) v_f. \tag{4.11}$$

The quantity v_f can be expressed as follows

$$v_f = \sqrt{1 - \left(\frac{m_\eta}{m_X}\right)^2 \left(1 - \frac{v^2}{4}\right)}. \tag{4.12}$$

We may make a velocity expansion of v_f

$$v_f \simeq \sqrt{1 - \frac{m_\eta^2}{m_X^2}} \left(1 + \frac{m_\eta^2 v^2}{8(m_X^2 - m_\eta^2)}\right). \tag{4.13}$$

Note that for $m_\eta \ll m_X$ the $v_f \approx 1$ and we recover the standard velocity expansion for the cross section. Furthermore, observe that the velocity expansion for v_f breaks down for $m_X \approx m_\eta$. The annihilation integral for $m_X > m_\eta$ and away from the threshold region $m_X \approx m_\eta$, may be approximated thus

$$J_{m_X \gtrsim m_\eta} \simeq \frac{\left(a_t I_a + \frac{3 b_t I_b}{x_f}\right)}{x_f}, \tag{4.14}$$

where a_t and b_t are the coefficients from the velocity expansion of the cross section corresponding to t-channel $\overline{X}X \to \eta\eta$. The factors $I_{a,b}$ account for the final state velocities of the produced states and are given by

$$\begin{aligned} I_a &= \frac{x_f}{a_t} \int_{x_f}^{\infty} \frac{\langle a_t v_f \rangle}{x^2} \mathrm{d}x, \\ I_b &= \frac{2x_f^2}{b_t} \int_{x_f}^{\infty} \frac{\langle b_t v^2 v_f \rangle}{6x^2} \mathrm{d}x. \end{aligned} \tag{4.15}$$

The explicit form of the factors $I_{a,b}$ given in eq. (4.15) depend on v_f. Away from the threshold region the approximation in eq. (4.13) is valid, however near the threshold one must use the exact form for v_f. Moreover, since the interacting states have non-zero

velocities, processes which would be forbidden at zero velocity may be accessible and lead to the dominant decay channels. We construct the total annihilation integral as a piecewise function

$$J = \begin{cases} J_{m_X \lesssim m_\eta} & m_X < 0.97 \times m_\eta \\ J_{\text{Threshold}} & 0.97 \times m_\eta \leq m_X \leq \times 1.03 m_\eta \\ J_{m_X \gtrsim m_\eta} & 1.03 \times m_\eta < m_X \end{cases} , \tag{4.16}$$

where $J_{\text{Threshold}}$ is identical in form to $J_{m_X \gtrsim m_\eta}$ but the $I_{a,b}$ factors are evaluated using the exact form for v_f. The factors $I_{a,b}$ are given explicitly in [198], which we reproduce below

$$I_a = \begin{cases} \frac{4z}{3\sqrt{\pi x_f}} \left(1 - 3x_f \left(\frac{m_\eta - m_X}{m_X}\right)\right) & \text{Threshold} \\ \sqrt{1 - \frac{m_\eta^2}{m_X^2}} \left(1 + \frac{3m_\eta^2}{8(m_X^2 - m_\eta^2)x_f}\right) & m_X \gtrsim m_\eta \end{cases} , \tag{4.17}$$

and

$$I_b = \begin{cases} \frac{32z}{15\sqrt{\pi x_f}} \left(1 - \frac{5}{6} x_f \left(\frac{m_\eta - m_X}{m_X}\right)\right) & \text{Threshold} \\ \sqrt{1 - \frac{m_\eta^2}{m_X^2}} \left(1 + \frac{5m_\eta^2}{6(m_X^2 - m_\eta^2)x_f}\right) & m_X \gtrsim m_\eta \end{cases} . \tag{4.18}$$

To calculate the relic density with light mediators we must use the corrected annihilation integral, eq. (4.16), in eq. (3.3):

$$Y_X = \frac{\Delta_X}{1 - \exp\left[-\Delta_X J \omega\right]}, \qquad Y_{\overline{X}} = \frac{\Delta_X}{\exp\left[\Delta_X J \omega\right] - 1}.$$

Then, as previously, we require that the asymmetric component alone accounts for the relic density by the requirement on the symmetric component given in eq. (3.10.) At this stage, for a given model, one can numerically evaluate the analytic forms

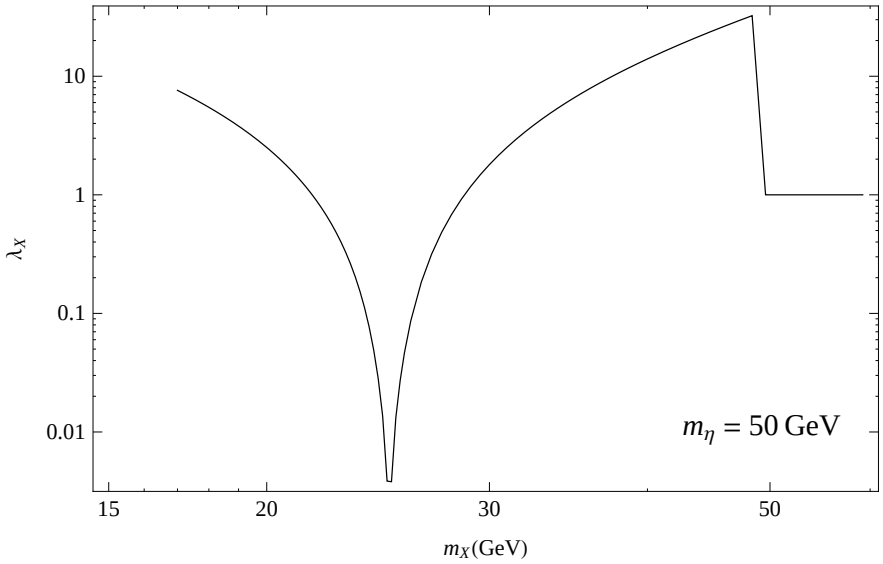

Figure 10. Relic density constraint on annihilation of the symmetric component to the visible sector through a 50 GeV scalar mediator, derived via a semi-analytic approach. Note that the aspect of the plot is comparable to the results obtained using `micrOMEGAs`, as displayed in Fig. 8 (right), and thus supports the findings of the numerical analysis.

above. This semi-analytic computation gives comparable results to those obtained from `micrOMEGAs`, as is shown in Fig. 10 for a mediator of mass $m_\eta = 50$ GeV. This semi-analytic analysis could be improved to better match the numerical results and some details of how this might be achieved are given in [198]. However, by comparing Fig. 8 & 10, it is already reasonable to conclude that the general features appearing in the numerical analysis are correct and understood.

4.4 Discussion

In Chap. 3 we demonstrated that most contact operators are very strongly constrained and that all of the operators were essentially excluded in the interesting, motivated ADM mass region 1 GeV $\lesssim m_X \lesssim$ 10 GeV. The validity of this effective operator description breaks down for mediators lighter than other scales appearing in the model,

this is $\lesssim$100 GeV for LHC physics and around the DM mass for processes which determine the annihilation cross section, at which point resonance and threshold effects become important in determining the exclusion limits. Both the monojet limits and the DM relic density are very sensitive to the DM mass, with both curves featuring resonances and mass threshold effects. In contrast to the effective operator analysis, where ADM was excluded up to 100 GeV by collider searches, the monojets limits for light mediators $m_a \lesssim$100 GeV are weakened to the extent that for natural couplings they present no appreciable constraint. Indeed the monojet limits are only visible in the plots of Fig. 9 in the resonance region $m_a \approx 2m_X$.

For $m_a \neq 2m_X$ the DM annihilation is via a virtual mediator and this leads to a large suppression in the cross section, thus for natural values of the parameter the mediator and DM masses must typically be arranged such that the annihilation of the symmetric component proceeds via resonant s-channel processes or t-channel pair production of the mediator states. In particular, if the DM is heavier than the mediator then there will generally be unconstrained parameter space in which efficient annihilation of the symmetric component to the visible sector can be achieved.

As can be seen in Fig. 8 & 9, if the mediator states are light then successful models of ADM can be constructed. However, for mediators with mass $\sim 10 - 100$ GeV there remain strong limits in cases where direct detection bounds are strong and to satisfy these constraints it is often required that the DM and mediator masses are arranged such that the DM annihilation is resonantly enhanced. This requires a degree of fine-tuning which is theoretically disfavoured. On the other hand if the direct detection bounds are suppressed as in the case of the pseudoscalar then there is no requirement for the DM and mediator masses to be tuned to the resonance region and thus such scenarios are very appealing.

We would like to highlight that pseudoscalars provide a viable, well motivated possibility for connecting the hidden and visible sectors in the ADM scenario. Not only do they allow the efficient annihilation of the symmetric component without conflicting with direct searches or requiring resonant (or similar) enhancement, but such light states arise quite naturally as PNGBs. In the next chapter we shall consider an alternative approach to removing the symmetric component of ADM, in which the DM annihilates to light hidden sector states and we shall examine the leading limits which constrain this scenario. Notably, we shall argue that in this case pseudoscalars also provide one of the best means of implementing this scenario.

5 Towards Successful Annihilation of the Symmetric Component:

Annihilation to hidden sector states

This chapter is based on work done in collaboration with John March-Russell and Stephen West, appearing in [2].

In the antecedent sections we have argued that if the symmetric component annihilates directly to the SM then large classes of ADM models face stringent constraints from collider and direct detection experiments. The introduction of new light states is perhaps the most interesting and well motivated manner to avoid the strong constraints examined previously. If the DM belongs to an extended hidden sector, containing lighter states into which the symmetric component can annihilate, then the limits from both direct search constraints and cosmological requirements are greatly ameliorated.

In this chapter we focus on the case where the hidden sector contains light degrees of freedom Y into which the symmetric component can annihilate. There are two distinct scenarios, firstly the $X\overline{X}$ could decay to light hidden sector particles Y which later decay to SM states. In this case the production and scattering cross sections are loop suppressed and the tension between the relic density requirements and the search constraints can be resolved. Alternatively, if the Y are stable on cosmological time scales then the initial energy density of the symmetric component will be effectively depleted by the ratio of masses m_Y/m_X. (Here we are assuming that the annihilation process is $X\overline{X} \to YY$.) Hence for the residual abundance of X set by the DM asymmetry to be the dominant contribution to $\Omega_{\rm DM}$ it is required that $m_Y \ll m_X$.

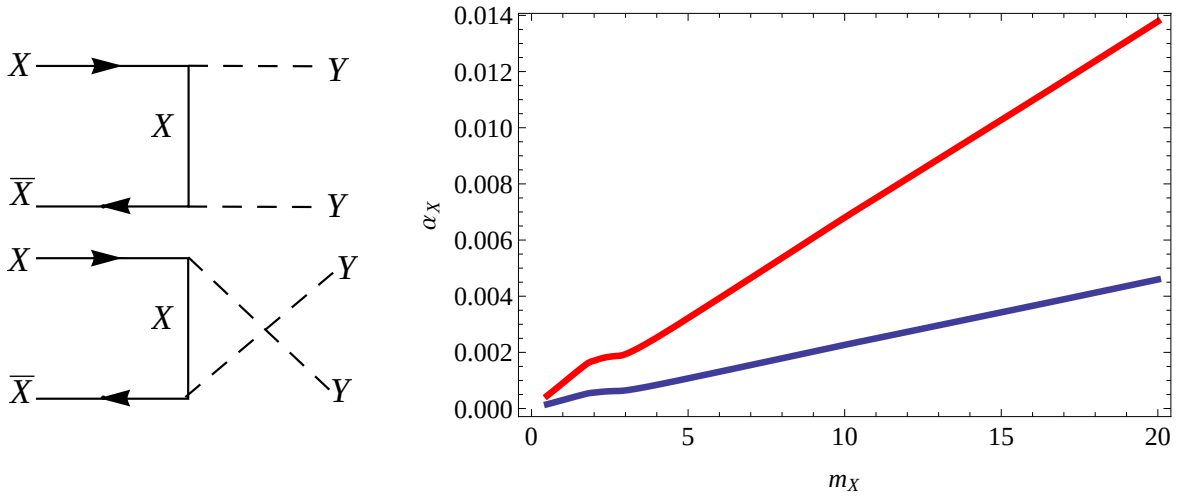

Figure 11. *left.* Dominant annihilation channels of the fermion DM X to hidden sector states Y. *right.* Minimum $\alpha_X = \lambda_X^2/4\pi$, where λ_X is the $YX\overline{X}$ coupling, required for efficient annihilation of the symmetric component in the limit $m_Y \ll m_X$, for Y a scalar (blue) or psuedoscalar (red).

Note, however, that for sub-keV (meta) stable Y states there are limits from structure formation and determinations of the number of relativistic species at CMB and BBN [199–206]. Additionally, for sub-10 MeV hidden sector states with couplings to SM particles there are potentially further constraints, such as invisible quarkonium decay [168, 170, 171]. Henceforth, in this work we generally consider the regime where the light hidden sector states are MeV or heavier.

We shall first discuss the requirements on the DM couplings to achieve successful annihilation of the symmetric component to light hidden sector scalar or pseudoscalar states. Subsequently, in Sect. 5.2 we discuss the leading limits on DM self-interactions and use these to constrain the hidden sector scenario. Some remarks about specific implementations are given in the Discussion section.

5.1 Efficient annihilation to hidden sector states

Let us examine the scenarios in which the symmetric component is removed primarily due to annihilations to light hidden sector degrees of freedom $X\overline{X} \to YY$ for Y a scalar or pseudoscalar state. Couplings of the DM (here assumed to be a Dirac fermion for definiteness) to scalar or pseudoscalar states are, respectively, $\lambda_X^{(\phi)} Y X \overline{X}$ and $\frac{1}{f_a}\partial_\mu Y X \gamma^\mu \gamma^5 \overline{X}$. The latter can be re-expressed as $\frac{2im_X}{f_a} Y X \gamma^5 \overline{X}$ and thus we define $\lambda_X^{(\mathrm{a})} = \frac{2m_X}{f_a}$. In the special case that the DM state X is a composite state, analogous to the proton, and the pseudoscalar states Y are the nearly massless PNGB "pions" of an associated spontaneously broken chiral symmetry, then one expects the relation $m_X \sim 4\pi f_a$ to hold (here assuming that the associated chiral symmetry is not badly explicitly broken), analogous to the Goldberger-Treiman relation of SM hadronic physics. Hence in this analogue to the hadronic sector of the SM the psedoscalar coupling is fixed to be $\lambda_X^{(\mathrm{a})} \simeq 4\pi$ (cf. $g_{\pi NN} \approx 13$ in the SM). Note that this relation is certainly not necessarily the case as the pseudoscalar might not be an analogue of the pion, but instead the PGNB of some other global symmetry spontaneously broken at a scale much higher than the mass scale of the DM states, rather like the QCD axion in the SM case. In this case f_a and thus $\lambda_X^{(\mathrm{a})}$ are free parameters.

Making an expansion $\sigma v = a + bv^2 + \cdots$ in the annihilation cross-section [1, 133], the symmetric yield after freeze-out is given by

$$Y_{\mathrm{sym}} \simeq \frac{\Delta_X}{\exp\left[\frac{4\pi}{\sqrt{90}}\Delta_X m_X M_{\mathrm{Pl}}\sqrt{g_*}\left(\frac{a}{x_f}+\frac{3b}{x_f^2}\right)\right]-1} \,. \tag{5.1}$$

The yield is related to the present relic density as follows

$$\Omega_{\mathrm{DM}}h^2 = 2.76\times 10^8 \left(\Delta_X + Y_{\mathrm{sym}}\right)\left(\frac{m_X}{\mathrm{GeV}}\right) \,. \tag{5.2}$$

To ensure that it is the asymmetry which determines $\Omega_{\rm DM}$ we shall again demand that the symmetric component is responsible for $\leq 1\%$ of the DM relic density, and this leads to a lower bound on the annihilation cross section.

The cross-section for fermion DM annihilating to scalar (ϕ) or pseudoscalar (a) states via t- and u-channel processes (as illustrated in Fig. 11) are given, to leading order in v, by

$$\begin{aligned}(\sigma v)_\phi &= \frac{\lambda_X^4 v^2 m_X \sqrt{m_X^2 - m_\phi^2}\left(9m_X^6 - 17m_\phi^2 m_X^4 + 10m_\phi^4 m_X^2 - 2m_\phi^6\right)}{24\pi\left(m_\phi^2 - 2m_X^2\right)^4\left(m_X^2 - m_\phi^2\right)}\ , \\ (\sigma v)_a &= \frac{\lambda_X^4 m_X v^2\left(m_X^2 - m_a^2\right)^{5/2}}{24\pi\left(m_a^2 - 2m_X^2\right)^4}\ .\end{aligned} \tag{5.3}$$

Note that the annihilation is p-wave suppressed in both cases. These scenarios reduce to one-parameter models in the limit $m_Y \ll m_X$ for $Y = \phi, a$; expressed in terms of $\alpha_X \equiv \lambda_X^2/4\pi$

$$(\sigma v)_\phi \simeq \frac{3\alpha_X^2 v^2 \pi}{8m_X^2}\ , \qquad\qquad (\sigma v)_a \simeq \frac{\alpha_X^2 v^2 \pi}{24 m_X^2}\ . \tag{5.4}$$

Substituting the above into eq. (5.1) leads to a rough order of magnitude limit on α_X,

$$\begin{aligned}\alpha_X^{(\phi)} &\gtrsim 1\times 10^{-3}\left(\frac{m_X}{5\ \text{GeV}}\right)\ , \\ \alpha_X^{(a)} &\gtrsim 3\times 10^{-3}\left(\frac{m_X}{5\ \text{GeV}}\right)\ ,\end{aligned} \tag{5.5}$$

where we have dropped a very slow dependence of x_f on the couplings.

This bound can be determined more precisely by taking into account the temperature variation of g_* through a numerical analysis. In Fig. 11 we plot the minimum α_X required for efficient annihilation of the symmetric component as a function of DM mass. The freeze-out temperature is determined numerically and the temperature

dependence of $g_*(T)$ is taken from the tables in DarkSUSY [135]. By inspection of Fig. 11 we note that the previous rough analytic approximation compares well with the precise numerical result. In the next section we shall compare the requirements on α_X necessary for efficient annihilation to constraints on DM self-interactions and we will find that in some cases this leads to considerable tension.

5.2 Model independent bounds on hidden sectors of ADM

One of the leading constraints on light hidden sector states which must be satisfied is the requirement that the observed ellipticity of DM halos is not destroyed by DM-DM elastic self-interactions [70, 207] mediated by the light state(s) in the DM sector and the precise limits vary depending on the interaction-type, which we examine in detail below. In particular, if the DM annihilates to light hidden sector states, then this interaction will also lead to DM scattering events which affect halo ellipticity and, consequently, there can exist tension between the requirement that the symmetric component annihilates efficiently and the limits coming from observations of DM halos. Important differences arise between models depending upon the nature of the state which mediates the DM interactions. A particular focus of the present work is the investigation of the case of (one or more) light PNGB state(s), and we argue that this scenario has many attractive features compared to the other possibilities investigated in the literature.

There are a number of astrophysical bounds on DM self-interactions, namely the observation of elliptical galaxy clusters [18] and elliptical DM halos [207], and from colliding clusters i.e. Bullet Cluster (1E 0657-558) constraints [13]. These constraints have been previously discussed for the case of scalar and vector DM in [70, 207], in which they note that halo ellipticity provides the leading bounds. We return to examine these

limits, in particular we show that in the (well motivated) scenario of a light pseudoscalar mediator these limits are significantly ameliorated. However, if the mediator is lighter than $m_X v_{\rm rel}$ then it is likely that bound states of DM will form [208, 211], this can drastically alter the analysis and we omit this case here. In the converse scenario we find that there is a tension with limits coming from halo ellipticity for light hidden sector scalars.

If the DM has self interactions which are mediated via a light state then this can lead to elastic scattering which can erase velocity anisotropies, resulting in spherical halos. Some initial work on this constraint of hidden sectors of ADM have previously been discussed in [70], we shall comment on this earlier study and also note some interesting variants in which certain limits are relaxed. Following [70, 207], we extract constraints on DM scattering cross-sections from galaxy NGC720 which is observed to possess an elliptical halo at 5 kpc. Following the literature [70, 207], the impact on halo morphology of DM self-interactions can be parametrised in terms of the average rate of $\mathcal{O}(1)$ changes in the DM velocities

$$\Gamma_{\Delta v\sim v} \simeq \int {\rm d}^3 v_1 {\rm d}^3 v_2 f(v_1) f(v_2) n_X \sigma_T v_{\rm rel} \left(\frac{v_{\rm rel}^2}{v_0^2}\right) \ , \tag{5.6}$$

where n_X is the halo DM density and $v_{\rm rel} = |\vec{v}_1 - \vec{v}_2| \sim 10^{-3}$ is the relative DM speed. The factor σ_T is the so-called transfer scattering cross-section which is the cross-section weighted by the momentum transfer

$$\sigma_T \equiv \int {\rm d}\Omega_* (1 - \cos\theta_*) \frac{{\rm d}\sigma}{{\rm d}\Omega_*} \ , \tag{5.7}$$

where σ is the scattering cross-section, θ_* the scattering angle in the centre of momentum frame, and Ω_* the associated solid angle. To estimate the limits on the DM

self-interactions, we will assume the Standard Halo Model, in which case the distributions $f(v)$ are of the form

$$f(\vec{v}) = \frac{e^{-v^2/v_0^2}}{(v_0\sqrt{\pi})^2} \ . \tag{5.8}$$

Observations of NGC720 suggest a local density of $m_X n_X \simeq 4$ GeV/cm^3 and radial velocity dispersion $v_0^2 \simeq 2(240\text{km/s})^2$. The existence of elliptical halos implies that the average time in which $\mathcal{O}(1)$ changes in the DM velocity occur must be greater than the lifetime of the galaxy, which corresponds to the constraint [207]:

$$\Gamma_{\Delta v \sim v} \lesssim \frac{1}{10^{10} \text{ years}} \ . \tag{5.9}$$

This can be translated into bounds on various mediator interactions following [207]. Note, Ref. [207] examines the cases of vector and scalar mediators, but not pseudoscalar mediators, which as we will see, lead to very different limits.

5.2.1 Constrains on DM self-interactions via scalar mediators

To set the scene, and for the sake of comparison, we begin with a reprise from [70, 207] of the constraints on the interactions of DM with non-derivatively coupled light scalar states. The form of the DM self-interaction potential for such a scalar mediator is simply $V(r) = -\alpha_X \frac{e^{-m_\phi r}}{r}$, where m_ϕ is the mediator mass and $\alpha_X = \frac{g_X^2}{4\pi}$ is related to the size of the coupling involved in DM self-interactions g_X. The transfer cross-section follows from $V(r)$, and in the Born approximation is given by

$$\sigma_T \simeq \frac{32\pi}{m_\phi^2 m_X^2 v_{\text{rel}}^4} [\alpha_X m_\phi]^2 \left(\ln(1+R^2) - \frac{R^2}{1+R^2} \right) \ . \tag{5.10}$$

Note that the factor in square brackets is proportional to the potential at the effective range of the force $V(r \sim m_\phi^{-1})$, while R is proportional to the ratio of the interaction range of the force to the de Broglie wavelength

$$R \equiv \frac{m_X v_{\rm rel}}{m_\phi} \ . \tag{5.11}$$

We shall work in the regime $R \ll 1$, as in this limit bound states of DM do not form [208, 211] and thus the following analysis is valid. Away from this limit the DM will often coalesce into bound states which can significantly alter the analysis, and for increasing R the cross-section blows-up. Since we expect ADM to respect $m_X \lesssim 10$ GeV, this corresponds to $m_\phi \gg 10$ MeV (since $v_{\rm rel} \sim 10^{-3}$). In this regime the DM self-interactions are well described by contact interactions, since the mediator mass is significantly larger than the momentum transfer in DM scatterings, and the transfer cross-section simplifies to the following approximate form[3]

$$\sigma_T \simeq \frac{32\pi\alpha_X^2}{m_X^2 v_{\rm rel}^4}\left(\frac{R^4}{2}\right) = 16\pi\alpha_X^2\frac{m_X^2}{m_\phi^4} \ . \tag{5.12}$$

Since this result is independent of $v_{\rm rel}$ the integral defining $\Gamma_{\Delta V \sim V}$ in eq. (5.9) simplifies and evaluating we obtain $\sigma_T \lesssim 4.4 \times 10^{-27}{\rm cm}^2 \ m_X \ {\rm GeV}^{-1}$ or equivalently $\sigma_T \lesssim 10 \ m_X{\rm GeV}^{-3}$ [70]. Moreover, by eq. (5.12) this translates into a bound on the α_X for $m_\phi \gg m_X v_{\rm rel}$

$$\alpha_X \lesssim 2 \times 10^{-3}\left(\frac{m_\phi}{100 \text{ MeV}}\right)^2\left(\frac{5 \text{ GeV}}{m_X}\right)^{1/2} \ . \tag{5.13}$$

We observe that the elliptical halo constraints provides an upper bound on the size

[3]Note that we find a factor of 2 difference compared with [207].

of α_X. However, we recall that large DM self-interactions are required to annihilate the symmetric component and thus there is also a lower bound on α_X as derived in Sect. 5.1 in the limit $m_\phi \ll m_X$. Combining these two bounds we observe a tension between experimental and theoretical requirements in the case of a scalar mediator with $m_X v_{\rm rel} \ll m_\phi \ll m_X$:

$$1 \times 10^{-3} \left(\frac{m_X}{5\ \text{GeV}}\right) \lesssim \alpha_X \lesssim 2 \times 10^{-3} \left(\frac{m_\phi}{100\ \text{MeV}}\right)^2 \left(\frac{5\ \text{GeV}}{m_X}\right)^{1/2} . \tag{5.14}$$

Note that the lower bound has a linear mass dependence, whereas the upper bound depends on the square root of the mass thus allowing for a potential larger allowed parameter space if one deviates from the standard picture of ~ 5 GeV ADM. Further, the limit $m_\phi \ll m_X$ is realistic, since, as argued previously, we expect that unless ϕ quickly decays to lighter states, the energy density of the symmetric component will be stored in these degrees of freedom with an effective dilution of the symmetric component energy density by a factor m_ϕ/m_X. Therefore in order for the ADM to be the dominant component of the DM relic density this ratio of masses must be $m_\phi/m_X \ll 1$.

In the next section we consider the case of DM self-interactions via a pseudoscalar mediator and we shall see that this leads to significant deviations.[4]

5.2.2 Constrains on DM self-interactions via pseudoscalar mediators

In Sect. 5.1 we derived a lower bound on the pseudoscalar-DM coupling required to remove the symmetric component of the DM. We now wish to compare this bound to limits arising from halo ellipticity in analogue to the previous discussion of the scalar mediator. We find that this scenario is decidedly different and that generically the upper bound on α_X (cf. eq. (5.14)) is no longer constricting. To study the elastic DM

[4] Vector mediators have similar bounds to the scalar case [70, 207].

scattering due to exchange of a PNGB we examine an effective Lagrangian which is constructed in direct analogue to the nucleon-pion Lagrangian in the limit that explicit chiral symmetry breaking is small. Moreover, since momentum transfer is small, the non-relativistic limit is a good approximation, and we consider the following effective chiral Lagrangian

$$\mathcal{L} = X^\dagger \left(i\partial_t - \frac{\nabla^2}{2m_X} \right) X - \lambda_X X^\dagger (\vec{\sigma} \cdot \vec{a}) X + \cdots \tag{5.15}$$

where the σ are the Pauli spin matrices and the ellipsis indicate contact interactions due to multiple pseudoscalar exchange, which are significantly suppressed [212–214]. The pseudoscalar field can be decomposed as follows

$$\vec{a} \equiv \frac{1}{\sqrt{2} f_a} \vec{\nabla} a + \cdots \tag{5.16}$$

The corresponding potential, which is the analogue of the standard one pion exchange potential [215], is given by

$$V_a(\vec{q}) = -\left(\frac{\lambda_X^2}{2 f_a^2} \right) (\tau_1 \cdot \tau_2) \frac{(\vec{\sigma}_1 \cdot \vec{q})(\vec{\sigma}_2 \cdot \vec{q})}{|\vec{q}|^2 + m_a^2} \ , \tag{5.17}$$

where τ_i are isospin matrices. This can be re-expressed via Fourier transformation to obtain

$$V_a(\vec{r}) = -\frac{\lambda_X^2 m_a^2}{24\pi f_a^2} (\tau_1 \cdot \tau_2) \left[\left(1 + \frac{3}{m_a r} + \frac{3}{(m_a r)^2} \right) L_2 \frac{e^{-m_a r}}{r} + L_0 \frac{e^{-m_a r}}{r} \right] + \cdots \tag{5.18}$$

where and the factors $L_{0,2}$ are proportional to angular momentum projectors with forms

$$\begin{aligned} L_0 &= \sigma_1 \cdot \sigma_2 \ , \\ L_2 &= 3\hat{r} \cdot \sigma_1 \hat{r} \cdot \sigma_2 - \sigma_1 \cdot \sigma_2 \ . \end{aligned} \tag{5.19}$$

It follows from eq. (5.17) that the transfer cross-section is of the form

$$\sigma_T^{(a)} \simeq 24\pi \left(\frac{27}{16}\right)^2 \frac{1}{m_a^2 m_X^2 v_{\rm rel}^4} \left[\frac{\alpha_X m_a^3}{f_a^2}\right]^2 \left(\ln(1+R^2) - \frac{R^2}{1+R^2}\left(1 + \frac{R^2}{2} - \frac{R^4}{6}\right)\right) \ . \tag{5.20}$$

where R is as given in eq. (5.11) (except with m_a replacing m_ϕ) and the factor in square brackets is the potential at the effective range of the force $V(r \sim m_a^{-1})$. At first view the scalar and pseudoscalar cross-sections seem comparable, the main difference being the factors contained in square brackets and the factor $(1 + \frac{R^2}{2} - \frac{R^4}{6})$, however these differences will turn out to be significant. In the limit $R \ll 1$

$$\sigma_T^{(\rm a)} \simeq 2\pi \left(\frac{27}{16}\frac{\alpha_X m_X}{f_a^2}\right)^2 R^4 \ . \tag{5.21}$$

It follows, comparing with the halo ellipticity bounds as in Sect. 5.2.1, that

$$\alpha_X \lesssim 8 \times 10^2 \left(\frac{f_a}{1\ \text{GeV}}\right)^2 \left(\frac{m_a}{100\ \text{MeV}}\right)^2 \left(\frac{5\ \text{GeV}}{m_X}\right)^{5/2} \left(\frac{10^{-3}}{v_{\rm rel}}\right)^2 \ . \tag{5.22}$$

Thus there is essentially no upper bound on the size of the coupling from DM self-interactions in this case.

Another important difference between the scalar and pseudoscalar mediators is that, whilst in the scalar case the cross-section blew-up in the large R limit, equivalently $m_\phi \to 0$, for the pseudoscalar in the large R limit the cross-section is well behaved and

reduces to the one-parameter model

$$\sigma_T^{(a)} \simeq 4\pi \left(\frac{27}{16} \frac{\alpha_X m_X}{f_a^2} \right)^2 , \tag{5.23}$$

which leads to the following constraint on the DM-pseudoscalar interaction

$$\alpha_X \lesssim 0.2 \left(\frac{f_a}{1 \text{ GeV}} \right)^2 \left(\frac{m_X}{5 \text{ GeV}} \right)^{1/2} . \tag{5.24}$$

5.3 Discussion

A particularly interesting example of PNGB is the case that the DM states X are composites arising from a new non-abelian gauge symmetry which both confines and breaks a (hidden) matter chiral symmetry. In this case light pseudoscalars arise from spontaneous chiral symmetry breaking, analogous to the pions of QCD, and they interact strongly with the heavy X states as do pions with baryons. Specifically, consider a scaled version of 2-quark-flavor QCD with the non-perturbative scale of the hidden sector gauge symmetry increased by a factor of 5. In this case the DM X states are identified with the hidden nucleons with, by the usual naïve dimensional analysis arguments,

$$m_X \simeq 4\pi f_a \simeq 5 \times 4\pi f_\pi \simeq 5 m_p . \tag{5.25}$$

For simplicity we assume that the current masses of the hidden quarks preserve a hidden SU(2) isopsin symmetry, and that there is no analog of electromagnetism in the hidden sector. In this case the lowest-lying spin 1/2 hidden nucleons form degenerate isospin doublets interacting with a degenerate isotriplet of hidden pion-like pseudoscalar states. Further, in the relevant limit of small explicit breaking of the hidden chiral symmetry, so that the hidden pions are parametrically light compared to m_X, the dark-sector pion

couplings to the X states are dominantly derivative in nature, and satisfy an analog of the Goldberger-Treiman relation

$$\lambda^{(a)} \sim \frac{m_X}{f_a} \sim 4\pi \ . \tag{5.26}$$

The mass of the hidden pions depends on the scale of explicit chiral symmetry breaking in the hidden sector (in QCD this occurs both due to the non-zero quark masses, and to the coupling the $U(1)_{\rm EM}$). In the absence of explicit chiral symmetry breaking the Nambu-Goldstone bosons are massless, and thus the $R \to \infty$ limit, eqs. (5.23,5.24), of the scattering is appropriate (trivially dressed by numerical factors arising from hidden isospin contractions). Using the Goldberger-Treiman relation of eq. (5.26) this leads to a momentum-transfer cross-section that is clearly excluded by the constraints from halo ellipticity.

Alternatively, if we assume that the pion masses scale-up from QCD similar to the DM mass, then $m_a \simeq 5m_\pi \simeq m_X/10$, and this corresponds to the scenario in which $R < 1$ with momentum-transfer scattering cross-section

$$\begin{aligned} \sigma_T^{(\rm a)} &\simeq 4\pi \left(\frac{27}{16}\frac{\alpha_X m_X}{f_a^2}\right)^2 \frac{R^4}{2} \\ &\simeq 3\times 10^{-2}\ {\rm GeV}^{-2} \left(\frac{m_X}{5\ {\rm GeV}}\right)^2 \left(\frac{v_{\rm rel}}{10^{-3}}\right)^4 \left(\frac{b}{4\pi}\right)^8 \left(\frac{500\ {\rm MeV}}{m_a}\right)^4 \ , \end{aligned} \tag{5.27}$$

where we have introduced the quantity $b \equiv \frac{m_X}{f_a}$ to parameterise deviations from the Goldberger-Treiman relation. This is sufficiently small to satisfy DM self-interaction constraints and also satisfies the requirement for annihilating the symmetric component as can be seen from Fig, 11. However, since $m_a \not\ll m_X$, if the PGNB's are stable then the contribution of the relic density due to the pseudoscalar states will likely be comparable to the DM density due to the asymmetry. Since $\Omega_{\rm Asym} \sim \epsilon\ \Omega_{\rm Sym}$ and we

expect that $\epsilon \sim 10^{-3\pm1}$, it follows that for $m_a > 10^{-3} m_X$ (i.e. $R > 1$) in order to for the relic density to be set by the asymmetry then we require that the pseudoscalar states can decay to the visible sector.

In this chapter we have endeavoured to highlight the best motivated settings for ADM model building, in which these limits are naturally alleviated or circumvented. Specifically, we considered hidden sector models with extend field content and dynamics. In particular, we suggested that the scenarios in which the hidden sector features light pseudoscalars, into which the symmetric component of ADM can annihilate, is perhaps one of the best motivated and least constrained. We showed that for pseudoscalar states a the tension between limits from elliptical halos and relic density requirements are greatly relaxed (by a factor $(m_a/f_a)^2$, which is generally small) compared to analogous models with light scalars or vectors. Moreover, light pseudoscalars are very well motivated as they naturally emerge in many frameworks as PNGB's.

Conversely, in the case that the symmetric component annihilates into light hidden sector scalars or vectors, the limits from elliptical halos significantly constrain the parameter space of these models. Notably, over much of the remaining parameter space (i.e. away from the limit $R \ll 1$), one generically expects that the formation of DM bound states is possible. Such bound states can have a significant effect on the physics and lead to a wealth of new phenomenology [208, 211]. This is a research direction which we are currently pursuing and will be discussed further in [2].

6 Evading the Symmetric Component Problem:

The Exodus mechanism

This chapter is based on work appearing in [3].

The matter of the observable universe, the *visible sector*, exhibits a rich structure of interacting states and, a priori, one might expect that the DM could be part of an equally complicated (set of) hidden sector(s). Such a suggestion is not implausible from a UV perspective as, for example, it has been argued that the topological complexity of generic string theory compactifications results in a large number of hidden sectors [216–219]. In this context it is quite conceivable that exchanges between dark and visible sectors can have cosmological consequences (beyond the usual moduli problem) and this reasoning motivates us to propose a new mechanism for cogenerating the DM relic density $\Omega_{\rm DM}$ and baryon density Ω_B in such a way that the close coincidence $\Omega_{\rm DM} \approx 5\Omega_B$ is explained without necessarily resorting to the assumption that that the DM itself carries a particle-antiparticle asymmetry.

In this chapter we first provide an qualitative overview of the mechanism and discuss the general requirements for connecting $\Omega_{\rm DM}$ and Ω_B in this model. We discuss aspects of model building and general constraints in this framework, in Sect. 6.1 & Sect. 6.2, respectively. Notably, in contrast to traditional ADM models, the DM can be a real scalar or Majorana fermion and thus presents distinct phenomenology. In Sect. 6.3 we examine the Boltzmann equations which describe the evolution of particle yields in the exodus mechanism in a general setting. Further, we present a specific

SUSY example in which we use this mechanism, in the setting of the MSSM, to obtain the correct DM relic density for a bino LSP in Sect. 6.4. In Sect. 6.5 we add some further comments, in particular we discuss argue that this mechanism circumvents the usual symmetric component problem of ADM.

6.1 Outline of the exodus mechanism

Hidden sectors can readily accommodate large CP violation which can lead to asymmetries in hidden sector states, for instance, via analogues of traditional baryogenesis mechanisms. If this asymmetry is transferred to the visible sector then it can generate the baryon asymmetry and thus set the present day baryon density [66, 76–78, 82]. In the new framework presented here the interplay between two hidden sectors, connected via a weak trisector coupling involving the visible sector, is used to explain the coincidence of cosmological densities $\Omega_{\rm DM} \approx 5\Omega_B$. An asymmetry in some approximately conserved quantum number is generated in a hidden *genesis sector* resulting in an asymmetry between a state X and its anti-partner $\overline{X}$. The genesis sector then evolves such that the symmetric component of X annihilates away and the abundance of X is set by the asymmetry. Subsequently, the asymmetric component of X decays to the visible sector and a second hidden sector, the *relic sector*, in a manner that cogenerates the DM and the baryon asymmetry. This scenario is illustrated schematically in Fig. 12. Since the mechanism proposed here occurs after the genesis of a hidden sector asymmetry, and the DM and baryon asymmetry are due to energy leaving the genesis sector, we refer to this mechanism as *exodus*.

The mechanism presented here is related to models of ADM [54–124] and also DM assimilation [220]. However, the construction and phenomenology of the exodus framework is quite distinct, and, notably, unlike existing models our mechanism *allows the*

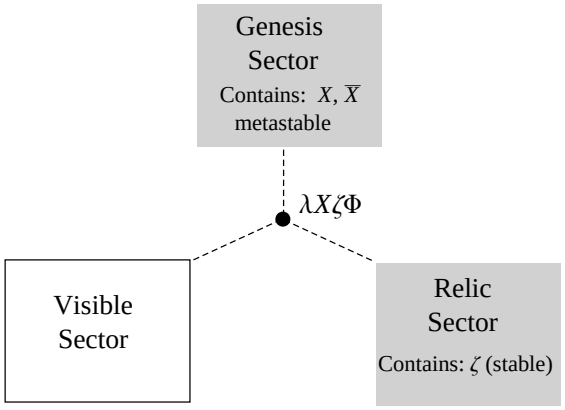

Figure 12. Illustration of the three sectors connected via a weak trisector interaction $\lambda X\zeta\Phi$, where Φ is some SM singlet operator involving SM states which violates $B-L$.

generation of self-conjugate or ADM, whilst simultaneously explaining the coincidence $\Omega_{\rm DM} \approx 5\Omega_B$. In particular, we shall argue that this framework provides a new possibility for obtaining the correct DM relic density composed of (nearly) pure bino LSP, a scenario which is generally not viable in the conventional freeze-out picture.

In the framework proposed here the observed DM relic density $\Omega_{\rm DM}$ is due to an abundance of stable states ζ in the relic sector. The genesis sector features large C- and CP-violating processes and appropriate out-of-equilibrium dynamics (therefore satisfying the Sakharov conditions [125]) which results in a sizeable asymmetry between the states X and $\overline{X}$, with some approximately conserved quantum number which we denote $\mathscr{X}$. The state X transforms under the DM stabilising symmetry, but $m_\zeta < m_X$ and the X do not comprise the present day DM relic density. The state X can decay to ζ, however, only via a suppressed intersector interaction, which violates $\mathscr{X}$ and B (and/or L) but conserves some combination of these quantum numbers, e.g. $B-L+\mathscr{X}$. For this mechanism to link Ω_ζ and Ω_B there are are three general requirements which must be satisfied:

- The intersector coupling must be sufficiently small that decays of X do not occur until after the symmetric component of X has been removed via pair annihilation.
- The number density of DM states n_ζ in the relic sector is due only to decays of the residual asymmetric component of X via the trisector coupling, i.e. $n_\zeta\big|_{\text{initial}} \simeq 0$.
- The relic DM produced via X decays must be entirely responsible for the DM relic density, and not due to thermally produced DM from heating of the relic sector.

These conditions ensure that the baryon asymmetry and the DM number density are linked $n_\zeta \propto n_{b-\bar{b}}$, as we will discuss in detail below. We assume that the initial abundance of DM states ζ is negligible, perhaps due to preferential inflaton decay [221, 222] which results in the relic sector reheating to a temperature lower than m_ζ (alternative scenarios could be envisaged). This type of cold hidden sector is similar to that considered in models of freeze-in production of DM [25, 121], as briefly discussed in Chap. 1. Importantly the temperature must be significantly lower that m_ζ to ensure that the tail of the thermal distribution does not populate ζ. For the case of weak-scale ζ self-interactions this translates into the requirement that $T^{\text{RH}}_{\text{relic}} \lesssim m_\zeta/25$ for X decays to be solely responsible for the DM relic density.

Immediately after the $\mathscr{X}$-genesis in the hidden sector (shaded red in Fig. 13) there is no asymmetry in B or L, the number density of X is set by the asymmetry in $\mathscr{X}$ and $n_\zeta, n_{\overline{X}} \approx 0$. At a later time the X states decay via the trisector coupling producing the DM and an asymmetry in the visible sector which sets the baryon asymmetry (green in Fig. 13). As the temperature drops below the baryon mass (~ 1 GeV) the baryon number density becomes suppressed and reveals the baryon asymmetry inherited from the

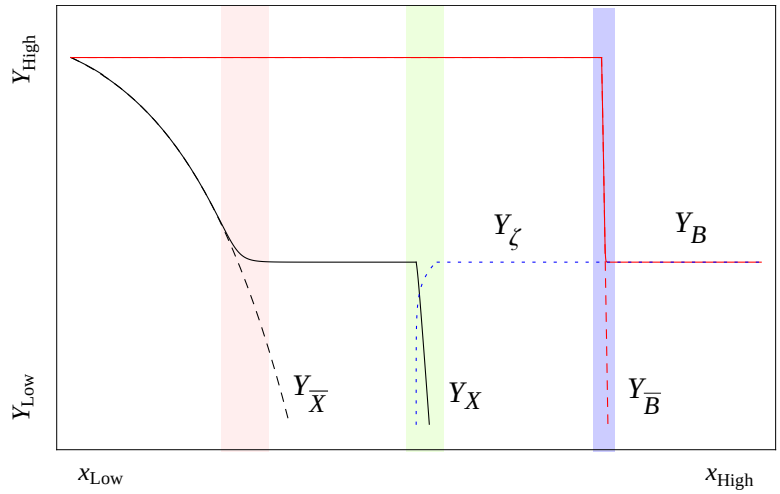

Figure 13. Log plot illustrating the cosmological history, it shows (schematically) particle yields $Y \equiv \frac{n}{s}$, where s is the entropy density, against $x \propto T^{-1}$. Black, red and blue solid lines give, respectively, the yields for X, the baryons and the relic DM ζ (antiparticles shown dashed). The red shaded region indicates where the X density becomes dominated by the asymmetry, the green region highlights the decays of X and subsequent generation of DM and visible sector asymmetry. In blue is shown the mass threshold of protons past which their number density is Boltzmann suppressed and the baryon density is set by the asymmetry.

genesis sector (blue in Fig. 13). We examine the Boltzmann equations which describe the asymmetry transfer shortly.

The decay of the asymmetric component of X from the genesis sector is solely via the trisector interaction $\lambda X\zeta\Phi$, for Φ some SM singlet operator involving SM states which violates $B-L$. For preferential inflationary reheating to occur the sectors must be only feebly coupled to each other and consequently, we expect the coefficient of the intersector portal λ to be small. In many realisations the operator $X\zeta\Phi$ has high mass dimension and the effective coupling is set by the inverse power of some mass scale M, for example $\frac{1}{M^3}X\zeta u^c d^c d^c$, as discussed in Sect. 2.3.

One of the main factors upon which the phenomenology of these models depends is whether the DM particle ζ carries $\mathscr{X}$ number. If ζ does not carry $\mathscr{X}$ then it can be self-conjugate state (a real scalar or Majorana fermion), thus resulting in symmetric DM.

In this case DM annihilations are possible and can lead to indirect detection signals with annihilation profiles [169]. On the other hand, if ζ is non-self-conjugate (a Dirac fermion or complex scalar), with non-zero $\mathscr{X}$ number, then these states will inherit the asymmetry of the genesis sector, like the baryons, resulting in ADM.

6.2 Constraints on the exodus mechanism

6.2.1 Lifetime constraints

To explain the comparable sizes of the cosmic relic densities $\Omega_\zeta/\Omega_B \approx 5$ via the exodus mechanism it is required that the $\mathscr{X}$ asymmetry alone be responsible for the DM relic density. Consequently we require that the symmetric component annihilates within the lifetime of X. Here we calculate the minimum lifetime of X required such that decays of the X states occur only after the symmetric component is removed via pair annihilation. The X and $\overline{X}$ could annihilate to either light hidden sector states which do not carry $\mathscr{X}$, and subsequently redshift away the energy density, or to visible sector states which thermalise before Big Bang nucleosynthesis (BBN). In order for the symmetric component of X to be sufficiently depleted it is necessary that the $X\overline{X}$ annihilations do not freeze-out too quickly, as illustrated in Fig. 3 (Chap. 2).

At high temperatures the X and $\overline{X}$ are in thermal equilibrium with the other states of the genesis sector and when the temperature of the genesis sector $T_{\rm gen}$ drops below the mass of X the number densities of these states decrease exponentially (provided $m_X > |\mu_X|$)

$$n_X^{\rm eq} = \left(\frac{m_X T_{\rm gen}}{2\pi}\right)^{3/2} e^{-\frac{m_X-\mu_X}{T_{\rm gen}}}, \qquad n_{\overline{X}}^{\rm eq} = \left(\frac{m_X T_{\rm gen}}{2\pi}\right)^{3/2} e^{-\frac{m_X+\mu_X}{T_{\rm gen}}}. \tag{6.1}$$

However, once the interaction rate falls below the Hubble rate H the $X\overline{X}$ annihilations

freeze-out and their co-moving number densities plateau. The temperature at which annihilations freeze-out $T_{\rm gen}^{\rm (FO)}$ can be determined by adapting a standard calculation [9]. Freeze-out occurs when the production and decay rate is too low to maintain the state in equilibrium and the freeze-out condition can be expressed in terms of the Boltzmann equation for antiDM. As $n_{\overline{X}}$ is greatly suppressed at low temperatures we can neglect DM-antiDM annihilations and only consider DM pair production

$$\dot{Y}_X \sim \sigma s Y_X^{\rm eq} Y_{\overline{X}}^{\rm eq} \ . \tag{6.2}$$

where σ is the $X\overline{X}$ annihilation cross section. We can rewrite $n_{\overline{X}}^{\rm eq}$ as follows

$$n_{\overline{X}}^{\rm eq} = \frac{1}{n_X}\left(\frac{m_X T_{\rm gen}}{2\pi}\right)^3 e^{-2m_X} = \frac{m_X^3}{\eta_X} e^{-2m_X}. \tag{6.3}$$

where the latter equality is derived using $n_X = \eta_X n_\gamma$. Then it follows from the Boltzmann equation that the condition of freeze-out is given by

$$\frac{m_X}{T_{\rm gen}^{\rm (FO)}} H\left(T_{\rm gen}^{\rm (FO)}\right) \sim \left(T_{\rm gen}^{\rm (FO)}\right)^3 \eta_X \sigma \ . \tag{6.4}$$

Using the standard definition $H(T) = \frac{1.66\sqrt{g_*}T^2}{M_{\rm Pl}}$, we solve eq. (6.4) to obtain an expression for the freeze-out temperature

$$T_{\rm gen}^{\rm (FO)} \sim \sqrt{\frac{1.66\sqrt{g_*} m_X}{M_{\rm Pl}\eta_X \sigma}} \ . \tag{6.5}$$

Next we calculate the critical temperature $T_{\rm gen}^{\rm (C)}$ for which the number density of X states becomes primarily due to the asymmetry, or equivalently the temperature at which $Y_{\overline{X}}^{\rm eq} \ll Y_X$. For concreteness we shall insist that $Y_{\overline{X}}^{\rm eq} < \eta_X/100$. The critical

temperature below which this depletion of the symmetric component is achieved is a function of the DM mass. The number density for states with an asymmetry is given by eq. (6.3) and we use $s = \frac{2\pi^2}{45} g_*^s T^3$ to express the depletion condition as follows

$$Y_{\overline{X}}^{\rm eq} \sim \frac{2\pi^2}{45} \frac{g_*^s \left(T_{\rm gen}^{\rm (C)}\right)^3 m_X^3}{\eta_X} e^{-\frac{2m_X}{T_{\rm gen}^{\rm (C)}}} = \frac{\eta_X}{100} \ . \tag{6.6}$$

In Fig. 14 we plot the critical temperature $T_{\rm gen}^{\rm (C)}$ necessary for sufficient annihilation of the symmetric component against m_X, taking $\eta_X = 6.2 \times 10^{-10}$, equal to the baryon asymmetry. In the case that the genesis sector is radiation dominated,[5] time can be related to temperature via $t \sim 1/H(T) \sim M_{\rm Pl}/\sqrt{\rho(T)}$, in terms of the energy density $\rho(T) \sim \frac{3M_{\rm Pl}^2}{8\pi} H(T)^2$, and we can re-express the critical temperature $T_{\rm gen}^{\rm (C)}$ in terms of the minimum time t_* required to adequately deplete the symmetric component

$$t_* \sim \frac{M_{\rm Pl}}{1.66\sqrt{g_*}\ T_{\rm vis}^2} \sim 10^{-6}\ {\rm s} \left(\frac{R}{1}\right)^2 \left(\frac{\rm GeV}{T_{\rm gen}^{\rm (C)}}\right)^2 , \tag{6.7}$$

where $R = T_{\rm vis}/T_{\rm gen}$ is the quotient of the temperatures of the genesis and visible sector.

In many constructions it is reasonable to assume that in the early universe the genesis sector and visible sector were in thermal equilibrium, before later decoupling. In this case the thermal evolution of the genesis and visible sectors may be very similar and we can compare the critical temperature $T_{\rm gen}^{\rm (C)}$ to important thresholds in the visible sector, such as BBN and the EWPT, as is shown in Fig. 14. Of course, if the genesis sector and visible sector are not in thermal equilibrium in the early universe, or evolve very differently after decoupling, then the critical temperature can not be readily compared with visible sector milestones.

[5] The time-temperature relationship for matter-dominance is of the form $t \sim H^{-1} \sim \frac{M_{\rm Pl}}{\sqrt{\rho}}(1+z)^{-3/2}$ where z is the redshift. For simplicity we shall assume a radiation dominated genesis sector henceforth.

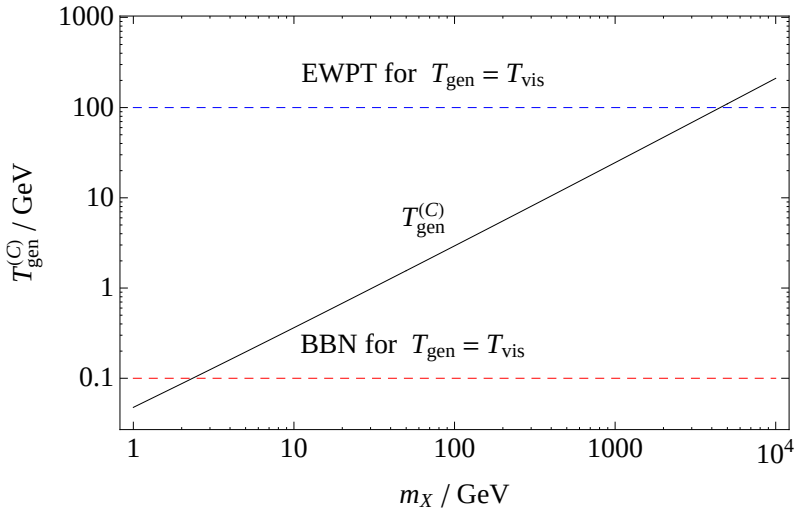

Figure 14. The critical temperature $T^{(C)}_{gen}$, below which the symmetric component of X states is sufficiently depleted, for varying m_X, with $\eta_X = 6.2 \times 10^{-10}$. In the simplest scenarios the genesis and visible sectors are in thermal equilibrium and we indicate the temperature at BBN (red dashed) and EWPT (green dashed) for this case.

To demonstrate that viable models can be constructed we must compare the X lifetime to the minimum time required to annihilate the symmetric component. For simplicity, let us examine the lifetime of the X states assuming decays via a renormalisable operator with coupling constant λ to a two-body final state

$$\tau_X = \Gamma_X^{-1} \simeq 1 \times 10^{-4}\ \mathrm{s} \left(\frac{10^{-10}}{\lambda}\right)^2 \left(\frac{10\,\mathrm{GeV}}{m_X}\right) . \tag{6.8}$$

In several scenarios X decays to a multi-body final state via a high dimension operator dressed by the reciprocal of an appropriate scale M, this leads to additional phase space suppression of Γ_X and the coupling λ should be replaced by a ratio of scales, parametrically, $(m_X/M)^n$ for a $4+n$ dimensional operator. To construct a proof of principle, let us further assume that the temperatures of the visible and genesis sectors are equal and evolve together $T_{vis} = T_{gen}$. The minimum time required to

sufficiently deplete the symmetric component t_* is given by eq. (6.7), with $R = 1$. Further, from inspection of Fig. 14, the critical temperature behaves like $T_{\rm gen}^{\rm (C)} \sim \frac{m_X}{30}$ and thus parametrically

$$t_* \sim 10^{-5} \left(\frac{10 \text{ GeV}}{m_X}\right)^2 \text{ s} \,. \tag{6.9}$$

Comparing with eq. (6.8) we conclude that viable models, with $\tau_X > t_*$, can be constructed.

6.2.2 Constraints on energy injection

In order for the exodus mechanism to set the relic density rather than the conventional freeze-out mechanism it is required that the number density of the relic DM n_ζ is entirely due to decays of X states. It is important that the temperature of the relic sector remains lower than m_ζ such that the DM can not be thermally produced. Note that the requirement $T_{\rm relic} \ll m_\zeta < m_X$ implies that, for there to be initially a thermal distribution of X states, the reheat temperature of the X sector must be significantly higher than the relic sector, which could be due to preferential inflaton decay. Crucially, if the temperature of the relic sector is raised due to energy injection to the point that the exponential tail of the DM distribution is populated, then freeze-out of this thermally produced DM will likely dominate over the DM component produced via X decays and thus ruin the exodus mechanism. If one assumes that the ζ have weak-scale self-interactions, then to avoid populating the tail of the distribution it is required that $T_{\rm relic} \lesssim m_\zeta/25$. Note that changes in the interaction strength will only lead to logarithmic deviations in the temperature bound. Additionally, a weaker requirement is that the three sectors should not equilibrate, in which case we expect a negligible X relic density which will disrupt the relationship $\Omega_{\rm DM} \approx 5\Omega_B$.

Consider the decays $X \to \zeta b$, for some final state b carrying baryon number $B = 1$.

In order to satisfy the requirement that $T_{\rm relic} \lesssim m_\zeta/25$ it must be that the X decay products have non-relativistic momenta and, working in this regime, we calculate the temperature of the relic sector after energy injection from the genesis sector $T^{(\infty)}_{\rm relic}$. The temperature of the ζ final states is related to the average kinetic energy

$$\frac{3}{2}k_B T^{(\infty)}_{\rm relic} = \langle {\rm KE} \rangle = \frac{\langle p_\zeta^2 \rangle}{2m_\zeta} \ . \tag{6.10}$$

The kinematic variables are related via $p_X^2 = (p_b + p_\zeta)^2$ and $m_X^2 = m_b^2 + m_\zeta^2 + 2p_b \cdot p_\zeta$. Working in the rest frame of X we have $p_\zeta = (E_\zeta, p_\zeta)$ and $p_b = (E_b, -p_\zeta)$; it follows that

$$m_X^2 - (m_b^2 + m_\zeta^2) \simeq 2(m_b m_\zeta + p_\zeta^2) \ . \tag{6.11}$$

Solving for p_ζ and substituting into eq. (6.10) yields

$$\langle p_\zeta \rangle \simeq 2m_b m_\zeta + 6T^{(\infty)}_{\rm relic} m_\zeta \ . \tag{6.12}$$

From which we can find the temperature of the relic sector after energy injection

$$T^{(\infty)}_{\rm relic} \simeq \frac{m_X^2 - (m_b + m_\zeta)^2}{6m_\zeta} \ . \tag{6.13}$$

Thus the constraint $T^{(\infty)}_{\rm relic} \lesssim m_\zeta/25$ can be recast in terms of the masses; in the simplest scenarios we expect that $m_\zeta \sim 5$ GeV and $m_B \simeq 1$ GeV in order to explain $\Omega_{\rm DM} \approx 5\Omega_B$ and substituting values for m_B and m_ζ, eq. (6.13) reduces to

$$\frac{T^{(\infty)}_{\rm relic}}{\rm GeV} \simeq \left(\frac{m_X}{6\ {\rm GeV}}\right)^2 - 1 \ , \tag{6.14}$$

and the constraint $T^{(\infty)}_{\rm relic} \lesssim m_\zeta/25$ places an upper bound on $m_X \lesssim 6.5$ GeV. We note

that in a wide range of scenarios there is sufficient freedom to choose the relative sizes of m_ζ and m_X and thus viable models can be constructed.

6.3 Boltzmann equations for exodus

To understand quantitatively the transfer in the $\mathscr{X}$ asymmetry $n_{\mathscr{X}} \equiv n_X - n_{\overline{X}}$ from the genesis sector to the visible sector we can use the Boltzmann equations (see e.g. [9, 10]). To first order in the small trisector coupling λ, assuming two-body X decays to DM states ζ and baryons b, this can be expressed as

$$\begin{aligned}\dot{n}_{\mathscr{X}} + 3Hn_{\mathscr{X}} = &\int \mathrm{d}\Pi_X \mathrm{d}\Pi_b \mathrm{d}\Pi_\zeta (2\pi)^4 \delta^{(4)}(p_X - p_b - p_\zeta) \left[|M|^2_{b\zeta\to X} f_b f_\zeta - |M|^2_{X\to b\zeta} f_X\right] \\ &- \int \mathrm{d}\Pi_X \mathrm{d}\Pi_b \mathrm{d}\Pi_\zeta (2\pi)^4 \delta^{(4)}(p_X - p_b - p_\zeta) \left[|M|^2_{b\overline{\zeta}\to \overline{X}} f_{\overline{b}} f_{\overline{\zeta}} - |M|^2_{\overline{X}\to b\overline{\zeta}} f_{\overline{X}}\right]\end{aligned} \tag{6.15}$$

where we have neglecting statistical factors. Note, $\mathrm{d}\Pi_i = \frac{\mathrm{d}^3 p_i}{(2\pi)^3 2E_i}$ and the phase space distribution function f_i is related to the number density by

$$n_i = \frac{g_i}{(2\pi)^3} \int \mathrm{d}^3 p f_i \ , \tag{6.16}$$

where g_i is the number of internal spin degrees of freedom. For a state in thermal equilibrium at temperature T the phase space distribution function is of the form

$$f_i \simeq \exp\left(-\frac{E_i}{T} \pm \frac{\mu_i}{T}\right) \ , \tag{6.17}$$

where μ_i is the chemical potential which describes unbalances between particle-antiparticle number densities due to asymmetries: $\eta_i \propto \mu_i/T$. This term takes opposite signs for particles and antiparticles and is absent in the case of self-conjugate fields.

Immediately prior to X decays the number density of relic DM is negligible $n_{\zeta,\bar{\zeta}} \approx 0$

and it follows $f_\zeta \approx f_{\overline{\zeta}} \approx 0$. Moreover, as the processes do not feature large CP violation, X and $\overline{X}$ processes can be treated equally, hence $|M|^2_{b\zeta\to X} = |M|^2_{\overline{b\zeta}\to\overline{X}}$ and by CPT invariance $|M|^2_{b\zeta\to X} = |M|^2_{\overline{X}\to\overline{b\zeta}}$. Thus eq. (6.15) reduces to

$$\dot{n}_{\mathscr{X}} + 3Hn_{\mathscr{X}} \simeq \int \mathrm{d}\Pi_X 2m_X\Gamma_X \left(f_{\overline{X}} - f_X\right) \ , \tag{6.18}$$

where we have introduced the decay width

$$\Gamma_X = \frac{1}{2m_X}\int \Pi_b \mathrm{d}\Pi_\zeta (2\pi)^4\delta^{(4)}(p_X - p_b - p_\zeta)|M|^2_{X\to b\zeta} \ . \tag{6.19}$$

Converting the integration variable from momentum to energy (following [25]) we obtain

$$\begin{aligned}\dot{n}_{\mathscr{X}} + 3Hn_{\mathscr{X}} &\simeq \int_{m_X}^{\infty} \frac{\mathrm{d}E_X}{2\pi^2} m_X\Gamma_X\sqrt{E_X^2 - m_X^2}e^{-E_X/T}\left(e^{\mu_X/T} - e^{-\mu_X/T}\right) \\ &\simeq \frac{m_X^2\Gamma_X T}{2\pi^2}K_1\left(\frac{m_X}{T}\right)\left(e^{\mu_X/T} - e^{-\mu_X/T}\right) \ ,\end{aligned} \tag{6.20}$$

where K_i a the modified Bessel function of the second kind. Re-expressing this in terms of Δ_X, and using the asymptotic form of the Bessel function $K_1(x) \sim \sqrt{\frac{\pi T}{2m_X}}\exp\left(-\frac{m_X-\mu}{T}\right)$ gives

$$\dot{\Delta}_X \simeq \frac{\Gamma_X}{s}\left(\frac{m_X T}{2\pi}\right)^{3/2}\left(e^{-(m_X+\mu_X)/T} - e^{-(m_X-\mu_X)/T}\right) \simeq -\Gamma_X\Delta_X \ , \tag{6.21}$$

where we have collected terms into the number densities, as stated in eq. (2.4). It follows that

$$\int \frac{\mathrm{d}\Delta_X}{\Delta_X} \simeq -\int \mathrm{d}t\ \Gamma_X \simeq \Gamma_X\int \mathrm{d}T\ \frac{1}{HT} \ , \tag{6.22}$$

and integrating between early time and late time, at temperature T, yields

$$\log\left(\frac{\Delta_X^{(\rm init)}}{\Delta_X(T)}\right) \simeq -\frac{\Gamma_X}{2}\frac{M_{\rm Pl}}{1.66\sqrt{g_*}}\left(\frac{1}{T_{\rm UV}^2}-\frac{1}{T^2}\right) . \tag{6.23}$$

where $\Delta_X^{(\rm init)}$ is the initial $\mathscr{X}$ asymmetry and $\Delta_X(T)$ is the asymmetry at temperature T. The quantity $T_{\rm UV}^2$ is the temperature at which the primordial $\mathscr{X}$ asymmetry is generated and which in certain cases may be taken to be the reheat temperature.

For the asymmetry to be transferred we require that $\Delta_X(T) \ll \Delta_X^{\rm init}$, thus

$$\Delta_X(T) \sim \Delta_X^{\rm init} \times 10^{-9} \exp\left[2\left(1-\left(\frac{\rm GeV}{T}\right)^2\left(\frac{\Gamma_X}{10^{-18}\ {\rm GeV}}\right)\left(\frac{10}{\sqrt{g_*}}\right)\right)\right] . \tag{6.24}$$

For instance, for the asymmetry to be transferred via X decays prior to $T \sim$ GeV (assuming that the visible and hidden sectors maintain comparable temperatures) the width must be $\Gamma \sim 10^{-18}$ GeV and, hence, the lifetime of X is $\tau \sim 10^{-6}$ s. Conversely, to ensure that the asymmetry is transferred before BBN at $T \sim$MeV one requires $\Gamma \sim 10^{-24}$ GeV, hence $\tau \sim 1\ s$, as expected. In the case that the temperatures between the sectors undergo different thermal evolutions then $R \equiv T_{\rm vis}/T_{\rm gen} \neq 1$ and the above equation will depend on this quantity

$$\Delta_X(T) \sim \Delta_X^{\rm init} \times 10^{-9} \exp\left[2\left(1-\left(\frac{\rm GeV}{T_{\rm vis}}\right)^2\left(\frac{R}{100}\right)^2\left(\frac{\Gamma_X}{10^{-22}\ {\rm GeV}}\right)\left(\frac{10}{\sqrt{g_*}}\right)\right)\right] . \tag{6.25}$$

Further, by conservation of the combination of quantum number $B-L+X$ it follows that $\eta_X \propto -\eta_B \propto -\eta_\zeta$. Moreover, for two body X decays or in the case that ζ does not carry a conserved charge (e.g. for self-conjugate ζ) then $\eta_X = -\eta_B$, which is

clear from analysis of the corresponding Boltzmann equation

$$\begin{aligned}\dot{n}_B + 3Hn_B = &\int \mathrm{d}\Pi_X \mathrm{d}\Pi_b \mathrm{d}\Pi_\zeta (2\pi)^4 \delta^{(4)}(p_X - p_b - p_\zeta) \left[|M|^2_{X\to b\zeta} f_X - |M|^2_{b\zeta\to X} f_b f_\zeta\right] \\ &- \int \mathrm{d}\Pi_X \mathrm{d}\Pi_b \mathrm{d}\Pi_\zeta (2\pi)^4 \delta^{(4)}(p_X - p_b - p_\zeta) \left[|M|^2_{\overline{X}\to \overline{b\zeta}} f_{\overline{X}} - |M|^2_{\overline{b\zeta}\to \overline{X}} f_{\bar{b}} f_{\bar{\zeta}}\right]\end{aligned} \tag{6.26}$$

Then, similarly to previously, as $f_\zeta \approx f_{\bar{\zeta}} \approx 0$ this reduces to

$$\dot{\Delta}_B \simeq \frac{1}{s}\int \mathrm{d}\Pi_X 2m_X \Gamma_X \left(f_X - f_{\overline{X}}\right) \simeq -\dot{\Delta}_X \ , \tag{6.27}$$

where the final equality can be seen by comparison to eq. (6.18). A similar argument can be made for the $\mathscr{X}$ asymmetry inherited by the ζ states in the case that they carry $\mathscr{X}$ number. On the other hand, in the case that the relic DM ζ is self-conjugate then the Boltzmann equation which describes their evolution is

$$\begin{aligned}\dot{n}_\zeta + 3Hn_\zeta = &\int \mathrm{d}\Pi_X \mathrm{d}\Pi_b \mathrm{d}\Pi_\zeta (2\pi)^4 \delta^{(4)}(p_X - p_b - p_\zeta) \left[|M|^2_{X\to b\zeta} f_X - |M|^2_{b\zeta\to X} f_b f_\zeta\right] \\ &+ \int \mathrm{d}\Pi_X \mathrm{d}\Pi_b \mathrm{d}\Pi_\zeta (2\pi)^4 \delta^{(4)}(p_X - p_b - p_\zeta) \left[|M|^2_{\overline{X}\to \bar{b}\zeta} f_{\overline{X}} - |M|^2_{\bar{b}\zeta\to \overline{X}} f_{\bar{b}} f_\zeta\right]\end{aligned} \tag{6.28}$$

Thus, following analogous steps to (6.18)-(6.21), this implies

$$\dot{Y}_\zeta \simeq \Gamma_X \left(\frac{n_X + n_{\overline{X}}}{s}\right) \simeq \Gamma_X \Delta_X \simeq -\dot{\Delta}_X \ , \tag{6.29}$$

where in the intermediate step we have written $n_X + n_{\overline{X}} = s\Delta_X + 2n_{\overline{X}}$ and used that $n_{\overline{X}} \approx 0$. These results conform with our expectations, as outlined in the previous sections and as depicted in Fig. 13. Note that washout effects enter only at order λ^2 and higher in the feeble trisector coupling and thus can be neglected.

6.4 Exodus in the MSSM

Next we present a simple SUSY realisation which offers a resolution to the well known problem of obtaining the correct relic abundance for (nearly) pure bino DM. The bino generally falls foul of relic density constraints since its annihilation cross section is p-wave suppressed.[6] However, in the exodus mechanism the relic density is not set by the annihilation cross section and the bino can provide a viable DM candidate. In this section we consider an implementation of the exodus framework in which the MSSM is appended with a genesis sector, we will not provide a full description of this sector, but we assume that it contains a SM singlet chiral superfield $\boldsymbol{X}$ which carries a conserved quantum number $\mathscr{X} = 1$ with a particle-antiparticle asymmetry.

If the inflaton decays preferentially to the genesis sector, it is conceivable that the reheat temperature of the genesis sector could be much higher than the visible sector $T^{\rm RH}_{\rm vis} \ll T^{\rm RH}_{\rm gen}$. If the reheat temperature of the visible sector is lower than the mass of the LSP then (initially) there will be no abundance of R_p odd states. Moreover, if the genesis sector is heated to temperature greater than the lightest R_p odd state in the genesis sector, then visible sector superpartners can be generated through the decays from the genesis sector. This realises the exodus mechanism with the set of R_p odd states identified with the relic sector and where the reheat temperatures of the relic and visible sectors are equal.

Little is known about the reheat temperature of the universe after inflation apart from that it should be higher than the temperature of BBN (few MeV). In order to construct a viable model of bino DM via exodus production we require that the following

[6] However, it is possible to have phenomenologically viable bino DM with the relic density due to freeze-out if the bino can annihilate via slepton coannihilation or Z-resonance [46, 167].

hierarchy is respected

$$T_{\rm vis}^{\rm RH} \ll m_{\rm LSP} < m_X < T_{\rm gen}^{\rm RH} \ . \tag{6.30}$$

This ensures that the bino is not thermally produced (as discussed in Sect. 6.2.2) and that there is initially a thermal abundance of X states. In minimal models we expect that $m_{\rm LSP} \sim 5$ GeV in order to explain $\Omega_{\rm LSP} \approx 5\Omega_B$ and thus we require $T_{\rm vis}^{\rm RH} < m_{\rm LSP}/25 \sim 200$ MeV. For a 5 GeV neutralino LSP to be phenomenologically viable the state must be essentially purely bino in order to avoid direct production limits and invisible quarkonium decays [168, 170, 171]. Aspects of light bino phenomenology has been studied in [46, 220, 223, 224].

The temperature of the early universe was certainly in excess of a few MeV at some stage, as a colder universe would alter the relative abundance of nucleons and deviations in these quantities are very restricted [199–202]. There are two possible cosmological histories which could be realised in this model depending on the reheat temperature of the visible sector. In order to avoid observable deviations from BBN predications we require that either $T_{\rm vis}^{\rm RH} >$ few MeV or, if $T_{\rm vis}^{\rm RH} \lesssim$ MeV, that the energy injection due to X decays must be sufficient to raise the temperature of the visible sector such that primordial nucleons are destroyed ($T_{\rm vis} \gtrsim 100$ MeV), otherwise there is a risk that the experimentally verified ratios of nucleons may be disrupted. In the latter scenario, the requirement that energy injection heats the visible sector to $T_{\rm vis}^{\rm RH} \gg 1$ MeV, combined with the condition that the energy injection must not lead to thermal bino production, results in a window for viable models and allows predictive scenarios to be constructed. Referring to the calculation of Sect. 6.2.2, the temperature of the bino DM generated through X decays for a 5 GeV bino LSP is parametrically $T_{\rm vis}^{(\infty)} \sim ((m_X/6\ {\rm GeV})^2 - 1)$ GeV and, for an appropriate value of m_X, X decays are sufficient to heat the visible sector to $T_{\rm vis} \gtrsim 100$ MeV.

Additionally, it must be that the X states generally decay well before the universe cools to $T \sim$MeV and that there are very few residual X decays after this point, since injection of hadronic energy during BBN is greatly constrained [199–202]. Suppose that the exodus mechanism proceeds via the portal operator $\epsilon_{jk}\boldsymbol{X}\boldsymbol{U}_i\boldsymbol{D}_j\boldsymbol{D}_k$, where i, j, k are generation indices. Under the generalised definition of R-parity, $R_p = (-1)^{2s+3(B-L+\mathscr{X})}$, the $\boldsymbol{X}$ scalar (denoted ϕ_X) is R_p odd. The asymmetric component of the hidden sector state ϕ_X decays via a dimension five B-violating interaction producing an (off-shell) squark which subsequently decays to the bino LSP, as shown in Fig. 15. Note that this is the lowest dimension B-violating trisector portal operator which can be constructed. The decay width due to this interaction is parametrically

$$\Gamma_X \sim \frac{\lambda^2 g'^2}{m_{\tilde{q}}^4} \frac{\Delta^7}{512\pi^5} \frac{1}{M^2} \ , \tag{6.31}$$

where $\Delta \equiv m_X - m_{\rm LSP} - m_b$, the baryonic decay product has mass $m_b \simeq 1$ GeV, and the operator $\epsilon_{jk}\boldsymbol{X}\boldsymbol{U}_i\boldsymbol{D}_j\boldsymbol{D}_k$ is dressed by the scale M in the Lagrangian. Therefore typically the size for the decay width is

$$\Gamma_X \sim 10^{-22}\ \text{GeV} \left(\frac{\Delta}{5\ \text{GeV}}\right)^7 \left(\frac{1.5\ \text{TeV}}{m_{\tilde{q}}}\right)^4 \left(\frac{\lambda}{1}\right)^2 \left(\frac{10^4\ \text{GeV}}{M}\right)^2 \ , \tag{6.32}$$

which corresponds to a lifetime $\tau_X \sim 10^{-2}$ s, with the indicated choices of parameters, and thus models is which the X states decay before BBN can be constructed. Note that here the B-violating operator is suppressed by a scale $M \sim 10$ TeV and therefore we do not expect collider constraints on this contact operator. Furthermore, order of magnitude changes in scale M can be accommodated given $\mathcal{O}(1)$ changes in Δ.

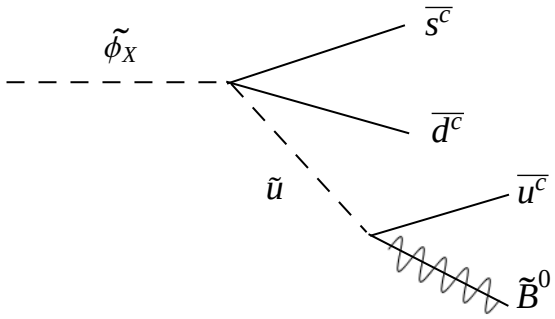

Figure 15. A bino LSP provides good candidate for exodus dark matter.

6.5 Discussion

In this chapter we have outlined a new framework for explaining the observed relation $\Omega_{\rm DM} \approx 5\Omega_B$. The exodus scenario assumes that the number density of the DM state is initially near-zero and is only generated due to decays from a second hidden sector possessing a particle-antiparticle asymmetry. This produces DM and generates a $B-L$ asymmetry, resulting finally in the observed baryon asymmetry. In contrast to models of ADM, the DM can be a real scalar or Majorana fermion, thus presenting distinct phenomenology. In particular, models of ADM can not typically have annihilation signals, however, if the exodus DM state ζ is a real scalar or Majorana fermion DM annihilations can occur, and thus potentially produce observable indirect detection signals with annihilation profiles [225].

Furthermore, in traditional models of ADM the symmetric component of the DM must annihilate in order for the asymmetry to set the relic density and this leads to strong constraints. As discussed in earlier chapters, these limits rule out large classes of models if the symmetric component annihilates directly to the visible sector and there may remain strong constraints on annihilations to light hidden sector states from DM self-interactions. In contradistinction, the genesis sector states X of exodus

models, which possess a particle-antiparticle asymmetry, can have large annihilation cross sections to the visible sector or to light hidden sector states whilst avoiding these bounds, since the DM relic density is not composed of the X states, but rather the relic sector states ζ (which do not necessarily carry an asymmetry). Thus the exodus mechanism detailed here avoids the tension between experimental searches for DM interactions and relic density constraints of traditional ADM models discussed in previous chapters. One potential observable of annihilations to light hidden sector states is that this could increase the effective number of neutrino species, similar to as studied in [226]. Some further comments concerning this scenario appear in [3].

7 Summary and Closing Remarks

This thesis has studied various aspects of asymmetric dark matter and related scenarios. In particular, we have highlighted the tension between direct searches for DM and efficient annihilation of the symmetric component of DM-antiDM pairs required for the DM relic density to be set by the DM asymmetry rather than by conventional freeze-out. In Chap. 3 we outlined the symmetric component problem in detail and we presented a careful study of the case where ADM annihilates to quarks via heavy mediators, for which an effective field theory approach is valid. It was demonstrated that this scenario is effectively excluded for all models due to null search results from the LHC and DM direct detection experiments. Subsequently, in Chap. 4 & 5 we went beyond the simplified effective field theory and examined, respectively, the case of light mediators, and the scenario in which the symmetric component annihilates dominantly to light states in the hidden sector.

The contact operator description used in Chap. 3 breaks down for mediator masses comparable to LHC energies as resonance and mass threshold effects become important in determining the exclusion limits. It was seen in Chap. 4 that with light mediators, successful models of ADM can be constructed, in particular collider limits are greatly ameliorated in this case. However, in models where the scattering cross sections are unsuppressed (by velocity or momentum transfer) stringent constraints remain from direct detection, which are generally only satisfied for resonantly enhanced annihilations. Further, it was argued that light pseudoscalars provides an attractive possibility as such states are well motivated, since they naturally occur in the context of pseudo-Nambu-Goldstone bosons, and the experimental bounds can be more readily satisfied as the scattering cross section, thus direct detection bounds, are heavily suppressed.

Alternatively, the symmetric component could annihilate to light hidden sector states. In Chap. 5 we considered the case where these light hidden sector states are stable. In this scenario the tension between direct searches and efficient annihilation of the symmetric component is evaded as the annihilation cross section and the DM-nucleon scattering cross section are no longer directly connected. However, the annihilation cross section is now related to the DM-DM scattering cross section and thus limits on DM self-interactions can lead to renewed tension with the successful depletion of the symmetric component. We argued that whilst DM self-interaction bounds coming from the observation of elliptical halos strongly constrain the case where the light hidden sector states are scalars, these limits are much weaker for pseudoscalars and this scenario is a viable and well motivated possibility for realising models of ADM. It could also be that the light hidden states late decay to the visible sector, this scenario still decouples the direct search constraints and the relic density requirements, but may lead to observable cosmological signals due to energy injection in the early universe. This latter case will be discussed further in a forthcoming publication [2].

In Chap. 6 we outlined an interesting variant on the traditional ADM framework, which allows for self-conjugate DM with the relic density set by an asymmetry (in contrast to standard ADM models) and also evades the symmetric component problem. It is important that the DM can be self-conjugate since it allows for distinct phenomenology compared to other ADM models. In particular it is possible to produce indirect detection signals from DM annihilations, which are not generally expected in ADM models. Thus signatures of annihilating DM with a mass of 1-10 GeV would be a good indication that this mechanism may be realised in nature. Notably indirect detection signals for decaying DM and annihilating DM have different morphologies as the decays depend linearly on the DM density, whereas annihilations have a quadratic dependence

[227, 228]. The exodus mechanism of Chap. 6 evades the symmetric component problem which strongly constrains other ADM constructions since the annihilation of the symmetric component occurs in a meta-stable particle species which then later decays to the DM. Thus the limits on DM scattering cross sections do not bound the efficient removal of the symmetric component. It would be interesting to study this setting in further detail and investigate other possible realisations in future work.

Before concluding this thesis it is interesting to briefly note the status of searches for light DM at the time of writing. In April 2013 the CDMS collaboration [53] reported the observation of three nuclear recoil events in their silicon detectors consistent with DM-nucleon scattering (at roughly 2-3σ significance), suggestive of a DM state with mass around 5-20 GeV and scattering cross section $\sim 10^{-41}$ cm^2. Further, the CoGeNT collaboration [51] have also presented possible hints of DM which are aligned with the CDMS region; their tentative signal corresponds to 7-10 GeV DM with a cross section comparable to the CDMS signal.[7] Whilst a proportion of the CDMS signal region is in tension with exclusion bounds from Xenon100, it has been claimed that under mild variation of certain assumptions and approximations that this can be alleviated to some degree [229–233]. It is expected that this region of parameter space can be independently probed at several new direct detection experiments, in particular LUX, COUPP, and SuperCDMS, due to report in the near future. Finally, we remark that it has also been suggested that certain indirect detection signals from the galactic centre could be indicative of annihilating 1-10 GeV DM [234, 235]. Notably, in most formulations of ADM annihilations do not occur as the DM is non-self-conjugate and the abundance of $\overline{X}$ is negligible. However, such a signature could arise if the DM is produced via the exodus mechanism of Chap. 6 and this possibility is worth investigating further.

[7] Additionally, CRESST [52] and DAMA/LIBRA [49, 50] also have presented possible hints of light mass DM, however these are more challenging to reconcile with other experiments.

Given the increasing tension on the traditional WIMP framework from direct detection and (SUSY) collider searches, the theoretical motivation for ADM as an attempt to explain the observed coincidence $\Omega_{\rm DM} \simeq 5\Omega_B$, and the tantalising hints of light DM in direct detection experiments, ADM is fast becoming a serious competitor to the 'WIMP miracle'. Moreover, should the current tentative signals of light DM be verified in the future, then it is likely that ADM may become the standard paradigm in our attempt to understand the structure of the dark sector. There are still many interesting aspect of ADM to investigate, and indeed some intriguing possibilities for future research directions have been alluded to in this work.

References

[1] J. March-Russell, J. Unwin and S. M. West, *Closing in on Asymmetric Dark Matter I: Model independent limits for interactions with quarks,* JHEP **1208** (2012) 029, arXiv:1203.4854 [hep-ph].

[2] J. March-Russell, J. Unwin and S. M. West, *Asymmetric Dark Matter: Self-Interactions and Light Pseudoscalars*, forthcoming.

[3] J. Unwin, *Exodus: Hidden origin of dark matter and baryons,* JHEP **1306** (2013) 090, arXiv:1212.1425 [hep-ph].

[4] U. Haisch, F. Kahlhoefer and J. Unwin, *The impact of heavy-quark loops on LHC dark matter searches,* JHEP **1307** (2013) 125, arXiv:1208.4605 [hep-ph].

[5] J. Unwin, *R-symmetric High Scale Supersymmetry,* Phys. Rev. D **86** (2012) 095002, arXiv:1210.4936 [hep-ph].

[6] E. Hardy, J. March-Russell and J. Unwin, *Precision Unification in λ SUSY with a 125 GeV Higgs,* JHEP **1210** (2012) 072, arXiv:1207.1435 [hep-ph].

[7] J. Unwin, *A Sharp 141 GeV Higgs Prediction from Environmental Selection,* arXiv:1110.0470 [hep-ph].

[8] J. Unwin, *Vacuum stability and the Cholesky decomposition,* Eur. Phys. J. C **71** (2011) 1663, arXiv:1102.2896 [hep-ph].

[9] D. S. Gorbunov and V. A. Rubakov, *Introduction to the theory of the early universe: Hot big bang theory,* Hackensack, USA: World Scientific (2011)

[10] E. W. Kolb and M. S. Turner, *The Early universe,* Front. Phys. **69** (1990) 1.

[11] F. Zwicky, *Spectral displacement of extra galactic nebulae,* Helv.Phys.Acta **6** (1933) 110.

[12] K.G. Begeman, A.H. Broeils and R.H. Sanders, *Extended rotation curves of spiral galaxies: Dark haloes and modified dynamics,* Mon.Not.Roy.Astron.Soc. **249** (1991) 523.

[13] M. Markevitch, A. H. Gonzalez, D. Clowe, A. Vikhlinin, L. David, W. Forman, C. Jones and S. Murray *et al.*, *Direct constraints on the dark matter self-interaction cross-section from the merging galaxy cluster 1E0657-56,* Astrophys. J. **606** (2004) 819, astro-ph/0309303.

[14] D. Clowe, M. Bradac, A. H. Gonzalez, M. Markevitch, S. W. Randall, C. Jones and D. Zaritsky, *A direct empirical proof of the existence of dark matter,* Astrophys. J. **648** (2006) L109, astro-ph/0608407.

[15] **MACHO Collaboration**, C. Alcock *et al. The MACHO project: Microlensing results from 5.7 years of LMC observations,* Astrophys. J. **542** (2000) 281, astro-ph/0001272.

[16] **EROS-2 Collaboration**, P. Tisserand *et al. Limits on the Macho Content of the*

Galactic Halo from the EROS-2 Survey of the Magellanic Clouds, Astron. Astrophys. **469** (2007) 387, astro-ph/0607207.

[17] M. Bartelmann and P. Schneider, *Weak gravitational lensing,* Phys. Rept. **340** (2001) 291, astro-ph/9912508.

[18] J. Miralda-Escude, *A test of the collisional dark matter hypothesis from cluster lensing,* astro-ph/0002050.

[19] G. Hinshaw, D. Larson, E. Komatsu, D. N. Spergel, C. L. Bennett, J. Dunkley, M. R. Nolta and M. Halpern *et al.*, *Nine-Year Wilkinson Microwave Anisotropy Probe (WMAP) Observations: Cosmological Parameter Results,* arXiv:1212.5226 [astro-ph.CO].

[20] J. F. Navarro, C. S. Frenk and S. D. M. White, *The Structure of cold dark matter halos,* Astrophys. J. **462** (1996) 563, astro-ph/9508025.

[21] J. Preskill, M. B. Wise and F. Wilczek, *Cosmology of the Invisible Axion,* Phys. Lett. B **120** (1983) 127.

[22] M. Dine and W. Fischler, *The Not So Harmless Axion,* Phys. Lett. B **120** (1983) 137.

[23] L. F. Abbott and P. Sikivie, *A Cosmological Bound on the Invisible Axion,* Phys. Lett. B **120** (1983) 133.

[24] J. E. Kim and G. Carosi, *Axions and the Strong CP Problem,* Rev. Mod. Phys. **82** (2010) 557 [arXiv:0807.3125 [hep-ph]].

[25] L. J. Hall, K. Jedamzik, J. March-Russell and S. M. West, *Freeze-In Production of FIMP Dark Matter,* JHEP **1003**, 080 (2010), arXiv:0911.1120 [hep-ph].

[26] T. Moroi, H. Murayama and M. Yamaguchi, *Cosmological constraints on the light stable gravitino,* Phys. Lett. B **303** (1993) 289.

[27] R. D. Peccei and H. R. Quinn, *CP Conservation in the Presence of Instantons,* Phys. Rev. Lett. **38** (1977) 1440.

[28] **The Particle Data Group Collaboration**, J. Beringer *et al.*, *Review of Particle Physics (RPP),* Phys. Rev. D **86** (2012) 010001.

[29] G. 't Hooft, *Naturalness, chiral symmetry, and spontaneous chiral symmetry breaking,* NATO Adv. Study Inst. Ser. B Phys. **59** (1980) 135.

[30] S. Weinberg, *A New Light Boson?,* Phys. Rev. Lett. **40** (1978) 223.

[31] F. Wilczek, *Problem of Strong p and t Invariance in the Presence of Instantons,* Phys. Rev. Lett. **40** (1978) 279.

[32] M. Dine, W. Fischler and M. Srednicki, *A Simple Solution to the Strong CP Problem with a Harmless Axion,* Phys. Lett. B **104** (1981) 199.

[33] A. R. Zhitnitsky, *On Possible Suppression of the Axion Hadron Interactions.* Sov. J. Nucl. Phys. **31** (1980) 260 [Yad. Fiz. **31** (1980) 497].

[34] J. E. Kim, *Weak Interaction Singlet and Strong CP Invariance,* Phys. Rev. Lett. **43** (1979) 103.

[35] M. A. Shifman, A. I. Vainshtein and V. I. Zakharov, *Can Confinement Ensure Natural CP Invariance of Strong Interactions?,* Nucl. Phys. B **166** (1980) 493.

[36] J. Engel, D. Seckel and A. C. Hayes, *Emission and detectability of hadronic axions from SN1987A,* Phys. Rev. Lett. **65** (1990) 960.

[37] G. G. Raffelt, *Astrophysical axion bounds,* Lect. Notes Phys. **741** (2008) 51 [hep-ph/0611350].

[38] S. P. Martin, *A Supersymmetry primer,* In *Kane, G.L. (ed.): Perspectives on supersymmetry II* 1-153, hep-ph/9709356.

[39] L. E. Ibanez and G. G. Ross, *$SU(2)_L\times$ U(1) Symmetry Breaking as a Radiative Effect of Supersymmetry Breaking in Guts,* Phys. Lett. B **110** (1982) 215.

[40] L. Alvarez-Gaume, M. Claudson and M. B. Wise, *Low-Energy Supersymmetry,* Nucl. Phys. B **207** (1982) 96.

[41] K. Inoue, A. Kakuto, H. Komatsu and S. Takeshita, *Aspects of Grand Unified Models with Softly Broken Supersymmetry,* Prog. Theor. Phys. **68**, 927 (1982) [Erratum-ibid. **70**, 330 (1983)] [Prog. Theor. Phys. **70**, 330 (1983)].

[42] S. Dimopoulos, S. Raby and F. Wilczek, *Supersymmetry and the Scale of Unification,* Phys. Rev. D **24** (1981) 1681.

[43] H. Georgi and S. L. Glashow, *Unity of All Elementary Particle Forces,* Phys. Rev. Lett. **32** (1974) 438.

[44] G. Jungman, M. Kamionkowski and K. Griest, *Supersymmetric dark matter,* Phys. Rept. **267** (1996) 195, hep-ph/9506380.

[45] **The XENON100 Collaboration**, E. Aprile *et al.*, *Dark Matter Results from 100 Live Days of XENON100 Data,* Phys. Rev. Lett. **107** (2011) 131302, arXiv:1104.2549.

[46] C. Boehm, P. S. B. Dev, A. Mazumdar and E. Pukartas, *Naturalness of Light Neutralino Dark Matter in pMSSM after LHC, XENON100 and Planck Data,* JHEP **1306** (2013) 113, arXiv:1303.5386 [hep-ph].

[47] J. R. Ellis, S. F. King and J. P. Roberts, *The Fine-Tuning Price of Neutralino Dark Matter in Models with Non-Universal Higgs Masses,* JHEP **0804** (2008) 099, arXiv:0711.2741 [hep-ph].

[48] M. Perelstein and B. Shakya, *Fine-Tuning Implications of Direct Dark Matter Searches in the MSSM,* JHEP **1110** (2011) 142, arXiv:1107.5048 [hep-ph].

[49] **The DAMA Collaboration**, R. Bernabei *et al.*, *First results from DAMA/LIBRA and the combined results with DAMA/NaI,* Eur. Phys. J. C **56** (2008) 333, arXiv:0804.2741 [astro-ph].

[50] **The DAMA and LIBRA Collaborations**, R. Bernabei *et al.*, *New results from DAMA/LIBRA,* Eur. Phys. J. C **67** (2010) 39, arXiv:1002.1028 [astro-ph.GA].

[51] **The CoGeNT Collaboration**, C. E. Aalseth *et al.*, *Results from a Search for Light-Mass Dark Matter with a P-type Point Contact Germanium Detector,* Phys. Rev.

Lett. **106** (2011) 131301, arXiv:1002.4703 [astro-ph.CO].

[52] **The CRESST Collaboration**, G. Angloher, M. Bauer, I. Bavykina, A. Bento, C. Bucci, C. Ciemniak, G. Deuter and F. von Feilitzsch *et al.*, *Results from 730 kg days of the CRESST-II Dark Matter Search,* Eur. Phys. J. C **72** (2012) 1971, arXiv:1109.0702.

[53] **The CDMS Collaboration**, R. Agnese *et al.*, *Dark Matter Search Results Using the Silicon Detectors of CDMS II,* arXiv:1304.4279 [hep-ex].

[54] S. Nussinov, *Technocosmology: Could A Technibaryon Excess Provide A 'Natural' Missing Mass Candidate?,* Phys. Lett. B **165**, 55 (1985).

[55] R.S. Chivukula, T.P. Walker, *Technicolor Cosmology,* Nucl. Phys. **B329** (1990) 445.

[56] S. M. Barr, R. S. Chivukula and E. Farhi, *Electroweak fermion number violation and the production of stable particles in the early universe,* Phys. Lett. B **241**, 387 (1990).

[57] G. B. Gelmini, L. J. Hall, and M. J. Lin, *What is the cosmion?* Nucl. Phys. B281 (1987) 726.

[58] D. B. Kaplan, *A Single explanation for both the baryon and dark matter densities,* Phys. Rev. Lett. **68**, 741 (1992).

[59] D. Hooper, J. March-Russell and S. M. West, *Asymmetric sneutrino dark matter and the Omega(b)/Omega(DM) puzzle,* Phys. Lett. B **605**, 228 (2005), hep-ph/0410114.

[60] R. Kitano and I. Low, *Dark matter from baryon asymmetry,* Phys. Rev. D **71**, 023510 (2005), hep-ph/0411133.

[61] N. Cosme, L. Lopez Honorez and M. H. G. Tytgat, *Leptogenesis and dark matter related?,* Phys. Rev. D **72**, 043505 (2005), hep-ph/0506320.

[62] G. R. Farrar and G. Zaharijas, *Dark matter and the baryon asymmetry,* Phys. Rev. Lett. **96**, 041302 (2006), hep-ph/0510079.

[63] D. Suematsu, *Nonthermal production of baryon and dark matter,* Astropart. Phys. **24**, 511 (2006), hep-ph/0510251.

[64] M. H. G. Tytgat, *Relating leptogenesis and dark matter,* hep-ph/0606140.

[65] D. E. Kaplan, M. A. Luty and K. M. Zurek, *Asymmetric Dark Matter,* Phys. Rev. D **79**, 115016 (2009), arXiv:0901.4117 [hep-ph].

[66] D. E. Kaplan, G. Z. Krnjaic, K. R. Rehermann and C. M. Wells, *Atomic Dark Matter,* JCAP **1005** (2010) 021, arXiv:0909.0753 [hep-ph].

[67] T. Cohen and K. M. Zurek, *Leptophilic Dark Matter from the Lepton Asymmetry,* Phys. Rev. Lett. **104** (2010) 101301, arXiv:0909.2035 [hep-ph].

[68] A. L. Fitzpatrick, D. Hooper and K. M. Zurek, *Implications of CoGeNT and DAMA for Light WIMP Dark Matter,* Phys.Rev.D **81** (2010) 115005, arXiv:1003.0014 [hep-ph].

[69] C. Cheung and K. M. Zurek, *Affleck-Dine Cogenesis,* arXiv:1105.4612 [hep-ph].

[70] T. Lin, H. -B. Yu and K. M. Zurek, *On Symmetric and Asymmetric Light Dark Matter,* Phys. Rev. D **85** (2012) 063503, arXiv:1111.0293 [hep-ph].

[71] S. D. McDermott, H. B. Yu and K. M. Zurek, *Constraints on Scalar Asymmetric Dark Matter from Black Hole Formation in Neutron Stars,* Phys. Rev. D **85** (2012), arXiv:1103.5472 [hep-ph].

[72] T. Cohen, D. J. Phalen, A. Pierce, K. M. Zurek, *Asymmetric Dark Matter from a GeV Hidden Sector,* Phys. Rev. **D82** (2010) 056001, arXiv:1005.1655 [hep-ph].

[73] K. M. Zurek, *Asymmetric Dark Matter: Theories, Signatures, and Constraints,* arXiv:1308.0338 [hep-ph].

[74] S. Tulin, H. -B. Yu and K. M. Zurek, *Oscillating Asymmetric Dark Matter,* JCAP **1205** (2012) 013, arXiv:1202.0283 [hep-ph].

[75] D. E. Morrissey, D. Poland and K. M. Zurek, *Abelian Hidden Sectors at a GeV,* JHEP **0907** (2009) 050, arXiv:0904.2567 [hep-ph].

[76] J. Shelton and K. M. Zurek, *Darkogenesis,* Phys. Rev. D **82** (2010) 123512, arXiv:1008.1997 [hep-ph].

[77] N. Haba and S. Matsumoto, *Baryogenesis from Dark Sector,* Prog. Theor. Phys. **125** (2011) 1311, arXiv:1008.2487 [hep-ph].

[78] M. R. Buckley and L. Randall, *Xogenesis,* JHEP **1109** (2011) 009, arXiv:1009.0270.

[79] E. J. Chun, *Leptogenesis origin of Dirac gaugino dark matter,* Phys. Rev. D **83** (2011) 053004, arXiv:1009.0983 [hep-ph].

[80] P. H. Gu, M. Lindner, U. Sarkar and X. Zhang, *WIMP Dark Matter and Baryogenesis,* Phys. Rev. D **83** (2011) 055008, arXiv:1009.2690 [hep-ph].

[81] B. Dutta, J. Kumar, *Asymmetric Dark Matter from Hidden Sector Baryogenesis,* Phys. Lett. **B699**, 364-367 (2011), arXiv:1012.1341 [hep-ph].

[82] M. Blennow, B. Dasgupta, E. Fernandez-Martinez and N. Rius, *Aidnogenesis via Leptogenesis and Dark Sphalerons,* JHEP **1103** (2011) 014, arXiv:1009.3159 [hep-ph].

[83] A. Falkowski, J. T. Ruderman and T. Volansky, *Asymmetric Dark Matter from Leptogenesis,* JHEP **1105** (2011) 106, arXiv:1101.4936 [hep-ph].

[84] Z. Kang and T. Li, *Asymmetric Origin for Gravitino Relic Density in the Hybrid Gravity-Gauge Mediated Supersymmetry Breaking,* arXiv:1111.7313 [hep-ph].

[85] G. Kane, J. Shao, S. Watson and H. -B. Yu, *The Baryon-Dark Matter Ratio Via Moduli Decay After Affleck-Dine Baryogenesis,* JCAP **1111** (2011) 012, arXiv:1108.5178.

[86] S. D. Thomas, *Baryons and dark matter from the late decay of a supersymmetric condensate,* Phys. Lett. B **356** (1995) 256, hep-ph/9506274.

[87] R. Allahverdi, B. Dutta and K. Sinha, *Cladogenesis: Baryon-Dark Matter Coincidence from Branchings in Moduli Decay,* Phys. Rev. D **83** (2011) 083502, arXiv:1011.1286

[88] K. Kohri, A. Mazumdar, N. Sahu and P. Stephens, *Probing Unified Origin of Dark Matter and Baryon Asymmetry at PAMELA/Fermi,* Phys. Rev. D **80**, 061302 (2009), arXiv:0907.0622 [hep-ph].

[89] C. Arina and N. Sahu, *Asymmetric Inelastic Inert Doublet Dark Matter from Triplet Scalar Leptogenesis,* Nucl. Phys. B **854**, 666 (2012), arXiv:1108.3967 [hep-ph].

[90] A. Belyaev, M. T. Frandsen, S. Sarkar and F. Sannino, *Mixed dark matter from technicolor,* Phys. Rev. D **83** (2011) 015007, arXiv:1007.4839 [hep-ph].

[91] M. T. Frandsen, S. Sarkar and K. Schmidt-Hoberg, *Light asymmetric dark matter from new strong dynamics,* Phys. Rev. D **84** (2011) 051703, arXiv:1103.4350 [hep-ph].

[92] K. Petraki and R. R. Volkas, *Review of asymmetric dark matter,* arXiv:1305.4939.

[93] J. J. Heckman and S. -J. Rey, *Baryon and Dark Matter Genesis from Strongly Coupled Strings,* JHEP **1106** (2011) 120, arXiv:1102.5346 [hep-th].

[94] W. -Z. Feng, P. Nath and G. Peim, *Cosmic Coincidence and Asymmetric Dark Matter in a Stueckelberg Extension,* Phys. Rev. D **85** (2012) 115016, arXiv:1204.5752 [hep-ph].

[95] P. Fileviez Perez and M. B. Wise, *Baryon Asymmetry and Dark Matter Through the Vector-Like Portal,* JHEP **1305** (2013) 094, arXiv:1303.1452 [hep-ph].

[96] I. Goldman, R. N. Mohapatra, S. Nussinov, D. Rosenbaum and V. Teplitz, *Possible Implications of Asymmetric Fermionic Dark Matter for Neutron Stars,* arXiv:1305.6908.

[97] E. Del Nobile, C. Kouvaris and F. Sannino, *Interfering Composite Asymmetric Dark Matter for DAMA and CoGeNT,* Phys. Rev. D **84** (2011) 027301, arXiv:1105.5431.

[98] P. -H. Gu, *From Dirac neutrino masses to baryonic and dark matter asymmetries,* Nucl. Phys. B **872** (2013) 38, arXiv:1209.4579 [hep-ph].

[99] R. Lewis, C. Pica and F. Sannino, *Light Asymmetric Dark Matter on the Lattice: SU(2) Technicolor with Two Fundamental Flavors,* Phys. Rev. D **85** (2012) 014504, arXiv:1109.3513 [hep-ph].

[100] M. Ibe, S. Matsumoto and T. T. Yanagida, *The GeV-scale dark matter with B-L asymmetry,* Phys. Lett. B **708** (2012) 112, arXiv:1110.5452 [hep-ph].

[101] G. B. Gelmini, J. -H. Huh and T. Rehagen, *Asymmetric dark matter annihilation as a test of non-standard cosmologies,* arXiv:1304.3679 [hep-ph].

[102] M. Cirelli, P. Panci, G. Servant and G. Zaharijas, *Consequences of DM/antiDM Oscillations for Asymmetric WIMP Dark Matter,* JCAP **1203** (2012) 015, arXiv:1110.3809 [hep-ph].

[103] M. R. Buckley and S. Profumo, *Regenerating a Symmetry in Asymmetric Dark Matter,* Phys. Rev. Lett. **108** (2012) 011301, arXiv:1109.2164 [hep-ph].

[104] K. Kamada and M. Yamaguchi, *Asymmetric Dark Matter from Spontaneous Cogenesis in the Supersymmetric Standard Model,* Phys. Rev. D **85** (2012) 103530 arXiv:1201.2636.

[105] K. Blum, A. Efrati, Y. Grossman, Y. Nir and A. Riotto, *Asymmetric Higgsino Dark Matter,* Phys. Rev. Lett. **109** (2012) 051302, arXiv:1201.2699 [hep-ph].

[106] R. Foot and R. R. Volkas, *Was ordinary matter synthesized from mirror matter? An Attempt to explain why Omega(Baryon) approximately equal to 0.2 Omega(Dark),* Phys. Rev. D **68** (2003) 021304, hep-ph/0304261.

[107] T. R. Dulaney, P. Fileviez Perez and M. B. Wise, *Dark Matter, Baryon Asymmetry, and Spontaneous B and L Breaking,* Phys. Rev. D **83** (2011) 023520, arXiv:1005.0617.

[108] N. Bernal, S. Colucci, F. -X. Josse-Michaux, J. Racker and L. Ubaldi, *On baryogenesis from dark matter annihilation,* arXiv:1307.6878 [hep-ph].

[109] J. Casanellas and I. d. Lopes, *Constraints on asymmetric dark matter from asteroseismology,* arXiv:1307.6519 [astro-ph.SR].

[110] K. Agashe and G. Servant, *Baryon number in warped GUTs: Model building and (dark matter related) phenomenology,* JCAP **0502** (2005) 002, hep-ph/0411254.

[111] N. F. Bell, K. Petraki, I. M. Shoemaker and R. R. Volkas, *Pangenesis in a Baryon-Symmetric Universe: Dark and Visible Matter via the Affleck-Dine Mechanism,* Phys. Rev. D **84** (2011) 123505, arXiv:1105.3730 [hep-ph].

[112] D. H. Oaknin and A. Zhitnitsky, *Baryon asymmetry, dark matter and quantum chromodynamics,* Phys. Rev. D **71** (2005) 023519, hep-ph/0309086.

[113] G. Servant and S. Tulin, *Higgsogenesis,* arXiv:1304.3464 [hep-ph].

[114] S. Kasuya and M. Kawasaki, *Gravitino dark matter and baryon asymmetry from Q-ball decay in gauge mediation,* Phys. Rev. D **84** (2011) 123528, arXiv:1107.0403 [hep-ph].

[115] J. McDonald, *Generation of WIMP Miracle-like Densities of Baryons and Dark Matter,* arXiv:1201.3124 [hep-ph].

[116] C. Cheung and Y. Zhang, *Electroweak Cogenesis,* arXiv:1306.4321 [hep-ph].

[117] B. Bhattacherjee, S. Matsumoto, S. Mukhopadhyay and M. M. Nojiri, *Phenomenology of Fermionic Asymmetric Dark Matter,* arXiv:1306.5878 [hep-ph].

[118] H. An, S. L. Chen, R. N. Mohapatra and Y. Zhang, *Leptogenesis as a Common Origin for Matter and Dark Matter,* JHEP **1003**, 124 (2010), arXiv:0911.4463 [hep-ph].

[119] Y. Cui, L. Randall and B. Shuve, *Emergent Dark Matter, Baryon, and Lepton Numbers,* JHEP **1108** (2011) 073, arXiv:1106.4834 [hep-ph].

[120] R. Kitano, H. Murayama and M. Ratz, *Unified origin of baryons and dark matter,* Phys. Lett. B **669**, 145 (2008), arXiv:0807.4313 [hep-ph].

[121] L. J. Hall, J. March-Russell, S. M. West, *A Unified Theory of Matter Genesis: Asymmetric Freeze-In,* arXiv:1010.0245 [hep-ph].

[122] H. Davoudiasl, D. E. Morrissey, K. Sigurdson and S. Tulin, *Hylogenesis: A Unified Origin for Baryonic Visible Matter and Antibaryonic Dark Matter,* Phys. Rev. Lett. **105** (2010) 211304, arXiv:1008.2399 [hep-ph].

[123] J. March-Russell and M. McCullough, *Asymmetric Dark Matter via Spontaneous Co-Genesis,* JCAP **1203** (2012) 019, arXiv:1106.4319 [hep-ph].

[124] H. Davoudiasl and R. N. Mohapatra, *On Relating the Genesis of Cosmic Baryons and Dark Matter,* New J. Phys. **14** (2012) 095011, arXiv:1203.1247 [hep-ph].

[125] A. D. Sakharov, *Violation of CP Invariance, c Asymmetry, and Baryon Asymmetry*

of the Universe, Pisma Zh. Eksp. Teor. Fiz. **5** (1967) 32 [JETP Lett. **5** (1967) 24] [Sov. Phys. Usp. **34** (1991) 392] [Usp. Fiz. Nauk **161** (1991) 61].

[126] R. Barbieri, P. Creminelli, A. Strumia and N. Tetradis, *Baryogenesis through leptogenesis,* Nucl. Phys. B **575** (2000) 61, hep-ph/9911315.

[127] A. Pilaftsis, *CP-violation and baryogenesis due to heavy Majorana neutrinos,* Phys. Rev. D **56** (1997) 5431, hep-ph/9707235.

[128] M. Fukugita and T. Yanagida, *Baryogenesis Without Grand Unification,* Phys. Lett. B **174** (1986) 45.

[129] J. A. Harvey and M. S. Turner, *Cosmological baryon and lepton number in the presence of electroweak fermion number violation,* Phys. Rev. D **42** (1990) 3344.

[130] G. F. Giudice, A. Notari, M. Raidal, A. Riotto and A. Strumia, *Towards a complete theory of thermal leptogenesis in the SM and MSSM,* Nucl. Phys. B **685** (2004) 89, hep-ph/0310123.

[131] J. Schechter and J. W. F. Valle, *Neutrino Masses in SU(2) × U(1) Theories,* Phys. Rev. D **22** (1980) 2227.

[132] C. T. Hill and E. H. Simmons, *Strong dynamics and electroweak symmetry breaking,* Phys. Rept. **381** (2003) 235 [Erratum-ibid. **390** (2004) 553], hep-ph/0203079.

[133] H. Iminniyaz, M. Drees and X. Chen, *Relic Abundance of Asymmetric Dark Matter,* JCAP **1107** (2011) 003, arXiv:1104.5548 [hep-ph].

[134] M. L. Graesser, I. M. Shoemaker and L. Vecchi, *Asymmetric WIMP dark matter,* JHEP **1110** (2011) 110, arXiv:1103.2771 [hep-ph].

[135] P. Gondolo, J. Edsjo, P. Ullio, L. Bergstrom, M. Schelke and E. A. Baltz, *DarkSUSY: Computing supersymmetric dark matter properties numerically,* JCAP **0407** (2004) 008, astro-ph/0406204.

[136] M. Freytsis and Z. Ligeti, *On dark matter models with uniquely spin-dependent detection possibilities,* Phys. Rev. D **83** (2011) 115009, arXiv:1012.5317 [hep-ph].

[137] A. Kurylov and M. Kamionkowski, *Generalized analysis of weakly interacting massive particle searches,* Phys. Rev. D **69** (2004) 063503, hep-ph/0307185.

[138] J. Fan, M. Reece, L. -T. Wang, *Non-relativistic effective theory of dark matter direct detection,* JCAP **1011** (2010) 042, arXiv:1008.1591 [hep-ph].

[139] P. Agrawal, Z. Chacko, C. Kilic and R. K. Mishra, *A Classification of Dark Matter Candidates with Primarily Spin-Dependent Interactions with Matter,* arXiv:1003.1912.

[140] M. Beltran, D. Hooper, E. W. Kolb and Z. C. Krusberg, *Deducing the nature of dark matter from direct and indirect detection experiments in the absence of collider signatures of new physics,* Phys. Rev. D **80** (2009) 043509, arXiv:0808.3384 [hep-ph].

[141] P. J. Fox, R. Harnik, J. Kopp and Y. Tsai, *LEP Shines Light on Dark Matter,* Phys. Rev. D **84** (2011) 014028, arXiv:1103.0240.

[142] R. Harnik, G. D. Kribs, *An Effective Theory of Dirac Dark Matter,* Phys. Rev. **D79**

(2009) 095007, arXiv:0810.5557 [hep-ph].

[143] A. Rajaraman, W. Shepherd, T. M. P. Tait and A. M. Wijangco, *LHC Bounds on Interactions of Dark Matter,* Phys. Rev. D **84** (2011) 095013, arXiv:1108.1196 [hep-ph].

[144] P. J. Fox, R. Harnik, J. Kopp, Y. Tsai, *Missing Energy Signatures of Dark Matter at the LHC,* Phys. Rev. D **85** (2012) 056011, arXiv:1109.4398 [hep-ph].

[145] A. Friedland, M. L. Graesser, I. M. Shoemaker and L. Vecchi, *Probing Nonstandard Standard Model Backgrounds with LHC Monojets,* Phys. Lett. B **714** (2012) 267, arXiv:1111.5331 [hep-ph].

[146] I. M. Shoemaker and L. Vecchi, *Unitarity and Monojet Bounds on Models for DAMA, CoGeNT, and CRESST-II,* Phys. Rev. D **86** (2012) 015023, arXiv:1112.5457 [hep-ph].

[147] P. J. Fox, R. Harnik, R. Primulando and C. -T. Yu, *Taking a Razor to Dark Matter Parameter Space at the LHC,* Phys. Rev. D **86** (2012) 015010, arXiv:1203.1662 [hep-ph].

[148] K. Griest and D. Seckel, *Cosmic Asymmetry, Neutrinos and the Sun,* Nucl. Phys. B **283** (1987) 681 [Erratum-ibid. B **296** (1988) 1034].

[149] M. R. Buckley, *Asymmetric Dark Matter and Effective Operators,* Phys. Rev. D **84** (2011) 043510, arXiv:1104.1429 [hep-ph].

[150] R. Mertig, M. Bohm and A. Denner, *FEYN CALC: Computer algebraic calculation of Feynman amplitudes,* Comput. Phys. Commun. **64** (1991) 345.

[151] J. R. Ellis, A. Ferstl and K. A. Olive, *Reevaluation of the elastic scattering of supersymmetric dark matter,* Phys. Lett. B **481** (2000) 304, hep-ph/0001005.

[152] G. Belanger, F. Boudjema, P. Brun, A. Pukhov, S. Rosier-Lees, P. Salati and A. Semenov, *Indirect search for dark matter with micrOMEGAs2.4,* Comput. Phys. Commun. **182** (2011) 842, arXiv:1004.1092 [hep-ph].

[153] J. R. Ellis, K. A. Olive and C. Savage, *Hadronic Uncertainties in the Elastic Scattering of Supersymmetric Dark Matter,* Phys. Rev. D **77** (2008) 065026, arXiv:0801.3656.

[154] **The COMPASS Collaboration**, M. Alekseev *et al.*, *The Polarised Valence Quark Distribution from semi-inclusive DIS,* Phys. Lett. **B660** (2008) 458-465, arXiv:0707.4077.

[155] **The CRESST Collaboration**, M. F. Altmann *et al.*, *Results and plans of the CRESST dark matter search,* astro-ph/0106314.

[156] **The XENON10 Collaboration**, J. Angle *et al. A search for light dark matter in XENON10 data,* Phys. Rev. Lett. **107** (2011) 051301, arXiv:1104.3088 [astro-ph.CO].

[157] **The CDMS Collaboration**, D. S. Akerib *et al.*, *A low-threshold analysis of CDMS shallow-site data,* Phys. Rev. D **82** (2010) 122004, arXiv:1010.4290, [astro-ph.CO].

[158] **The DAMIC Collaboration**, J. Barreto *et al. Direct Search for Low Mass Dark Matter Particles with CCDs,* Phys. Lett. B **711** (2012) 264, arXiv:1105.5191.

[159] **The SIMPLE Collaboration**, M. Felizardo, T. Girard, T. Morlat, A. C. Fernandes, F. Giuliani, A. R. Ramos, J. G. Marques, M. Auguste *et al.*, *Final Analysis and Results of the Phase II SIMPLE Dark Matter Search,* arXiv:1106.3014 [astro-ph.CO].

[160] **The ATLAS collaboration**, *Search for New Phenomena in Monojet plus Missing Transverse Momentum Final States using 1* fb^{-1} *of pp Collisions at* $\sqrt{s} = 7$ *TeV with the ATLAS Detector* ATLAS-CONF-2011-096 (2011).

[161] **The CMS Collaboration**, S. Chatrchyan *et al. Search for dark matter and large extra dimensions in monojet events in pp collisions at* $\sqrt{s} = 7$ *TeV,* JHEP **1209** (2012) 094, arXiv:1206.5663 [hep-ex]. EXO11059 (2012).

[162] T. Hahn, *Generating Feynman diagrams and amplitudes with FeynArts 3,* Comput. Phys. Commun. **140** (2001) 418, hep-ph/0012260.

[163] A. Pukhov, *CalcHEP 2.3: MSSM, structure functions, event generation, batchs, and generation of matrix elements for other packages,* hep-ph/0412191.

[164] Y. Bai, P. J. Fox and R. Harnik, *The Tevatron at the Frontier of Dark Matter Direct Detection,* JHEP **1012** (2010) 048, arXiv:1005.3797 [hep-ph].

[165] G. Choudalakis, *How to Use Experimental Data to Compute the Probability of Your Theory,* arXiv:1110.5295 [hep-ph].

[166] **The CDF Collaboration**, T. Aaltonen *et al. A search for dark matter in events with one jet and missing transverse energy in* $p\overline{p}$ *collisions at* $\sqrt{s} = 1.96$ *TeV,* arXiv:1203.0742 [hep-ex];

[167] J. R. Ellis, T. Falk, K. A. Olive and M. Srednicki, *Calculations of neutralino-stau coannihilation channels and the cosmologically relevant region of MSSM parameter space,* Astropart. Phys. **13** (2000) 181, hep-ph/9905481.

[168] L. N. Chang, O. Lebedev and J. N. Ng, *On the invisible decays of the Upsilon and J/psi resonances,* Phys. Lett. B **441** (1998) 419, hep-ph/9806487.

[169] C. Boehm, T. A. Ensslin and J. Silk, *Can Annihilating dark matter be lighter than a few GeVs?,* J. Phys. G **30** (2004) 279, astro-ph/0208458.

[170] P. Fayet, *Invisible Upsilon decays into Light Dark Matter,* Phys. Rev. D **81** (2010) 054025, arXiv:0910.2587 [hep-ph].

[171] B. McElrath, *Invisible quarkonium decays as a sensitive probe of dark matter,* Phys. Rev. D **72** (2005) 103508, hep-ph/0506151.

[172] **The BABAR Collaboration**, B. Aubert *et al. A Search for Invisible Decays of the Upsilon(1S),* Phys. Rev. Lett. **103** (2009) 251801, arXiv:0908.2840 [hep-ex].

[173] D. T. Cumberbatch, J. .A. Guzik, J. Silk, L. S. Watson and S. M. West, *Light WIMPs in the Sun: Constraints from Helioseismology,* Phys. Rev. D **82** (2010) 103503, arXiv:1005.5102 [astro-ph.SR].

[174] M. T. Frandsen and S. Sarkar, *Asymmetric dark matter and the Sun,* Phys. Rev. Lett. **105** (2010) 011301, arXiv:1003.4505 [hep-ph].

[175] A. R. Zentner and A. P. Hearin, *Asymmetric Dark Matter May Alter the Evolution of Low-mass Stars and Brown Dwarfs,* arXiv:1110.5919 [astro-ph.CO].

[176] F. Iocco, M. Taoso, F. Leclercq and G. Meynet, *Main sequence stars with asymmetric*

dark matter, Phys. Rev. Lett. **108** (2012) 061301, arXiv:1201.5387 [astro-ph.SR].

[177] H. Davoudiasl, D. E. Morrissey, K. Sigurdson and S. Tulin, *Baryon Destruction by Asymmetric Dark Matter,* Phys. Rev. D **84** (2011) 096008, arXiv:1106.4320 [hep-ph].

[178] C. Kouvaris, P. Tinyakov, *Constraining Asymmetric Dark Matter through observations of compact stars,* Phys. Rev. **D83** (2011) 083512, arXiv:1012.2039 [astro-ph.HE].

[179] C. Kouvaris, P. Tinyakov, *Excluding Light Asymmetric Bosonic Dark Matter,* Phys. Rev. Lett. **107** (2011) 091301, arXiv:1104.0382 [astro-ph.CO].

[180] N. F. Bell, A. Melatos and K. Petraki, *Realistic neutron star constraints on bosonic asymmetric dark matter,* Phys. Rev. D **87** (2013) 123507, arXiv:1301.6811 [hep-ph].

[181] J. Bramante, K. Fukushima and J. Kumar, *Constraints on Bosonic Dark Matter From Observations of Old Neutron Stars,* Phys. Rev. D **87** (2013) 055012, arXiv:1301.0036.

[182] Y. -z. Fan, R. -z. Yang and J. Chang, *Constraining Asymmetric Bosonic Non-interacting Dark Matter with Neutron Stars,* arXiv:1204.2564 [astro-ph.HE].

[183] J. M. Cline, Z. Liu and W. Xue, *Millicharged Atomic Dark Matter,* Phys. Rev. D **85**, 101302 (2012), arXiv:1201.4858 [hep-ph].

[184] P. J. Fox and E. Poppitz, *Leptophilic Dark Matter,* Phys. Rev. D **79** (2009) 083528, arXiv:0811.0399 [hep-ph].

[185] J. L. Feng, J. Kumar, D. Marfatia and D. Sanford, *Isospin-Violating Dark Matter,* Phys. Lett. B **703** (2011) 124, arXiv:1102.4331 [hep-ph].

[186] **The XENON100 Collaboration**, E. Aprile *et al. Dark Matter Results from 225 Live Days of XENON100 Data,* Phys. Rev. Lett. **109** (2012) 181301 arXiv:1207.5988.

[187] **The ATLAS Collaboration**, G. Aad *et al. Search for dark matter candidates and large extra dimensions in events with a jet and missing transverse momentum with the ATLAS detector,* JHEP **1304** (2013) 075, arXiv:1210.4491 [hep-ex].

[188] P. J. Fox and C. Williams, *Next-to-Leading Order Predictions for Dark Matter Production at Hadron Colliders,* Phys. Rev. D **87** (2013) 054030 arXiv:1211.6390.

[189] B. Patt and F. Wilczek, *Higgs-field portal into hidden sectors,* hep-ph/0605188.

[190] J. March-Russell, S. M. West, D. Cumberbatch and D. Hooper, *Heavy Dark Matter Through the Higgs Portal,* JHEP **0807** (2008) 058, arXiv:0801.3440 [hep-ph].

[191] J. Hisano, S. Matsumoto, M. Nagai, O. Saito and M. Senami, *Non-perturbative effect on thermal relic abundance of dark matter,* Phys. Lett. B **646** (2007) 34, hep-ph/0610249.

[192] **The LEP Working Group for Higgs boson searches and ALEPH and DELPHI and L3 and OPAL Collaborations**, R. Barate *et al.*, *Search for the standard model Higgs boson at LEP,* Phys. Lett. B **565** (2003) 61 hep-ex/0306033.

[193] A. Djouadi, O. Lebedev, Y. Mambrini and J. Quevillon, *Implications of LHC searches for Higgs–portal dark matter,* Phys. Lett. B **709** (2012) 65, arXiv:1112.3299 [hep-ph].

[194] C. Englert, T. Plehn, D. Zerwas and P. M. Zerwas, *Exploring the Higgs portal,* Phys.

Lett. B **703** (2011) 298, arXiv:1106.3097 [hep-ph].

[195] L. Lopez-Honorez, T. Schwetz and J. Zupan, *Higgs portal, fermionic dark matter, and a Standard Model like Higgs at 125 GeV,* Phys. Lett. B **716** (2012) 179 arXiv:1203.2064.

[196] J. R. Espinosa, M. Muhlleitner, C. Grojean and M. Trott, *Probing for Invisible Higgs Decays with Global Fits,* JHEP **1209** (2012) 126, arXiv:1205.6790 [hep-ph].

[197] D. Ghosh, R. Godbole, M. Guchait, K. Mohan and D. Sengupta, *Looking for an Invisible Higgs Signal at the LHC,* arXiv:1211.7015 [hep-ph].

[198] K. Griest and D. Seckel, *Three exceptions in the calculation of relic abundances,* Phys. Rev. D **43** (1991) 3191.

[199] K. Jedamzik, *Big bang nucleosynthesis constraints on hadronically and electromagnetically decaying relic neutral particles,* Phys. Rev. D **74** (2006) 103509, hep-ph/0604251.

[200] K. Jedamzik, *Did something decay, evaporate, or annihilate during Big Bang nucleosynthesis?* Phys.Rev. **D70**:063524 (2004), astro-ph/0402344.

[201] M. Reno and D. Seckel, *Primordial Nucleosynthesis: The Effects of Injecting Hadrons* Phys.Rev. **D37**:3441 (1988).

[202] M. Kawasaki, K. Kohri, and T. Moroi, *Big-Bang nucleosynthesis and hadronic decay of long-lived massive particles* Phys.Rev. **D71**:083502 (2005), astro-ph/0408426.

[203] D. P. Finkbeiner, S. Galli, T. Lin, and T. R. Slatyer, *Searching for Dark Matter in the CMB: A Compact Parameterization of Energy Injection from New Physics* Phys.Rev. **D85**:043522, (2012), arXiv:1109.6322.

[204] X.-L. Chen and M. Kamionkowski, *Particle decays during the cosmic dark ages* Phys.Rev. **D70**:043502 (2004), astro-ph/0310473.

[205] J. L. Feng, A. Rajaraman and F. Takayama, *SuperWIMP dark matter signals from the early universe,* Phys. Rev. D **68** (2003) 063504, hep-ph/0306024.

[206] M. Kamionkowski and A. Kosowsky, *The Cosmic microwave background and particle physics,* Ann. Rev. Nucl. Part. Sci. **49** (1999) 77, astro-ph/9904108.

[207] J. L. Feng, M. Kaplinghat and H. -B. Yu, *Halo Shape and Relic Density Exclusions of Sommerfeld-Enhanced Dark Matter Explanations of Cosmic Ray Excesses,* Phys. Rev. Lett. **104** (2010) 151301, arXiv:0911.0422 [hep-ph].

[208] J. D. March-Russell and S. M. West, *WIMPonium and Boost Factors for Indirect Dark Matter Detection,* Phys. Lett. B **676** (2009) 133, arXiv:0812.0559 [astro-ph].

[209] R. J. Munn, E. A. Mason, and F. J. Smith, *Some Aspects of the Quantal and Semiclassical Calculation of Phase Shifts and Cross Sections for Molecular Scattering and Transport*, J. Chem. Phys. 41, 3978 (1964).

[210] S. Tulin, H. -B. Yu and K. M. Zurek, *Beyond Collisionless Dark Matter: Particle Physics Dynamics for Dark Matter Halo Structure,* arXiv:1302.3898 [hep-ph].

[211] W. Shepherd, T. M. P. Tait and G. Zaharijas, *Bound states of weakly interacting dark*

matter, Phys. Rev. D **79** (2009) 055022, arXiv:0901.2125.

[212] S. Weinberg, *Summing soft pions,* Phys. Rev. D **2** (1970) 674.

[213] L. S. Brown, *On summing soft pions,* Phys. Rev. D **2** (1970) 3083.

[214] J. F. Donoghue, E. Golowich and B. R. Holstein, *Dynamics of the standard model,* Camb. Monogr. Part. Phys. Nucl. Phys. Cosmol. **2**, 1 (1992).

[215] C. Bertulani, *Nuclear Physics in a Nutshell,* Princeton University Press (2007).

[216] B. von Harling and A. Hebecker, *Sequestered Dark Matter,* JHEP **0805** (2008) 031, arXiv:0801.4015 [hep-ph].

[217] X. Chen and S. -H. H. Tye, *Heating in brane inflation and hidden dark matter,* JCAP **0606** (2006) 011, hep-th/0602136.

[218] A. Hebecker and J. March-Russell, *The Ubiquitous throat,* Nucl. Phys. B **781**, 99 (2007), hep-th/0607120.

[219] M. Berg, D. Marsh, L. McAllister and E. Pajer, *Sequestering in String Compactifications,* JHEP **1106** (2011) 134, arXiv:1012.1858.

[220] F. D'Eramo, L. Fei and J. Thaler, *Dark Matter Assimilation into the Baryon Asymmetry,* JCAP **1203** (2012) 010, arXiv:1111.5615 [hep-ph].

[221] M. Cicoli and A. Mazumdar, *Reheating for Closed String Inflation,* JCAP **1009** (2010) 025, arXiv:1005.5076 [hep-th].

[222] M. Cicoli and A. Mazumdar, *Inflation in string theory: A Graceful exit to the real world,* Phys. Rev. D **83** (2011) 063527, arXiv:1010.0941 [hep-th].

[223] H. K. Dreiner, C. Hanhart, U. Langenfeld and D. R. Phillips, *Supernovae and light neutralinos: SN1987A bounds on supersymmetry revisited,* Phys. Rev. D **68** (2003) 055004, hep-ph/0304289.

[224] N. Arkani-Hamed, A. Delgado and G. F. Giudice, *The Well-tempered neutralino,* Nucl. Phys. B **741** (2006) 108, hep-ph/0601041.

[225] C. Boehm, J. Orloff and P. Salati, *Light Dark Matter Annihilations into Two Photons,* Phys. Lett. B **641** (2006) 247, astro-ph/0607437.

[226] M. Blennow, E. Fernandez-Martinez, O. Mena, J. Redondo and P. Serra, *Asymmetric Dark Matter and Dark Radiation,* JCAP **1207** (2012) 022, arXiv:1203.5803 [hep-ph].

[227] W. Buchmuller and M. Garny, *Decaying vs Annihilating Dark Matter in Light of a Tentative Gamma-Ray Line,* JCAP **1208** (2012) 035, arXiv:1206.7056 [hep-ph].

[228] C. Boehm, T. Delahaye and J. Silk, *Can the morphology of gamma-ray emission distinguish annihilating from decaying dark matter?,* Phys. Rev. Lett. **105** (2010) 221301, arXiv:1003.1225 [astro-ph.GA].

[229] M. T. Frandsen, F. Kahlhoefer, C. McCabe, S. Sarkar and K. Schmidt-Hoberg, *The unbearable lightness of being: CDMS versus XENON,* JCAP **1307** (2013) 023, arXiv:1304.6066 [hep-ph].

[230] N. Okada and O. Seto, *Isospin violating dark matter being asymmetric,* arXiv:1304.6791 [hep-ph].

[231] J. L. Feng, J. Kumar and D. Sanford, *Xenophobic Dark Matter,* arXiv:1306.2315.

[232] M. McCullough and L. Randall, *Exothermic Double-Disk Dark Matter,* arXiv:1307.4095 [hep-ph].

[233] D. Hooper, *Revisiting XENON100's Constraints (and Signals?) For Low-Mass Dark Matter,* arXiv:1306.1790 [hep-ph].

[234] D. Hooper, I. Cholis, T. Linden, J. Siegal-Gaskins and T. Slatyer, *Pulsars Cannot Account for the Inner Galaxy's GeV Excess,* arXiv:1305.0830 [astro-ph.HE].

[235] D. Hooper, *The Empirical Case For 10 GeV Dark Matter,* Phys. Dark Univ. **1** (2012) 1, arXiv:1201.1303 [astro-ph.CO].